

PACIFIC LAMPREY PASSAGE STRUCTURES AT BONNEVILLE DAM: DESIGN
GUIDELINES AND CATALOG OF QUALITATIVE HYDRAULIC CONDITIONS,
HYDRAULIC MODELING, AND INTEGRATING DIVERSE INFORMATION
SOURCES WITH 3D VISUAL MODELS TO CREATE A FISH PASSAGE WIKI

A Thesis

Presented in Partial Fulfillment of the Requirements for the

Degree of Master of Science

with a

Major in Civil Engineering

in the

College of Graduate Studies

University of Idaho

by

Hattie Zobott

November 2013

Major Professors: Ralph S. Budwig, Ph.D., P.E. and Christopher C. Caudill, Ph.D.

AUTHORIZATION TO SUBMIT THESIS

This thesis of Hattie Zobott, submitted for the degree of Master of Science with a major in Civil Engineering and titled “PACIFIC LAMPREY PASSAGE STRUCTURES AT BONNEVILLE DAM: DESIGN GUIDELINES AND CATALOG OF QUALITATIVE HYDRAULIC CONDITIONS, HYDRAULIC MODELING, AND INTEGRATING DIVERSE INFORMATION SOURCES WITH 3D VISUAL MODELS TO CREATE A FISH PASSAGE WIKI,” has been reviewed in final form. Permission as indicated by the signatures and dates given below, is now granted to submit final copies to the College of Graduate Studies for approval.

Major
Professor _____ Date _____
Ralph S. Budwig, Ph.D., P.E.

Major
Professor _____ Date _____
Christopher C. Caudill, Ph.D.

Committee
Member _____ Date _____
Daniele Tonina, Ph.D., P.E.

Department
Administrator _____ Date _____
Richard Nielson, Ph.D., P.E.

Discipline’s
College Dean _____ Date _____
Larry Stauffer, Ph.D., P.E.

Final Approval and Acceptance by the College of Graduate Studies

_____ Date _____
Jie Chen, Ph.D.

ABSTRACT

Pacific lamprey is an ancient anadromous fish that has declined in parallel with Pacific salmon. The focus on recovery within the Columbia River has led to the development of fishways specific for adult Pacific lamprey passage at dams. These novel structures exploit a natural and unusual climbing behavior of Pacific lamprey that allows them to ascend very steep slopes. The structures have been installed parallel to the existing fishways at several locations at Bonneville Dam. Each Lamprey Passage Structure (LPS) is unique because of the retrofit application. Here, I describe characteristics used in past LPS designs and criteria used to develop a new LPS at the Bonneville Dam Washington Shore fishway. LPS structures are composed of three major components, climbing ducts, rest boxes and traversing ducts. The traversing duct is a low slope ($S=0.0035$) rectangular channel with subcritical flow; while the climbing duct is a steep slope ($S=1.0$) structure with thin supercritical flow.

We developed a hydraulic model of both duct types. The result of the model is a series of operating curves for varying widths and slope that predict discharge and velocity based on flow depth. We also determined an appropriate roughness for the LPS systems based on reported operating conditions. The flow conditions within the ductwork are steady and uniform. In contrast, there are unique features implemented within each LPS that may present complex and challenging hydraulic conditions. Using the recent system installed at The Bonneville Dam Washington North Shore Fishway as a case study, we catalog the different features and their hydraulic conditions.

Pacific lamprey research and recovery efforts are occurring at a rapid pace. The complexity of researching and addressing the problems uncovered in real time is tedious. A large number of studies and modifications have been undertaken to improve passage of adult lamprey at Bonneville Dam. Integrating such diverse sets of information types in a spatially explicit context is a common challenge in many applied research settings. We developed a collaborative, visual model, which integrated the current information on Pacific lamprey with the structural elements of the Washington Shore Fishway to improve recovery efforts. The tool is a 3D visual model with overlaid and integrated information creating a fish passage “wiki”. Stakeholders will be able to investigate different aspects of Pacific lamprey recovery including research results, current and past modifications, and archive photos, all within the structural context of the fishway. The wiki aspect describes a potential for transparency and crowd sourced maintenance of the information. Stakeholders can use the fish passage wiki for both dissemination and synthesizing information, and prioritizing future management and conservation actions. The 3D-wiki tool is aimed at developing a more comprehensive understanding of the difficulties facing Pacific lamprey passage within the Columbia River basin.

ACKNOWLEDGEMENTS

I would like to thank my professors for their efforts during the development of this thesis: Ralph Budwig for mentoring me during all phases of my research, Chris Caudill for helping me grow into a more complex engineer, Matthew Keefer for his feedback, committee member Daniele Tonina for his time and feedback on my thesis, and Elowyn Yager, in addition to the aforementioned, for their flexibility during the implementation phases of my research.

A special thanks to the United States Army Corp of Engineers, Portland Office, for funding and supporting this research. I would also like to thank Sean Tackley for his administrative and technical assistance, Andrew Traylor for operational support, Natalie Richards and many others for their role in the installation of the Lamprey Passage Structure.

DEDICATION

I dedicate this work to my loving husband and family who supported my dream to understand and facilitate fish passage while gaining an advanced degree in engineering.

TABLE OF CONTENTS

Authorization to Submit Thesis	ii
Abstract.....	iii
Acknowledgements.....	v
Dedication.....	vi
Table of Contents.....	vii
List of Figures.....	ix
List of Tables	xii
Chapter One: Preface	1
Chapter Two: Design guidelines and catalog of qualitative hydraulic conditions for Pacific lamprey passage structures.....	3
1. Abstract	3
2. Introduction	4
3. Study Site and Apparatus	7
4. Results	10
5. Discussion and Recommendations.....	17
6. Acknowledgements	18
7. References	18
Chapter Three: Hydraulic modeling of channels in Pacific Lamprey Passage Structures.....	21
1. Abstract	21
2. Introduction	22
3. Methods	27
4. Results	32
5. Discussion and Recommendations.....	36
6. Acknowledgements	45
7. References	45
Chapter Four: Integrating diverse information sources with 3D visual models to create a fish passage wiki	50
1. Abstract	50
2. Introduction	51

3. Methods	53
4. Results	57
5. Discussion	60
6. Acknowledgements	62
7. References	63
Appendix A-Reported parameters investigated during roughness calculations*	65
Appendix B-Roughness calculation method	66
Appendix C-Climbing duct hydraulic model calculations	76
Appendix D-Traversing Duct Hydraulic Model Calculations	82

LIST OF FIGURES

Figure 2.1 Bonneville Dam complex: Washington Shore LPS located on the Washington Shore fishway	9
Figure 2.2 Schematic of LPS structure at Bonneville Dam Washington North Shore Fishway	10
Figure 2.3: Elevation view of climbing duct LPS 1) Attaches to the Lamprey Flume Structure. 2) First rest box and 180 degree turn. 3) Climbing duct section: width is 50cm, depth 15cm, 4) transition to a rest box. 5) Second rest box.....	13
Figure 2.4: Plan view of traversing ductwork over the fishway. 5) Second rest box 6) Step 7) Traversing duct, width 50 cm 8) 90 degree corner 9) Expansion from narrow duct, width 20cm, to wide traversing duct.....	13
Figure 2.5: Plan view of the LPS finale. 11) Jogging duct, 12) Expansion, same dimensions as contraction, 13) Climbing duct 14) Final Rest Box 15) Upwelling box Entrance 16) Upwelling Box 17) Upwelling box exit.....	14
Figure 2.6 Elevation view of traversing duct.....	14
Figure 2.7: Plan view of traversing section in long straightaway.....	14
Figure 2.8: a) Elevation of LPS platform section b) End view of LPS platform section	15
Figure 3.1: Geometry of LPS ductwork. Dimensions to outside of duct. Interior dimensions used in calculations a) Climbing duct cross section with Slope= 1. b) Traversing duct cross section with Slope= 0.0035 at Washington Shore Fishway LPS c) Traversing duct of Cascade Island, Bradford Island and Washington Shore AWS LPS systems with Slope=0.0035 d) LPS schematic.....	28

Figure 3.2: Operating Curves for LPS Ductwork: flow depth are shown with blue lines, mean velocity shown with black lines for $\epsilon=0.18\text{mm}$; a) Cascade Island, Bradford Island and Washington Shore AWS LPS systems where width is 19cm b) Washington Shore Fishway LPS system where width is 23 cm c) Bradford Island, Cascade Island, & Washington Shore Fishway LPS where width is 50cm d) Climbing duct for all LPS systems: Slope=1.0, width is 50cm..... 34

Figure 3.3: Drag force as a function of velocity. The fish is fully submerged in the flow. Blue lines represent a fish with girth, $G=0.08\text{m}$; Orange lines represent a fish with $G=0.10\text{m}$, and pink lines represent a fish with $G=0.12\text{m}$. F_{dcrit} is the drag force at the critical swim velocity of $0.8 \text{ m}\cdot\text{sec}^{-1}$ and the respective girth. $F_{d_{vb}}$ is the drag force at the upper swimming limit of $2.5 \text{ m}\cdot\text{sec}^{-1}$ and the respective girth. 38

Figure 3.4: Flow Depth with Increasing Slope. The duct shown is the traversing width ($b=19\text{cm}$) and ($Q=7.8L\cdot\text{s}^{-1}$). Flow depth is represented by the blue line, and velocity is represented by the black line. a) Represents subcritical slopes $< S_c=0.0047$, b) represents supercritical slopes where Slope $> S_c=0.0047$ 40

Figure 3.5: Drag force with decreasing slope ($S < S_c$) and constant discharge ($Q=7.8L\cdot\text{s}^{-1}$) for a given duct width, ($b=19\text{cm}$). Blue represents $G=0.08\text{m}$, Orange represents $G=0.1\text{m}$, and Pink represents $G=0.12\text{m}$. Dashed lines represent the F_{dcrit} calculated from the girth and ($U_{crit}=0.8\text{m}\cdot\text{s}^{-1}$) 41

Figure 4.1: Site Overview of Bonneville Dam Complex, The Washington North Shore Fishway is circled 54

Figure 4.2: Plan view of Bonneville Dam Complex 3D wiki model..... 58

Figure 4.3: Plan view of Powerhouse 2. Insets show tailrace elevation change and resulting overflow weir flooding 59

Figure 4.4: Snapshots of the 3D wiki functionality. The brightly colored objects are references to external data pertaining to their location (e.g. reports, charts, or pictures). a) Arrows show the hyperlinked external data of a graph and a picture of the North Downstream Entrance of the fishway (Inset pictures). b) Is a scene where the recent Lamprey Passage Flume modifications to the Washington North Shore Fishway are shown. 59

Figure 4.5: Data passage overlay on the visual 3D base model. The inset “Layers” box shows which layers are active in this view..... 60

LIST OF TABLES

Table 2.1: Catalog of hydraulic conditions.....	16
Table 2.2: Design guidelines for LPS systems	17
Table 3.1: Roughness Determination: for hydraulic modeling for discharge of $7.8 \text{ L}\cdot\text{s}^{-1}$ using the Haaland correlation to determine effective roughness	32
Table 3.2: Comparison of ductwork parameters and resulting flow conditions for $Q=7.8\text{L}\cdot\text{s}^{-1}$, and $\epsilon=0.18\text{mm}$. Climbing duct % change compared to nominal parameters in bold ($S=1.0$, $b=50\text{cm}$). Traversing duct compared to nominal parameters in bold ($S=0.0035$, $b=19\text{cm}$).	33
Table 3.3: Critical Flow Parameters for Ductwork: were critical flow occurs at Froude number= 1.0 and $\epsilon=0.18\text{mm}$ at a discharge of $Q=7.8\text{L}\cdot\text{s}^{-1}$	35
Table 3.4: Comparison of ductwork parameters and resulting flow conditions for $Q=7.8\text{L}\cdot\text{s}^{-1}$, and $\epsilon=0.18\text{mm}$. Climbing duct % change compared to nominal parameters in bold ($S=1.0$, $b=50\text{cm}$). Traversing duct compared to nominal parameters in bold ($S=0.0035$, $b=19\text{cm}$).	36
Table 3.5: Flow parameters of supercritical flow where Pacific lamprey are fully submerged. Girth=Flow depth, flow is supercritical for all cases shown with a constant Froude number. Results of the critical drag force ($F_{d_{\text{crit}}}$) and the velocity barrier drag force ($F_{d_{\text{vb}}}$), and corresponding Froude numbers for the two conditions are in bold	42
Table 4.1: Software platform selection table. Google Sketchup was the best suited based on our criteria.....	55

CHAPTER ONE: PREFACE

The format of this thesis is presented in the form of three journal papers, each contained in its own chapter in this thesis. Each paper is formatted discretely and includes: abstract, introduction, methods, results, discussion and recommendation sections, acknowledgements, & references.

We introduce the design and implementation of a Lamprey Passage Structure (LPS) in chapter Two, “Catalog of qualitative hydraulic conditions and design guidelines for Pacific lamprey passage structures.” We use the Washington North Shore Fishway LPS as a case study to determine hydraulic conditions that result from structural features of an LPS system. The features are catalogued by number and then categorized based on the water surface as either uniform, gradually varying, or rapidly varying flow. A short description accompanies each categorization. We also outline the best practices implemented when we designed the Washington Shore Fishway LPS.

Chapter Three, “Hydraulic modeling of channels in Pacific Lamprey Passage Structures” analyzes the hydraulic conditions within the basic components of Pacific Lamprey Passage Structures (LPS). The factors included in this research include flow depth, Froude number, channel width, discharge, and velocity. The roughness is determined theoretically based on solutions to the Haaland correlation for the Darcy friction factor. The resulting operating curves are presented for the calculated effective roughness based on reported hydraulic conditions for the LPS ductwork.

Chapter Four, “Fish Passage Wiki: Using collaborative visual modeling to communicate fish passage information,” describes the implementation of a collaborative

modeling tool for compiling Pacific lamprey passage information. The tool uses a visual three dimensional model as the base structure on which various information types are overlaid. Multiple file types are integrated within the model. The intent of the tool is to create a visual wiki page where stakeholders can update information as it becomes available to maintain an accurate description of research and conservation efforts at Bonneville Dam.

CHAPTER TWO: DESIGN GUIDELINES AND CATALOG OF QUALITATIVE HYDRAULIC CONDITIONS FOR PACIFIC LAMPREY PASSAGE STRUCTURES

Hattie Zobott¹, Christopher Caudill², Matthew Keefer², and Ralph Budwig¹, Mary Moser³

¹Center for Ecohydraulics Research

University of Idaho, Boise, ID

²Department of Fish and Wildlife Sciences

University of Idaho, Moscow, ID, 83844-1136

³Northwest Fisheries Science Center

National Marine Fisheries Services, Seattle, WA

1. Abstract

Development of fishways is a complex problem that necessitates biologists, engineers, and dam managers working as a team to develop, implement, and install components and structures. Fishways must fit within the context of the dam they support, resulting in large elevation changes within short distances. The slope of fishways is often determined by what fits, and not what is most biologically suitable. Historically, hydraulic conditions within fishways of the Columbia basin were optimized to facilitate the passage of salmonids. Passage of other species have become a priority since the original fishways were constructed. Innovative structures like Pacific Lamprey Passage Structures (LPS) accomplish fish passage improvement for an auxiliary species while minimizing potential impacts on salmonid passage. Currently, the structures are being considered for implementation at a wide variety of projects from low-head irrigation dams to large mainstem hydroelectric projects. In an effort to aid these efforts, we report design guidelines used in development of LPS systems, catalog the types of hydraulic conditions

within a typical LPS system, and correlate the structural elements with resulting hydraulic conditions. We used the recently installed LPS system at Bonneville Dam, Washington North Shore Fishway to highlight the types of structures used, types of hydraulic conditions within them, and provide recommendations for further improvement to LPS systems.

2. Introduction

Lamprey passage structures were developed in response to growing concern of Pacific lamprey decline. The fish have unique climbing and swimming mechanisms that allow them to complete one of the historically longest migrations of anadromous, with distributions similar to the anadromous Pacific salmonids. While salmon decline was well studied due to the economic impacts resulting from failed migration, Pacific lamprey were neglected or actively managed against. Often described as a “trash fish”, (e.g., Perkins & Smith 1973), the Pacific lamprey continued to decline without advocates. Cultural impacts and losses were substantial for the tribal groups that once relied on the Pacific lamprey (Close et al. 2002). Pacific lamprey were petitioned for protection under the Endangered Species Act in effort to help their recovery, but the petition was denied citing lack of information on population structure and other basic biological attributes (Moser & Close 2003, Keefer et al. 2009). Since then, the Columbia River Fish Accords identified Pacific lamprey as a priority species for recovery in 2008 (“Columbia River Fish Accords Salmon Restoration, Salmon Protection.”)

The resulting research helped outline likely factors contributing to Pacific lamprey declines. Visual monitoring within fishways revealed that the standard overflow weir presented passage problems that resulted in milling behavior and failed passage (Beck 1995, Hard & Kynard 1997, and Clabough et al. 2012). Delays can be critical as the aggregation

of fish at a barrier can increase predation, and subject the fish to physical damage and stress (Schilt 2006). As a result, research to quantify the Pacific lampreys swimming performance identified the limits of swimming performance in velocities around $0.8 \text{ m}\cdot\text{s}^{-1}$ (Mesa et al. 2003). When velocities exceed the swimming velocity barrier, the fish switch swimming modes and become saltatory. Combining periods of rest by attaching to smooth surfaces with short periods of burst swimming (Quintella et al. 2004). Maximum burst swimming velocities are estimated between $2.5 \text{ m}\cdot\text{s}^{-1}$ and $3.0 \text{ m}\cdot\text{s}^{-1}$ for fish with average length of approximately 70cm (Keefer et al. 2011). The range of migrating Pacific lamprey is from (16cm-72cm) (Beamish 1980). Telemetry results indicate that the smallest fish are less successful in migrating upstream to historic spawning locations (Keefer et al. 2009). Therefore, the velocity limits for the population may be lower. As a result, fishways must provide pathways with lower mean velocities than is suitable for salmonids. Greater heterogeneity of flow conditions may also help accommodate the full diversity of species within river systems (Katapodis 2005, Barret and Mallen-Cooper 2006).

Not only do the hydraulic conditions need to be quantified, but the behavioral elements of fish are critical to fishway success. One natural behavior of Pacific lamprey is that they can climb when confronted with a passage barrier. The Pacific lamprey climb Willamette Falls (12 m) on the Willamette River to reach upstream spawning habitats (Clemens et al. 2012). Researchers began to develop structures that allowed the fish to bypass dams using both normal anguilliform swimming and by exploiting lamprey climbing behavior (Moser et al. 2005). The resulting LPS systems rely on anguilliform swimming in low-slope ducts combined with climbing behavior of Pacific lamprey on steep slopes with sheeting flow (Moser et al. 2011). The different climbing slopes investigated were over a

wide range but limited to a few angles: 18°, 45°, & 90° with results indicating that up to 17% of Pacific lamprey will not climb a vertical face (Kemp et al. 2009). Although researchers determined a suitable slope for LPS climbing duct, other hydraulic parameters have not been investigated to establish a set of comprehensive fishway criteria. Discharge and slope angle are interrelated parameters of climbing behavior (Reinhardt et al. 2008). The behavior of fish as related to the structures are often confusing as some research results point to increased climbing efficiency with lowered discharge (Keefer et al. 2011b), and other research indicates that discharge has no effect (Moser et al. 2011). Recent research indicates that reducing discharge will reduce the drag force on climbing Pacific lamprey (Zobott et al. 2013).

The importance of engineers and biologists working together to design fishways is intuitive. Fishway success depends on the hydraulic conditions as well as the behavior of fish within them. The structure of the fishway determines the hydraulic conditions. Salmon fishways were not successful until considerable research into the hydraulics of pool weir designs were explored (Williams et al. 2012). The alternative designs that were implemented better matched the specific cues the fish needed to ascend the fishway (Williams et al. 2012). These designs were further modified to accommodate multiple species including interactions between salmonids and shad (Monk and Weaver 1989).

The Washington North Shore LPS was installed in spring of 2013 and operational June of 2013. The structure operated until August of 2013 with few lamprey (29 or ~0.1 % of those passing the Washington Shore Ladder, C. Caudill unpub. data) using the structure due to structural and installation problems in the lower LFS that remain unclear and minor

issues in the upper LPS. The Bradford Island LPS was installed in 2005 (Moser et al. 2006), while the Cascade Island LPS was installed in 2007 (Moser et al. 2011).

We qualitatively describe the hydraulic conditions within an operational LPS system at Bonneville Dam from the perspective of Pacific lamprey as they ascend the fishway as part of a larger effort to establish general design criteria for LPS systems that can be used in future passage improvements. Unlike previous LPS, which are stand-alone structures with LPS entrance located inside a traditional fishway, the Washington Shore LPS provides passage to a collection trap after lamprey enter one of two prototype lamprey-specific entrances located in the tailrace. The LPS completes the flume structure developed by the USACE to collect migrating Pacific lamprey into the LPS bypass. Multiple novel features were implemented in order to address the complexity of fishway retrofit. In this paper we 1) catalog the structural elements of the LPS and 2) Correlate the structural elements to hydraulic conditions.

3. Study Site and Apparatus

The study site is within the Bonneville Dam complex on the Columbia River (Figure 2.1). The LPS structure is on the Washington Shore Fishway (Figure 2.2). The LPS begins at the end of the Lamprey Flume Structure (LFS) at elevation 11.3 m (37 ft.) on the South wall of the fishway, and climbs up to the 16.8 m (55 ft.) elevation deck. A series of climbing ducts and rest boxes enable the fish to ascend to the deck. Once on the deck, the Pacific lamprey swim through ductwork of varying widths that travels over the fishway (Figure 2.4, Figure 2.6). A long series of narrow ductwork elements travels to the west end of the fishway (Figure 2.7). The final section before the trap boxes includes a short climb, a rest box, and an exit assembly that drops Pacific lamprey into a holding tank (Figure 2.5,

Figure 2.8). After initial testing, the USACE plans to extend the LPS to the dam fore bay to provide passage without trapping.

The design was based on correspondence with Mary Moser (NOAA-Fisheries) and her reported research (Moser et al. 2005, Moser et al. 2008, and Moser et al. 2011). Aluminum ducting bent into rectangular cross sections are bolted together in series. Ducting is either climbing, where the width is 50cm or traversing, where the widths are either 23cm or 50cm. The slopes of all climbing ducts are ≈ 1.0 ; while traversing ducts are ≈ 0.0035 . We used the reported values of depth and discharge to determine the base flow conditions for the climbing duct and traversing ducts from Moser et al. (2011). We will report parameter combinations in parenthesis, using: S for slope, b for width, y for depth, and Q for discharge. For the traversing duct where (b=19cm, S=0.0035, and $Q=7.8 \text{ L}\cdot\text{s}^{-1}$) the resulting flow depth (y=10cm). The climbing duct flow depth for (b=50cm, S=1.0, $Q=7.8 \text{ L}\cdot\text{s}^{-1}$) was (y= 3cm). Each critical structural feature is outlined in red and itemized by number as seen in (Figure 2.6). The features are defined in (**Error! Reference source not found.**) by the anticipated hydraulic condition and short description.

The hydraulic conditions are described by the flow types as described by Chow (1959). Flow was categorized as steady flow if the flow depth does not change within a given operational time period. Unsteady flow is defined as flow that varies in depth over time. Surging flow is a type of unsteady flow. When the flow depth doesn't change it is Uniform Flow (UF); while changing flow is described as Varied Flow VF. Varied flow can either be Rapidly Varied Flow RVF or Gradually Varied Flow GVF depending on the distance it takes for the flow to return to UF. We also included Froude descriptions of flow

as characterized by the comparison of mean velocity to the speed of gravitational wave speed, or:

$$Fr = \frac{U_{\text{mean}}}{\sqrt{g \cdot y}} \quad (\text{Eqn. 1})$$

Where U_{mean} is the mean velocity, g is gravity, and y is flow depth. When flow has a Froude number larger than one, flow is supercritical. Flow is considered critical at a Froude number of 1.0, and typically unsteady. Flows less than one are subcritical flows. Supercritical flow is fast and thin flow; while subcritical flow is slower and deeper. Both kinds of flow can

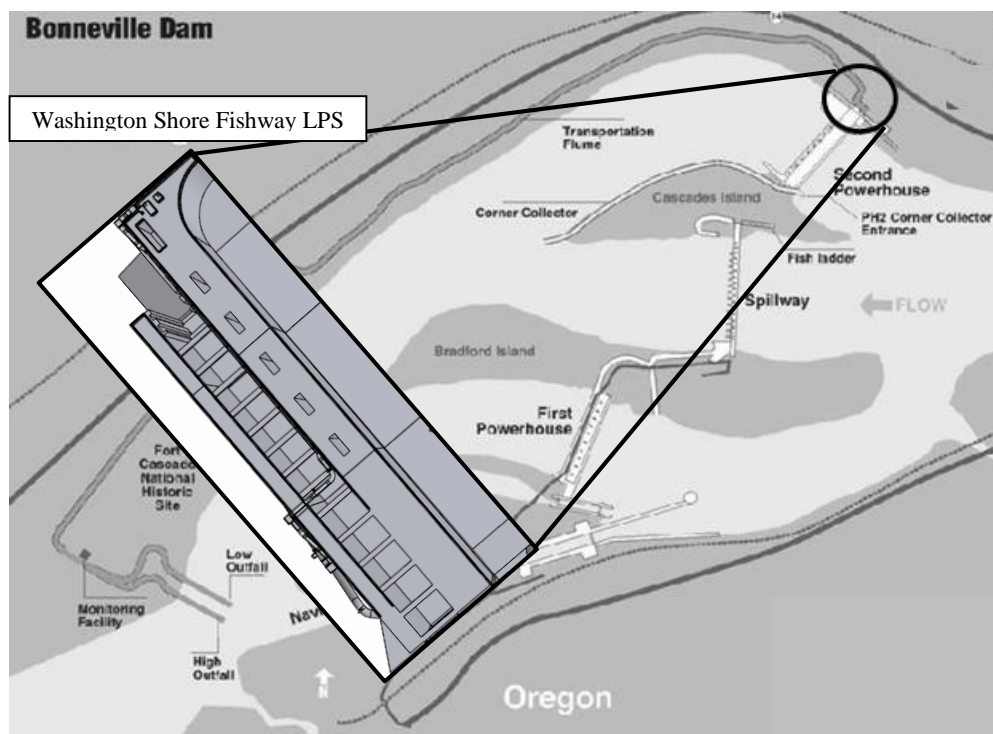


Figure 2.1 Bonneville Dam complex: Washington Shore LPS located on the Washington Shore fishway

exist in a cross section depending on slope for a given discharge.

For cases have not been documented, we determined a likely flow condition based on the slopes and structure of a feature. The flow condition of the features will be described by the water surface where: Gradually Varying Flow (GVF) is defined as flow that changes little over a distance, while Rapidly Varying Flow (RVF) changes quickly within a short

distance. If the structural feature is complex and the flow has not been documented, we will describe the condition as “unknown”.

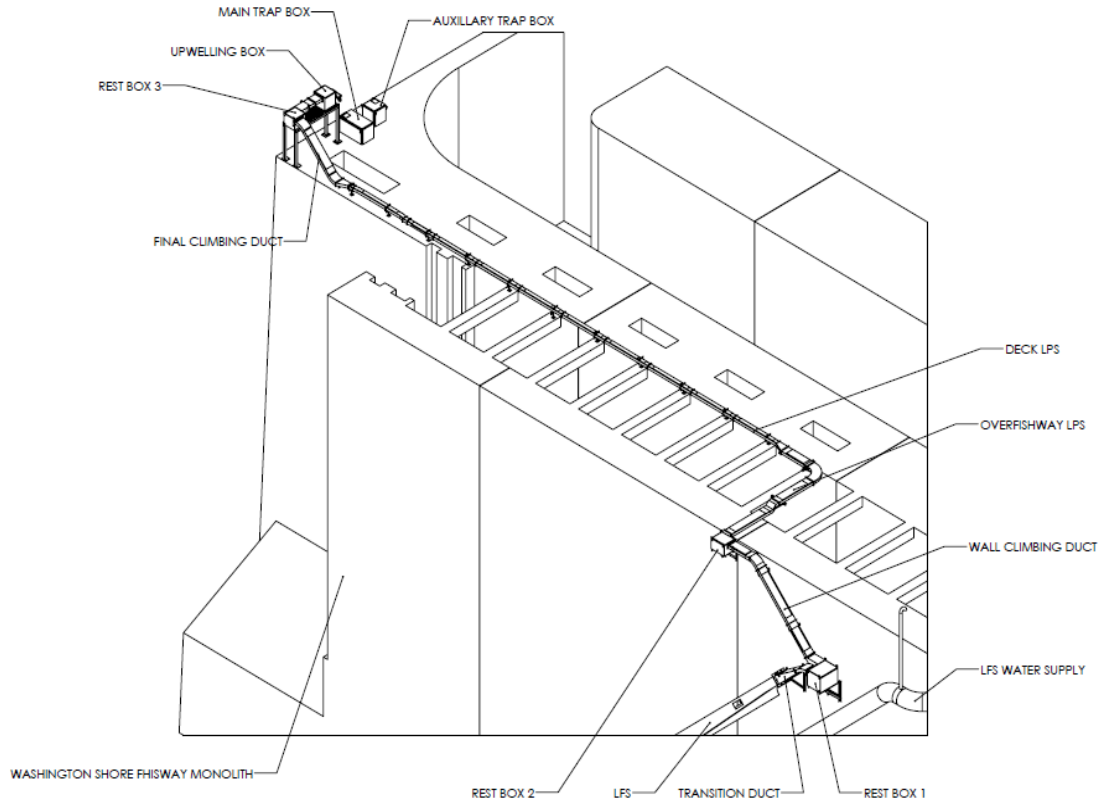


Figure 2.2 Schematic of LPS structure at Bonneville Dam Washington North Shore Fishway

4. Results

The flow conditions within the LPS are varied and sometimes complex. Flow within the duct work completes a series of transitions going through steady and unsteady phases depending on the structure. Along the wall climbing portion of the LPS the flow is generally very thin and fast starting at the end of the LFS at (Feature 1, Figure 2.3). The fish enter the first rest box through gradually varying flow coming over a crest. At the downstream opening of each rest box, the fish pass through a perforated fyke; which is designed to prevent fallback and attachment as the fish swim into the rest box (Feature not

shown, internal). The opening also serves as a weir that sets the flow depth within the channels. The resulting hydraulic interaction of the fyke with the weir is unknown.

The Flow conditions within a rest box are turbulent, but acceptable because velocities are low. The sheeting, supercritical flow on the climbing ducts collides with the subcritical flow within the rest boxes and develops a strong hydraulic jump. The fish pass through the hydraulic jump and into the climbing duct (Feature 3) where flows are supercritical and thin. The fish continue to climb through GVF at a second crest in Feature 4.

The flow will change from supercritical to subcritical as the slope decreases (Feature 3 to Feature 4). The fish now enter the second rest box through the downstream opening (Feature 5) and encounter markedly different conditions than rest box 1 (Feature 2). The fish pass through a similar fyke weir to rest box 1 when entering rest box 2. Here the flow is smoother, and nearly steady. The entrance flow is slower, and has only a few inches of descent over a small crest into the rest box. As a result, there is a very weak hydraulic jump that results in less turbulence within the rest box. Upstream of the second rest box begins the traversing section of the LPS.

From the second rest box, the fish will ascend a gradually sloped, wide traversing duct (Figure 2.4). The next hydraulic feature they encounter is the result of a step. Feature 6 was implemented in order to keep the slope in two conditions ($S=1.0$ or $S=0.0035$). In order to achieve the correct final elevation, we needed to rapidly gain height ($h \approx 20\text{cm}$) to maintain an overall traversing slope of ($S=0.0035$). Flow conditions within the step at Feature 6 will vary gradually through the crest and then rapidly at the end. There will be a

small hydraulic jump at the base of the step, the elevation of this height change is shown in (Feature 6, Figure 2.6). There will be unsteady flow at the top and bottom of the step similar to a riffle within a river.

The fish then continue through a region of gradually varying flow in the wide duct at the traversing slope ($b=50\text{cm}$, $S=0.0035$). The next feature the fish encounter is a wide radius, left hand turn (Feature 8, Figure 2.4). Flows within this turn are unsteady, and have secondary currents. The flow remains subcritical, and there is the possibility of an eddy on the inside corner as the fish approach the turn. Once the fish are through the corner, they approach a complex section where flow is transitioning from narrow traversing duct ($b=23\text{cm}$) to wide traversing duct ($b=50\text{cm}$), and goes through an expansion at Feature 9. Flow rapidly varies, has an eddy, and secondary flows.

The fish continue within the narrow traversing ductwork of the LPS ($b=23\text{cm}$) for approximately 30m (Feature 10, Figure 2.7). Flow conditions within this section are fully developed steady, subcritical, uniform flow except near the ends. At either end the flow is transitioning from wide ductwork ($b=50\text{cm}$) to narrow ductwork ($b=23$) or vice versa. Toward the end of this section, flow becomes unsteady as it passes through the transition. The next region of the LPS is the most complex and is called the terminating section. First the fish encounter a jog that goes around equipment on the deck. The flow is unsteady, has secondary flows, and eddies (Figure 2.5, Feature 11). The fish move through a complex feature where they encounter a hydraulic jump and a contraction (Figure 2.5, Feature 12). The hydraulic conditions are unknown, but likely turbulent with secondary flows. The fish enter the final climbing duct where the supercritical flows are similar to the previous climbs (Figure 2.8a, Feature 13). Finally, the lamprey pass over a crest with gradually varying

flow, swim through the final fyke at the downstream entrance, and end in the final rest box, where flow is steady and subcritical (Figure 2.8b, Feature 14).

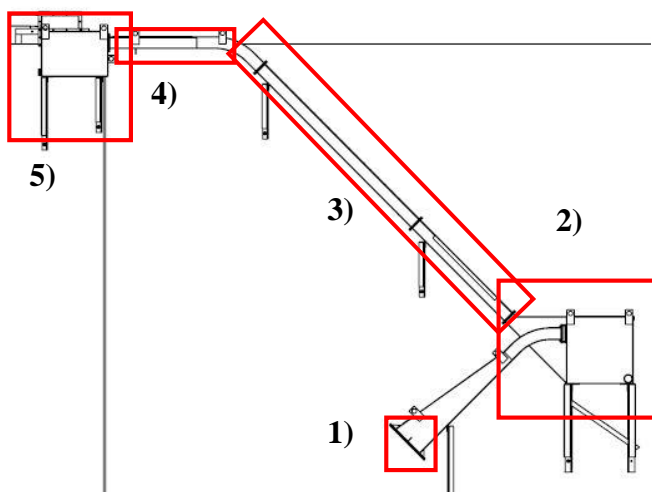


Figure 2.3: Elevation view of climbing duct LPS 1) Attaches to the Lamprey Flume Structure. 2) First rest box and 180 degree turn. 3) Climbing duct section: width is 50cm, depth 15cm, 4) transition to a rest box. 5) Second rest box

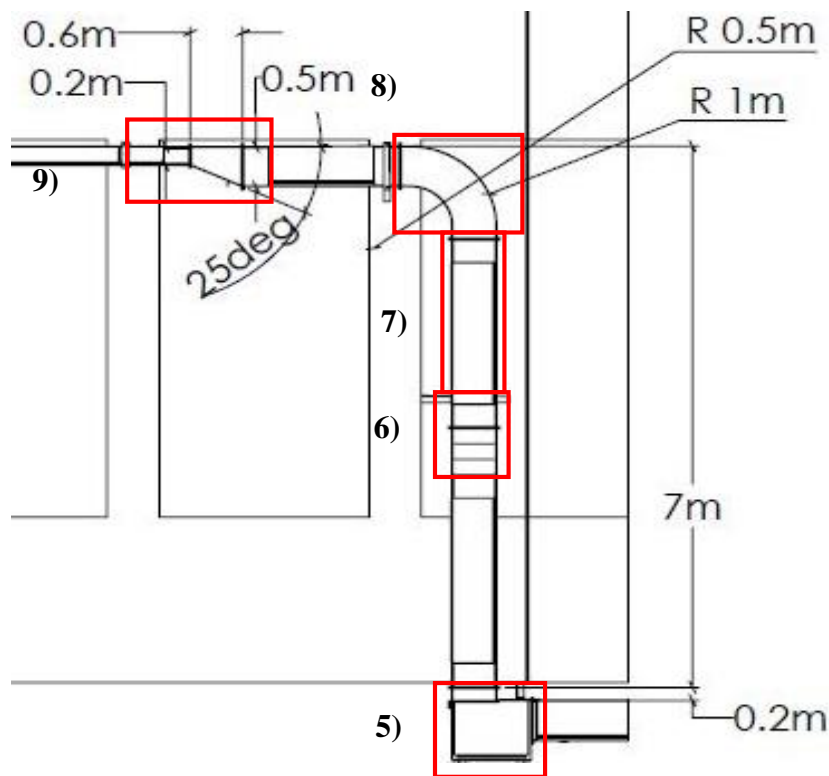


Figure 2.4: Plan view of traversing ductwork over the fishway. 5) Second rest box 6) Step 7) Traversing duct, width 50 cm 8) 90 degree corner 9) Expansion from narrow duct, width 20cm, to wide traversing duct

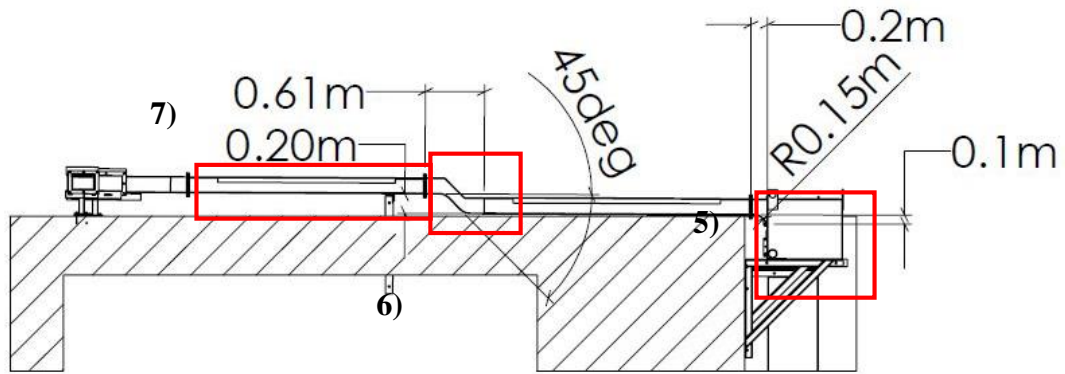


Figure 2.6 Elevation view of traversing duct.

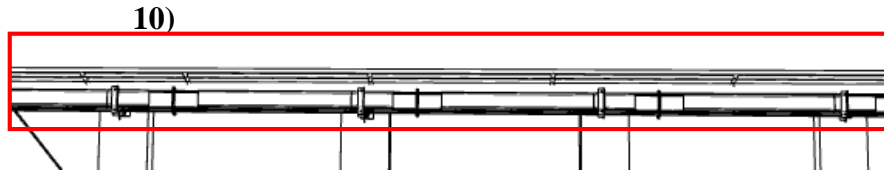


Figure 2.7: Plan view of traversing section in long straightaway

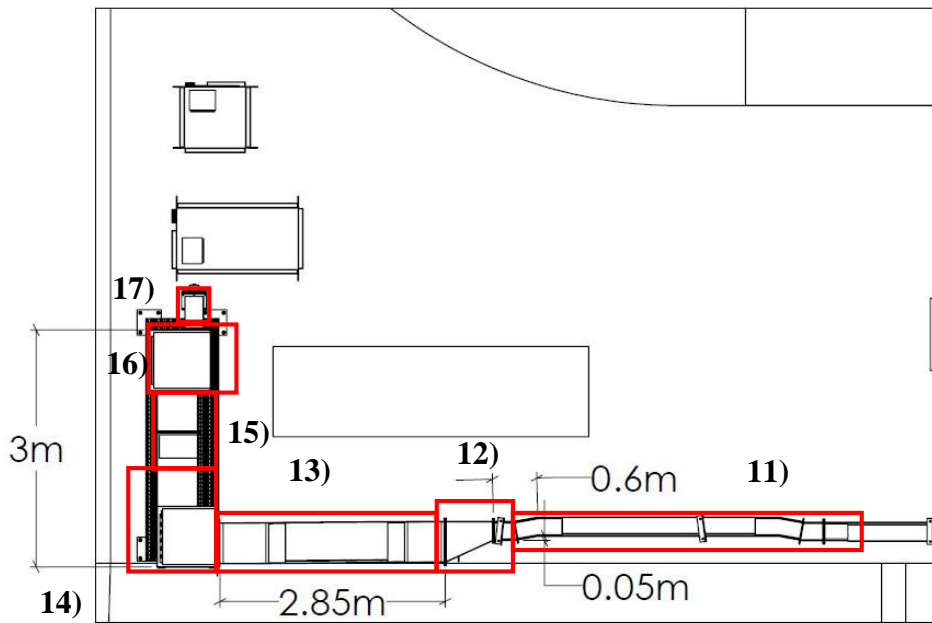


Figure 2.5: Plan view of the LPS finale. 11) Jogging duct, 12) Expansion, same dimensions as contraction, 13) Climbing duct 14) Final Rest Box 15) Upwelling box Entrance 16) Upwelling Box 17) Upwelling box exit

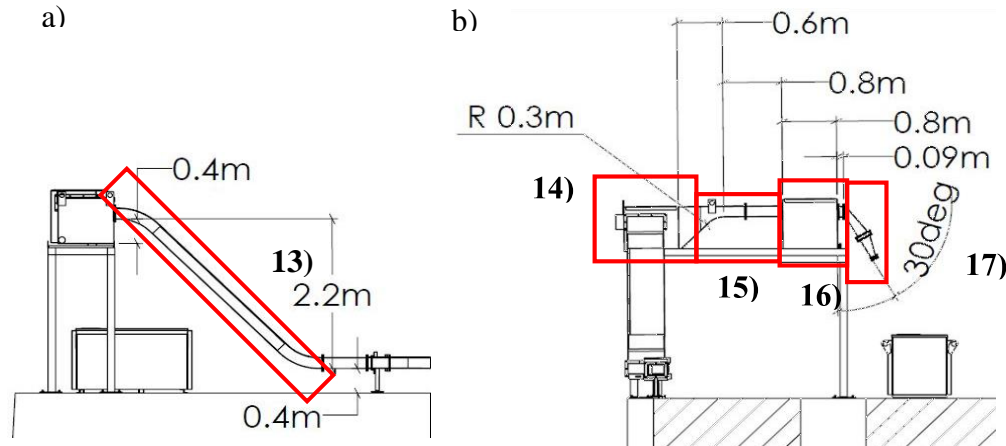


Figure 2.8: a) Elevation of LPS platform section b) End view of LPS platform section

This rest box functions as a direction change and slope transition in preparation for the straightaway needed for the exit. The path passes the fish through a small hydraulic jump, above which gradually varying flow descends over a radius (Figure 2.8b, Feature 15). The fish will swim into the upwelling box (Figure 2.8b, Feature 16) where the flow slows down to a minimal velocity, and then flows out the opposite end of the box. The design goal was to have the fish enter with sufficient velocity and inertia to pass through and out of the box before they notice the flow direction change. The fish begin to exit in a jet of rapidly varying flow once they pass the midline of Feature 16. The fish finally descend rapidly through the exit in a chute Feature 17 and into the trap boxes. Flow conditions within the upwelling box are unknown, but include jetting water out of the exit that may affect the exit hydraulics. The flow conditions within the exit chute should be uniform, supercritical, sheeting flow once it is fully developed. All features are compiled with the description of the hydraulic condition in (Table 2.1).

The design guidelines were based on conversations with Mary Moser throughout the project (Table 2.2). Critical design decisions were based on precedent at previous LPS

systems. Because of the complexity in retrofitting a fishway, we ultimately implemented several features that had never been tested including: the step (Feature 7), the contracting hydraulic jump (Feature 13), and the upwelling box (Feature 16).

Table 2.1: Catalog of hydraulic conditions

Feature #	Flow Depth	Water Surface	Description	Width	Hydraulic Description
1	≈0.004m	UF	Spillway	0.6m	Supercritical flow, sheeting
2	Varies≈0.6m	RVF	Pool	1.2m	Strong Hydraulic Jump
3	0.004m	UF	Spillway	0.5m	Supercritical flow, sheeting
4	Varies	GVF	Channel	0.5m	Subcritical flow
5	Varies≈0.4m	RVF	Pool	0.8m	Weak Hydraulic Jump
6	Varies	RVF	Spillway	0.5m	Supercritical flow, hydraulic jump
7	0.04m	UF	Channel	0.5m	Subcritical flow
8	Varies	RVF	90 Corner	0.5m	Secondary flow
9	Varies	RVF	Expansion	Varies	Subcritical flow, secondary flow
10	0.1m	UF	Channel	23cm	Subcritical flow
11	0.04m	RVF	Channel	23cm	Subcritical flow
12	Varies	RVF	Contraction	Varies	Unknown
13	≈0.004m	UF	Spillway	Varies	Strong Hydraulic Jump
14	Varies≈0.4m	RVF	Pool	0.5m	Supercritical flow
15	Varies	GVF	Spillway	1.5m	Gradually varying flow
16	Varies≈0.5m	RVF	Upwelling	0.5m	Unknown
17	≈0.004m	UF	Spillway	Varies	Supercritical flow

Table 2.2: Design guidelines for LPS systems

Traversing Duct Design Guidelines	
Traversing Slope	0.0035
Mean Velocity Traversing	0.4m/s
Duct width	19-50cm
Turning ductwork	50cm
Turning radius	50cm
Contraction Ratio	0.3
Max length without rest box	>60m
Climbing Duct Design Guidelines	
Climbing Slope	1.0
Mean Velocity Climbing	3.0 m/s
Fyke Opening	15 cm
Turning	None
Contraction	None
Rest Box Volume	Depends on spillway length
Average Rest Box Volume	0.2 m ³
Max Δ Height between Rest Boxes	<4m
Exit Duct Design Guidelines	
Chute Slope	1.13
Chute Surface	>40% porosity & 3/16" Dia. Holes
Discharge Flow	0.3-0.6 L/sec
Fish storage density	50% by volume

5. Discussion and Recommendations

We catalogued the anticipated features of LPS flow. The traversing duct generally has uniform, subcritical flow. The climbing duct always has uniform supercritical flow. Hydraulic jumps occur in all the rest boxes and upwelling box. Flow will rapidly vary because of the change from supercritical to subcritical flow. Features with the most complexity include the contraction (Feature 12), and the upwelling box (Feature 16). The contraction will likely be very turbulent and could be a barrier to fish passage. Flow within the upwelling box is more complex than other features and includes upwelling flows, gradually varying flows, and rapidly varying flows that exit as a jet into the exit chute.

The hydraulic conditions were not directly observed in most cases. Flow descriptions are qualitative, and meant to outline specific features that may need further investigation. One feature that seems significant is the combination of a hydraulic jump and contraction (Feature 12). The Pacific lamprey will likely encounter high turbulence and mean velocities in this feature. The other feature with the most complexity, the upwelling box (Feature 16), has low velocities, but multiple hydraulic conditions that could affect fish passage into the traps. Future research should carefully document the hydraulic conditions of the LPS structural feature including flow depth, width, and discharge.

6. Acknowledgements

Work supported by the United States Army Corp of Engineers, Portland office
The author acknowledges the guidance and support of Christopher Caudill, Matthew Keefer, and Ralph Budwig, and Mary Moser

7. References

- Barret, J. and M. Mallen-Cooper. 2006. The Murray River's 'Sea to Hume Dam' fish passage program: Progress to date and lessons learned, *Ecological Management & Restoration*, 7:3 173-183
- Beamish, R.J. 1980. Adult biology of the river lamprey (*Lampetra ayresi*) and the Pacific lamprey (*Lampetra tridentata*) from the Pacific coast of Canada. *Can. J. Fish Aquat. Sci.* 37:1906-1923
- Beck, L.M. 1995. Fish Behavior at Submerged Orifices, Overflow Weirs, and Vertical Slots in the Fish Ladder at Bonneville Second Powerhouse 1993-1994, Report of Research for U.S. Army Corp of Engineers
- Chow, V. T., 1959. *Open Channel Hydraulics*, 3-16, 201-203
- Clabough, T., M.L. Keefer, C.C. Caudill, E.L. Johnson, & C.A. Peery. 2012. Use of Night Video to Enumerate Adult Pacific Lamprey Passage at Hydroelectric Dams: Challenges and Opportunities to Improve Escapement Estimates, *North American Journal of Fisheries Management*, 32:4, 687-695, DOI:10.1080/02755947.2012.690820

- Clemens, B.J., M.G. Mesa, R.J. Magie, D.A. Young, C.B. Schreck. 2012. Pre-spawning migration of adult Pacific lamprey, *Entosphenus tridentatus*, in the Willamette River, Oregon, U.S.A. *Environ Biol Fish*, 93:245-254, doi10.1007/s10641-011-9910-3
- Close, D.A., M. S. Fitzpatrick, & H. W. Li. 2002. The Ecological and Cultural Importance of a Species at Risk of extinction, Pacific Lamprey, *Fisheries*, 27:7, 19-25, DOI:10.1577/1548-8446(2002)027<0019:TEACIO>2.0.CO;2
- “Columbia River Fish Accords Salmon Restoration, Salmon Protection.” 2013. *Columbia River Inter-Tribal Fish Commission*. Accessed July 31. <http://www.critfc.org/fish-and-watersheds/fish-and-habitat-restoration/columbia-basin-fish-accords/>
- Hard, A., B. Kynard. 1997. Video evaluation of passage efficiency of American Shad and Sea Lamprey in a modified Ice Harbor fishway, *North American Journal of Fisheries Management*, 17:4, 981-987, DOI:10.1577/1548-8675(1997)017<0981:VEOPEO>2.3.CO;2
- Katopodis, C. 2005. Developing a toolkit for fish passage, ecological flow management and fish habitat works, *Journal of Hydraulic Research*, 43:5, 451-467, DOI: 10.1080/0221680509500144
- Kemp, P.S., T. Tsuzaki, & M.L. Moser. 2009. Linking behavior and performance: intermittent locomotion in a climbing fish, *Journal of Zoology*, 277: 171-178
- Keefer, M. L., M.L. Moser, C.T. Boggs, W.R. Daigle, & C.A. Peery. 2009. Effects of Body Size and River Environment on the Upstream Migration of Adult Pacific Lampreys. *North American Journal of Fisheries Management*, 29:5, 1214-1224, DOI: 10.1577/M08-239
- Keefer, Matthew L., William R. Daigle, Christopher A Peery, Howard T. Pennington, Steven R. Lee, and Mary L. Moser. 2011. Testing Adult Pacific Lamprey Performance at Structural Challenges in Fishways. *North American Journal of Fisheries Management* 30:2, 376-385
- Mesa, M.G., J.M. Bayer, and J.G. Seelye. 2003. Swimming Performance and Physiological Responses to Exhaustive Exercise in Radio-Tagged and Untagged Pacific Lamprey, *Transactions of the American Fisheries Society*, 132:3, 483-492
- Monk, B., D. Weaver, C. Thompson, F. Ossiander. 1989. Effects of Flow and Weir Design on the Passage Behavior of American Shad and Salmonids in an Experimental Fish Ladder, *North American Journal of Fisheries Management* 9:60-67
- Moser, M.L., D.A. Close. 2003. Assessing Pacific Lamprey Status in the Columbia River Basin, *Northwest Science*, 77:2, 116-125

- Moser, M.L., D.A. Ogden, B.J. Burke, & C.A. Peery. 2005. Evaluation of a Lamprey Collector in the Bradford Island Makeup Water Channel, Bonneville Dam, 2003. Report of research to U.S. Army Corps of Engineers Portland Oregon.
- Moser, M.L., & D.A. Ogden, H. T. Pennington, W.R. Daigle & C.A. Peery. 2008. Development of Passage Structures for Adult Pacific Lamprey at Bonneville Dam, 2005. Report of Research to U.S. Army Corp of Engineers Portland Oregon
- Moser, M.L., M.L. Keefer, H.T. Pennington, D.A. Ogden, and J.E. Simonsen. 2011. Development of Pacific lamprey fishways at a hydropower dam. *Fisheries Management and Ecology* 18: 190-200
- Monk, B., D. Weaver, C. Thompson, F. Ossiander. 1989. Effects of Flow and Weir Design on the Passage Behavior of American Shad and Salmonids in an Experimental Fish Ladder, *North American Journal of Fisheries Management* 9:60-67
- Perkins, L.Z. & P.M. Smith. 1973. Modification of fish ladders Bonneville Dam, Columbia River Oregon and Washington Hydraulic Model Investigation, Technical Report No 141-1 for U.S. Army Corp of Engineers Portland Oregon
- Reinhardt, U.G., L. Eidietis, S.E. Friedl, and M.L. Moser. 2008. Pacific lamprey climbing behavior. *Canadian Journal of Zoology* 86: 1264-1272
- Quintella, B.R., N.O. Andrade, A. Koed, & P.R. Ameida. 2004. Behavioural patterns of sea lampreys' spawning migration through difficult passage areas studied by electromyogram telemetry, *Journal of Fish Biology*, 65: 961-972
- Schilt, C.R. 2006. Developing fish passage and protection at hydropower dams, *Applied Animal Behaviour Science*, 104:295-325
- Williams, J.G., G. Armstrong, C. Katapodis, M. Larinier, & F. Travade. 2012. Thinking like a fish: a key ingredient for development of effective fish passage facilities at river obstructions. *River Research and Applications*, 28:4, 407-417.
- Zobott, H. R. Budwig, C. Caudill. 2013. Pacific Lamprey Passage Structures at Bonneville Dam: Hydraulic Modeling, Cataloging Qualitative Design Criteria and Hydraulic Conditions, and Integrating Information from Diverse Information Sources to Create a Fish Passage Wiki (Master's thesis). University of Idaho, Moscow ID

CHAPTER THREE: HYDRAULIC MODELING OF CHANNELS IN PACIFIC LAMPREY PASSAGE STRUCTURES

Hattie Zobott¹, Ralph Budwig¹, Chris Caudill²

¹Center for Ecohydraulics Research

University of Idaho, Boise, ID

²Department of Fish and Wildlife Sciences

University of Idaho, Moscow, ID, 83844-1136

1. Abstract

Lamprey passage has become an important issue in the Pacific Northwest with declining numbers of migrating Pacific Lamprey (*Entosphenus tridentatus*) returning to the Columbia River. Here, I outline the materials, assembly methods, and the resulting hydraulic conditions for fully developed, uniform flow of a typical Lamprey Passage Structure (LPS) at Bonneville Dam, the first of up to nine dams Pacific lamprey encounter during upstream spawning migration. The LPS systems are installed where Pacific lamprey exhibit milling behavior. The entrance is placed on the wall and bottom of the fishway. Pacific lamprey enter voluntarily. Pacific Lamprey then climb the steep smooth surfaces of the LPS to bypass historic fishways designed for salmonids. The design of a LPS exploits the unique climbing behavior of Pacific lamprey to selectively route the fish through a series of climbing and traversing ductwork to route the fish over the fishway. The LPS hydraulic model is based off of reported operating conditions to establish the effective roughness range for operation (Moser et al. 2011, Reinhardt et al. 2008). Here, we determined an effective roughness for modeling the hydraulics within the LPS systems. We also created operating curves for a typical LPS system relating flow depth and mean velocity to

discharge. These values can be used for design of similar structures for Pacific lamprey at other locations.

2. Introduction

The hydraulic requirements for Salmon (*Oncorhynchus* spp) are relatively well understood with research spanning several decades (Monk et al. 1989, Johnson & Perkins 1968, Perkins & Smith 1973, and references therein). Conversely, Pacific lamprey research was limited prior to 2008 as the fish were perceived by western cultures as insignificant economically within the Columbia River basin, but remained an important resource to native cultures (Close et al. 2002, Moser & Close 2003). One technical report identified Pacific lamprey as “trash fish” (Perkins & Smith 1973).

Moser et al.’s (2002) telemetry study was a key step in assessing the decline through radiotelemetry studies that identified bottlenecks within the fishways and established the need for alternative routing (2002b). Development of fishway bypass systems known as Lamprey Passage Structures (LPS) enabled Pacific lamprey to bypass difficult sections within the fishway (Moser et al. 2011, Moser et al. 2005, and Moser et al. 2006). The LPS systems capitalize on the natural climbing behavior observed at natural migration barriers like Willamette falls.

The analogue to the LPS system is the ascent of waterfalls by Pacific lamprey at a natural barrier. One population, the Pacific lamprey in the Willamette River, is the only remaining harvestable population in the Columbia River Basin. During the Willamette River migration, Pacific lamprey climb over 12 meters, sometimes vertically, to pass Willamette Falls and reach spawning grounds (Clemens 2012). Lampreys may migrate as

far as 482 rkm before spawning (Clemens 2012). Conversely, approximately half of Pacific lamprey approaching each of four dams in the lower Columbia River pass and those passing upstream are larger on average at a comparable distance of 429rkm (Keefer et al. 2009). Telemetry and video studies of lamprey indicate that they have difficulty migrating upstream at barriers along the Columbia River (Beck 1995, Moser et al. 2002b, Clabough et al. 2012, Hard & Kynard 1997). The goal of the LPS systems is to provide a nature-like pathway to bypass otherwise impassable barriers in the Columbia River basin for Pacific lamprey.

The hydraulics of natural barriers is complex. Where Pacific lamprey pass and why is determined by many parameters including the hydraulics. In rivers and fishways, Pacific lamprey swim up to a critical swim speed and then attach to the substrate with their oral sucker. The fish will then burst and re-attach in a saltatory swim behavior. The fish cannot attach to certain substrate within fishways with uneven or porous surfaces like metal grating (Keefer et al. 2011b). Research results indicate that lamprey also avoid shear flows when migrating (Keefer et al. 2011b). One observed behavior indicating that the fish have encountered a hydraulically limiting feature is that the fish tend to congregate and mill prior to passage. The fish will also tend to orient to the bottom and sides of the fishway (Beck 1995, Hard & Kynard 1997, Keefer et al. 2010, Keefer et al. 2011b). Different hydraulics will enact different pressures on the fish, which will in turn determine the fish's locomotion and behavior.

Exactly when the fish begin to saltatory swim is a result of the critical swim speed of that individual. The results in laboratory settings estimated the critical swim speed of adult Pacific lamprey at approximately $0.8 \text{ m}\cdot\text{s}^{-1}$ for an average body length of 65.8 cm or 1.3

$\text{BL}\cdot\text{s}^{-1}$ (Mesa et al. 2003). Within an experimental fishway the results are similar, with critical swim speeds around $0.8 \text{ m}\cdot\text{s}^{-1}$ and maximum burst swimming between ($2.5\text{-}3.0 \text{ m}\cdot\text{s}^{-1}$) for Pacific Lamprey (Keefer et al. 2011b). Research on the similar, but larger sea lamprey are consistent with this research indicating that Sea lamprey migration can be mitigated with velocities exceeding $3.75 \text{ m}\cdot\text{s}^{-1}$ (Hunn and Young 1980). Although, some of the fish can attach to surfaces with their oral disc and hold position in current up to $3.9 \text{ m}\cdot\text{s}^{-1}$ (Hunn and Young 1980).

Once fish reach the critical swim velocity, they switch to saltatory swimming. The sea lamprey will increase saltatory swimming at difficult migration features by increasing the number of burst movements, but not increasing the burst length (Quintella et al. 2004). Similar behavior was observed within the fishways where Pacific lamprey sought refuge in lower velocity areas within the fishways, such as the Auxiliary Water Supply (AWS) channels that are inaccessible to other fish species (Johnson et al. 2009). The combination of milling, saltatory swimming, and refuge seeking behavior is evidence that Pacific lamprey experience difficulty ascending fishways along the Columbia River, which were designed for Salmonids and American Shad (Monk et al. 1989). Refuging, milling, and failed passage also highlights potential hydraulic limits on Pacific lamprey passage in fishways (Moser et al. 2002a, Moser et al. 2002b, Keefer et al. 2010, and Johnson et al. 2012). The trends of the research indicate that all Pacific lamprey experience some difficulty when migrating through fishways along the Columbia River (Keefer et al. 2013a). Ultimately, size may determine upriver migration distance because adults recorded upstream were larger than average when tagged near the beginning of upstream migration (Keefer et al. 2009).

The large size variation of adult migrating lamprey may impact the application of fishway modifications for Pacific lamprey. Adult migration length of Pacific lamprey can vary from 16cm to 76 cm (Beamish 1980). Smaller fish have lower velocity thresholds and often suffer passage difficulties at dams designed for salmonids (Haro et al. 2004, Mallen-Cooper & Brand 2007, and Barret & Mallen-Cooper 2006). The fish trapped for testing in these LPS systems are typically large and have lengths > 60cm (Moser et al. 2006, Moser et al. 2008, and Moser et al. 2011). It is unclear if the population averaged velocity barrier may be lower for the average migrating lamprey of a given year. Evidence the fish encountering a hydraulic barrier in the fishways is demonstrated by the effective passage rate of 49% for Pacific lamprey at Bonneville dam compared with >90% passage efficiency of salmonids (Caudill et al. 2007, Keefer et al. 2013a). Kemp observed that the climbing behavior for a given population is highly variable between individuals (2009).

Pacific lamprey use these novel structures at Bonneville Dam. The first LPS systems were installed in the Bradford Island Makeup Water Channel, an area near the top of the ladder used for hydraulic control which salmon cannot access. Pacific lamprey were observed to congregate in this area without any migration route beyond it. Moser et al. (2003) implemented a test system to determine orientation and location of the climbing ducts that access the LPS systems. Additional systems were implemented in other areas with lamprey congregations at Cascade Island and the Washington Shore AWS (Moser et al. 2011). A more complex collection system was developed and implemented this spring at Bonneville Dam North Shore Fishway entrance and is called the Lamprey Flume System. The structure we used as a case study for our research routes the Pacific lamprey from the LFS to the trap boxes on the fishway deck.

The LPS structures rely on Pacific lamprey climbing specialized rectangular ductwork with steep slopes and supercritical-sheeting flows. Success of the structures was highly dependent on location of the entrances and were most effective when placed in areas observed to have Pacific lamprey congregated (Moser et al. 2005, Moser et al. 2006, Moser et al. 2008, and Moser et al. 2011). Hydraulic conditions have not been extensively studied, although Pacific lamprey climbing observed in laboratory settings suggest that they can climb a range of slopes and discharges (Reinhardt et al. 2008, Kemp et al. 2009, and Keefer et al. 2011).

When the fish find and enter the LPS, they are relatively successful compared to the fishways at Bonneville Dam. LPS systems typically have passage rates >90% for Pacific lamprey (Moser et al. 2006, Moser et al. 2008, Moser et al. 2011). The rate of use increases over time. In 2006 Approximately 21% of the Pacific lamprey used the LPS system at Bradford Island (Moser et al). By 2008, approximately 40% of the migrating population at Bonneville dam used an LPS system to pass. The highest passage efficiency was at the Washington Shore AWS LPS with 100% passing using the LPS system (Moser et al. 2011). The systems have significantly higher passage rates than the fishways where only 40% of the Pacific lamprey pass the dam (Moser et al. 2011).

The systems are unique and use aluminum to form ductwork that route the fish from areas in the fishway that the Pacific lamprey congregate. The key parameters affecting hydraulic conditions in the LPS system are duct slope, surface roughness, and channel shape. Surface roughness describes the height of protrusions into the flow. The ratio of roughness to flow depth determines if the flow is hydraulically smooth, in the transitional roughness regime, or fully rough flow (Nezu & Nakagawa 1993). Very small roughness

ratios result in hydraulically smooth flow. Hydraulically smooth flow has a velocity profile that develops more gradually, and the maximum velocity near the surface (Nezu & Nakagawa 1993). Hydraulically rough flow has a maximum velocity closer to the bottom (Chow 1959). Slope describes the ratio of rise per length and determines gravitational influence. Flow depth decreases and velocity increases with increasing slope for a given discharge. Channel shape affects secondary flows and acts as an additional form of flow resistance similar to roughness. The resulting hydraulic conditions of flow depth and velocity vary depending on these parameters.

Previous research focused on the behavior of the fish exhibited during climbing and evaluated a range of slope and discharge conditions that provided adequate conditions to induce climbing behavior and passage of LPS structures. However, the hydraulic conditions of the structures were not characterized in previous studies. Our research was interested in developing a 1D model of the hydraulic conditions within the LPS for design and operating purposes. We investigated 1) an appropriate roughness value to use in modeling the hydraulic conditions of LPS systems 2) and operational curves for the LPS systems relating flow depth to discharge. The resulting curves will help future designers and operators develop, implement and operate these structures for Pacific lamprey passage at Bonneville Dam and other locations.

3. Methods

3.1 Apparatus

The Lamprey Passage Structures (LPS) used for this analysis were the Cascade Island LPS previously implemented at Bonneville Dam (Moser et al. 2005, Moser et al. 2006, Moser et al. 2008, and Moser et al. 2011) and the Washington North Shore fishway

LPS designed and installed during 2013 (Zobott et al. 2013). Each LPS has a series of climbing ducts with rest boxes for the ascent, and a combination of varying width ducts for the traversing sections (Figure 3.1). All ductwork was 15cm deep.

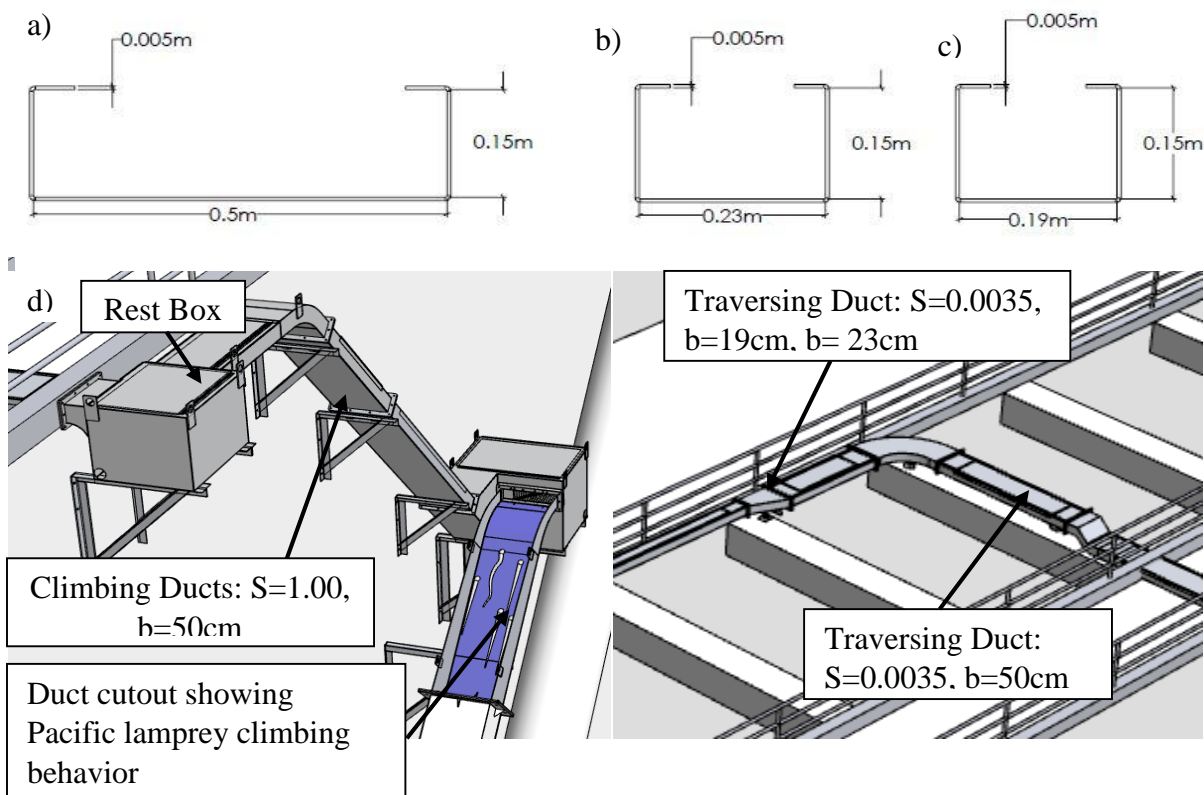


Figure 3.1: Geometry of LPS ductwork. Dimensions to outside of duct. Interior dimensions used in calculations a) Climbing duct cross section with Slope= 1. b) Traversing duct cross section with Slope= 0.0035 at Washington Shore Fishway LPS c) Traversing duct of Cascade Island, Bradford Island and Washington Shore AWS LPS systems with Slope=0.0035 d) LPS schematic

The duct widths for the Washington North Shore fishway LPS were: 23cm and 50cm for traversing duct. The climbing duct width is 50cm (Figure 3.1). The Cascade Island LPS traversing duct widths differed slightly, and were either 19cm, or 50cm.

The material used for the Washington Shore Fishway LPS was 4.8mm (3/16”), 5051 H32 Aluminum plate that was then formed with no radius interior bends. The Washington North Shore Fishway LPS also had a protective film covering the surfaces during manufacturing and was removed just prior to installation. There was no further surface

treatment prior to use in any system. The angle of the climbing duct was 45° (slope=1), and the angle of the horizontal duct was 0.2° (slope=0.0035). We also investigated climbing duct with a width of 50cm and at an angle of 18° (slope=0.325), as it was also reported in literature (Moser et al. 2006, Reinhardt et al. 2008, Moser et al. 2011).

The ductwork assembly required that the climbing duct pieces were bolted together periodically with silicone sealant in the interface to maintain water tight seal. Any two pieces of climbing duct were to be aligned with one another within a tolerance of ± 1.6 mm, while the horizontal duct alignment was ± 3.8 mm. Excess silicone was wiped out, or trimmed flush if dried.

3.2 Methods

The hydraulic model is a fully developed, open channel flow model, based on the energy equation with the losses accounted for using the Darcy friction factor:

$$S_o = \frac{f \cdot U_{\text{mean}}^2}{D_h \cdot 2 \cdot g} \quad (\text{Eqn. 1})$$

Where S_o is the slope, or rise versus run, of the channel, f is the Darcy friction factor that quantifies head loss, U_{mean} is the depth averaged velocity, D_h is the hydraulic diameter, and g

$$D_h = 4 \cdot R_h \quad \text{where} \quad R_h = \frac{A}{P}; \quad P = 2y + b \quad A = y \cdot b \quad (\text{Eqn. 2})$$

is gravity. The depth of flow is y , b is the width of the channel, A is the cross sectional area of the flow, and P is the wetted perimeter of the flow. We based the above parameters on the Reynolds number and Froude number of the functioning LPS systems. The Reynolds number, Re , is representative of the relationship between viscous and inertial forces:

$$Re = \frac{\rho \cdot U_{\text{mean}} \cdot R_h}{\mu} \quad (\text{Eqn. 3})$$

Where ρ is the density of water assumed to be $992 \text{ kg}\cdot\text{m}^{-3}$ and μ is the viscosity of water and is $1.307 \times 10^{-3} \text{ kg}\cdot\text{sec}^{-1}\cdot\text{m}^{-1}$ at 10°C . The Froude number compares the speed of the flow with the gravitational wave velocity (Eqn. 4):

$$\text{Fr} = \frac{U_{\text{mean}}}{\sqrt{g \cdot y}} \quad (\text{Eqn. 4})$$

Flows with values larger than 1.0 are considered supercritical; which are thin and fast flows like the flow observed within the climbing duct of the LPS systems. Froude number values less than 1.0 describe subcritical flows of the nearly horizontal duct sections of the LPS systems.

We first assumed a hydraulically smooth surface due to the smooth aluminum surface of the duct pieces with surface roughness ($\epsilon=0.002\text{mm}$). The hydraulically smooth model resulted in unreasonable velocities as compared to the findings of suitable velocities for Pacific lamprey passage (Moser et al. 2011, Reinhardt et al. 2008, and Keefer et al. 2011a). We then used the reported depth and discharge of the Bradford Island LPS to determine a functional friction factor using (Eqn. 1) and the Reynolds number (Table 3.1) (Moser 2011). We used the Moody diagram to determine that the flow was on the edge of the transitional roughness regime using the determined friction factor, Reynolds number, roughness, and hydraulic diameter. Therefore, we implemented the Haaland correlation (Eqn. 5) (Kakac et al. 1987) to explicitly solve for the Darcy friction factor as a function of effective roughness, where ϵ is the effective roughness:

$$f = 4 \cdot \left[3.4735 - 1.5635 \cdot \ln \left[\left(2 \cdot \frac{\epsilon}{D_h} \right)^{1.11} + 63.635 \cdot \frac{\rho}{\mu \cdot D_h \cdot U_{\text{mean}}} \right] \right]^{-2} \quad (\text{Eqn. 5})$$

Now we could develop a function relating flow depth to mean velocity. We did this by combining 1, 2, &5, resulting in the following equation:

$$0 = 8 \cdot S_o \cdot \left(\frac{y \cdot b}{2 \cdot y + b} \right) \cdot g - 4 \cdot \left[3.4735 - 1.5635 \cdot \ln \left[2 \cdot \frac{\epsilon}{\left(\frac{4y \cdot b}{2 \cdot y + b} \right)} \right]^{1.11} + 63.635 \cdot \frac{\rho}{\mu \cdot \left(\frac{4y \cdot b}{2 \cdot y + b} \right) \cdot U_{\text{mean}}} \right]^{-2} U_{\text{mean}}^2 \quad (\text{Eqn. 6})$$

To create the operating curves we needed to relate discharge (Q) to flow depth (y). We did this by using the definition of discharge and rewriting (Eqn. 7) to solve for the mean velocity, U_{mean} :

$$Q = U_{\text{mean}} \cdot A \quad ; \quad U_{\text{mean}} = \frac{Q}{A} \quad (\text{Eqn. 7})$$

We then substituted substituted (Eqn. 7) into (Eqn. 6):

$$0 = 8 \cdot S_o \cdot \left(\frac{y \cdot b}{2 \cdot y + b} \right) \cdot g - 4 \cdot \left[3.4735 - 1.5635 \cdot \ln \left[2 \cdot \frac{\epsilon}{4 \left(\frac{y \cdot b}{2 \cdot y + b} \right)} \right]^{1.11} + 63.635 \cdot \frac{\rho}{4 \cdot \mu \left(\frac{y \cdot b}{2 \cdot y + b} \right) \cdot \frac{Q}{b \cdot y}} \right]^{-2} \frac{Q^2}{(b \cdot y)^2} \quad (\text{Eqn. 8})$$

Then, we used a root solver within a loop program to solve (Eqn. 8) for flow depth (y) resulting from each discharge value within the range of ($1 \text{ L} \cdot \text{s}^{-1} < Q < 100 \text{ L} \cdot \text{s}^{-1}$), with ($\Delta Q = 1 \text{ L} \cdot \text{s}^{-1}$). Using the flow depth, we could calculate the mean velocity of the flow. The resulting operating curves relate flow depth, discharge and mean velocity.

The climbing duct was more difficult to model. First we assumed the same roughness for the climbing duct as the traversing duct. The resulting mean velocities did not match those reported in Reinhardt et al. (2008). Reinhardt took the velocity measurements with a high speed camera and a dredge (2008). We assumed that the measurements were equal to the mean velocity because we knew flow depth would be very thin. With the given discharge (Q) and the mean velocity (U_{mean}) we could solve for area (A) using (Eqn. 7). Then using the given width, we solved for flow depth. We tried to determine the effective roughness for all reported values from Reinhardt's research. Unfortunately, only one

velocity value, discharge, and slope, converged to a reasonable effective roughness value ($U_{\text{mean}}= 3.07 \text{ m/s}$, $Q=7.8 \text{ L}\cdot\text{s}^{-1}$), and slope ($S=1.0$). The complete matrix of parameters investigated, and the calculation coding for the roughness value are available in Appendix A and B. The calculation coding for the climbing duct is in Appendix C; while the traversing duct calculations are in Appendix D.

4. Results

We originally determined two roughness values based on the reported values from literature (Moser et al. 2011, Reinhardt et al. 2008) (Table 3.1). The effective roughness value of ($\epsilon=11\text{mm}$) for the traversing duct was unreasonable given the smooth surfaces of the aluminum ductwork. We determined that the climbing effective roughness value of ($\epsilon=0.18\text{mm}$) was reasonable given the additional periodic roughness of assembly tolerances ($1.6 \text{ mm} < \epsilon < 3.8$) mm and the surface roughness value of aluminum ($\epsilon=0.002 \text{ mm}$). The effective roughness should not vary with the width or slope. We applied the resulting effective roughness value from Reinhardt et al. (2008) for both traversing and climbing ducts.

Table 3.1: Roughness Determination: for hydraulic modeling for discharge of $7.8 \text{ L}\cdot\text{s}^{-1}$ using the Haaland correlation to determine effective roughness

Reported values and resulting effective roughness									
b(m)	y (m)	$\alpha=b/y$	S (m/m)	V(m/s)	f	Re #	Fr #	$\epsilon(\text{mm})$	Source
0.19	0.10	2	0.0035	0.41	0.079	1.53E+04	0.4	11	Moser et al 2011
0.50	0.0044	114	1	3.07	0.041	1.40E+04	14.8	0.18	Reinhardt et al 2008

The low slope of the traversing ducts is necessary to maintain subcritical flow in the ductwork. Within the operating slope used in the Bonneville Dam LPSs of $S=0.0035$: the effective roughness value we used resulted in a mean velocity difference of 2-20% between varying duct widths (Table 3.2). Due to the difference between widths, we created unique

operating curves for each width (Figure 3.3). Increasing the width by $\approx 20\%$ results in very small differences in mean velocity (Figure 3.3b). The widest duct width investigated will have the smallest flow depths, and highest Froude numbers (Figure 3.3c). Flows will be subcritical in all traversing ducts. Velocity changes across varying widths are $(0.49 \text{ m}\cdot\text{s}^{-1} < U_{\text{mean}} < 0.61 \text{ m}\cdot\text{s}^{-1})$ (Table 3.2). We note that the depth changes are substantial between the two widths of traversing duct, and the traversing duct flow may become supercritical if the slope is greater than nominal in the widest duct width where, $b=50\text{cm}$.

Table 3.2: Comparison of ductwork parameters and resulting flow conditions for $Q=7.8\text{L}\cdot\text{s}^{-1}$, and $\varepsilon=0.18\text{mm}$. Climbing duct % change compared to nominal parameters in bold ($S=1.0$, $b=50\text{cm}$). Traversing duct compared to nominal parameters in bold ($S=0.0035$, $b=19\text{cm}$)

Ductwork Parameters	$\alpha=b/y$	y (m)	U_{mean} (m/s)	Fr	Re	%Change y	%Change U_{mean}	%Change Fr
Climbing S=1.0, b=50cm	100	0.005 0	3.12	14.09	1.17E +04	0	0	0
Climbing S=0.325, b=50cm	72	0.007 0	2.23	8.54	1.16E +04	-40	28	39
Traversing S=0.0035, b=19cm	2.8	0.067	0.61	0.76	1.84E +04	0	0	0
Traversing S=0.0035, b=23cm	4.1	0.057	0.60	0.80	1.74E +04	12	2	-6
Traversing S=0.0035, b=50cm	16	0.032	0.49	0.87	1.06E +04	42	21	-15

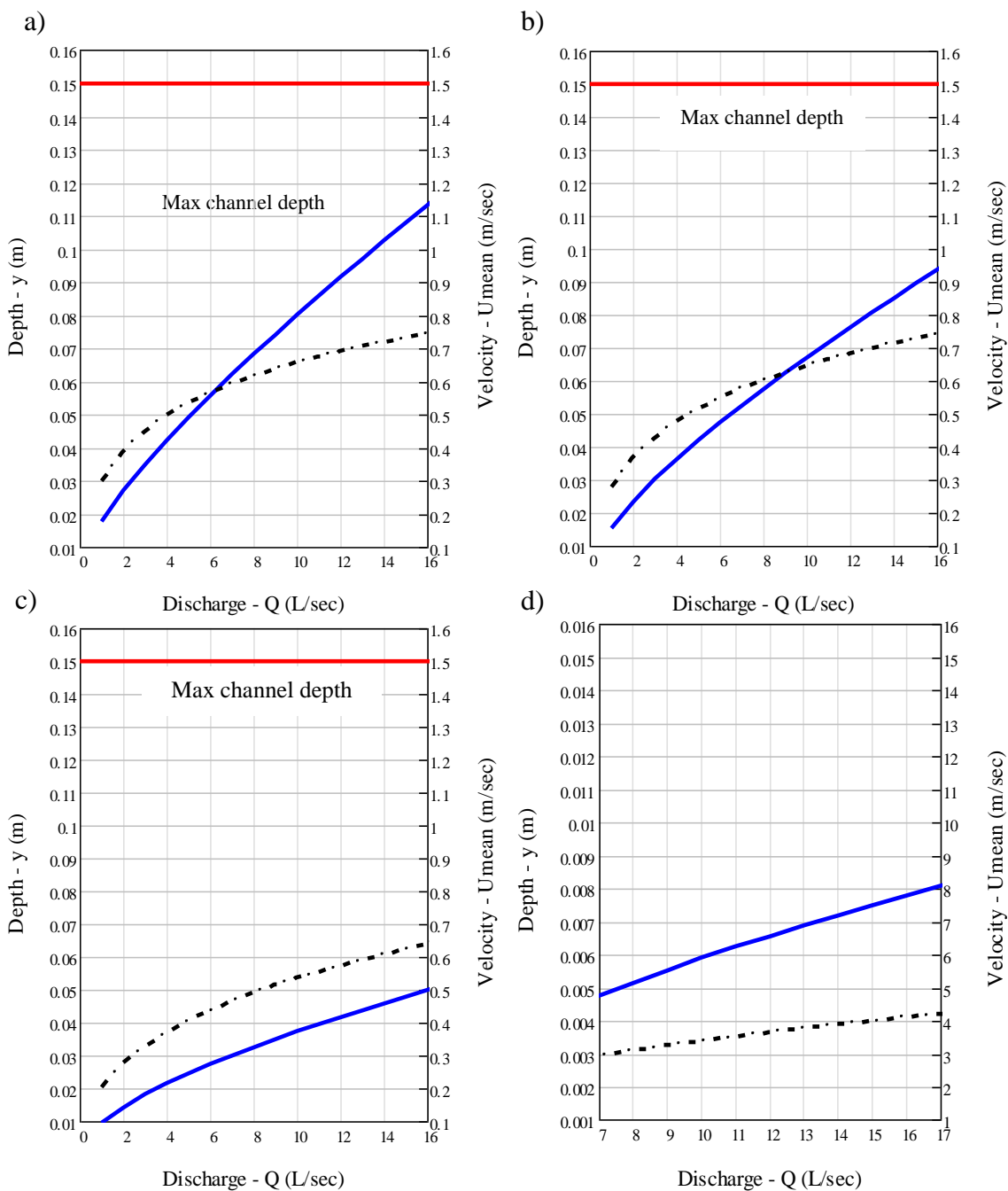


Figure 3.2: Operating Curves for LPS Ductwork: flow depth are shown with solid, blue lines, mean velocity shown with dashed, black lines for $\epsilon=0.18\text{mm}$; a) Cascade Island, Bradford Island and Washington Shore AWS LPS systems where width is 19cm b) Washington Shore Fishway LPS system where width is 23 cm c) Bradford Island, Cascade Island, & Washington Shore Fishway LPS where width is 50cm d) Climbing duct for all LPS systems: Slope=1.0, width is 50cm

When the slope increases beyond the critical slope, the flow condition changes from subcritical to supercritical for a given discharge. Critical slopes for the traversing duct widths at nominal discharge of $7.8 \text{ L}\cdot\text{s}^{-1}$ are summarized in (Table 3.3). The widest duct width will become supercritical at the lowest slope value for the nominal discharge. The narrowest duct will have the deepest depth, and the highest mean velocity at critical flow (Table 3.3). The widest width will have the lowest mean velocity at critical flow and the shallowest depth.

Table 3.3: Critical Flow Parameters for Ductwork: were critical flow occurs at Froude number=1.0 and $\varepsilon=0.18\text{mm}$ at a discharge of $Q=7.8\text{L}\cdot\text{s}^{-1}$

Critical Flow Parameters			
b(m)	y_c (m)	$U_{\text{mean},c}$ (m/sec)	S_c (m/m)
0.19	0.055	0.74	0.0047
0.23	0.049	0.69	0.0042
0.5	0.029	0.54	0.0037

Conversely, the climbing slope ($S=1.0$) results in supercritical flows regardless of the width or roughness for all functional discharges. We modeled the flow using the only convergent solution we developed from Reinhardt reported values, resulting in $\varepsilon=0.18\text{mm}$ at nominal discharges (2008). The results are significantly different from the traversing duct (Figure 3.2d). Flow depths are a factor of ten smaller, and velocities five times larger. The flow depth change from a 78% reduction in slope ($S=1.0$ to $S=0.325$), results in a 40% increase in depth (Table 3.2), but only a 28% decrease in velocity.

Table 3.4: Comparison of ductwork parameters and resulting flow conditions for $Q=7.8L\cdot s^{-1}$, and $\varepsilon=0.18mm$. Climbing duct % change compared to nominal parameters in bold ($S=1.0$, $b=50cm$). Traversing duct compared to nominal parameters in bold ($S=0.0035$, $b=19cm$)

Ductwork Parameters	$\alpha=b/y$	y (m)	U_{mean} (m/s)	Fr	Re	%Change y	%Change U_{mean}	%Change Fr
Climbing S=1.0, b=50cm	100	0.005 0	3.12	14.09	1.17E +04	0	0	0
Climbing S=0.325, b=50cm	72	0.007 0	2.23	8.54	1.16E +04	-40	28	39
Traversing S=0.0035, b=19cm	2.8	0.067	0.61	0.76	1.84E +04	0	0	0
Traversing S=0.0035, b=23cm	4.1	0.057	0.60	0.80	1.74E +04	12	2	-6
Traversing S=0.0035, b=50cm	16	0.032	0.49	0.87	1.06E +04	42	21	-15

5. Discussion and Recommendations

We developed an open channel hydraulic model for traversing ducts as well as climbing ducts of LPS systems installed at Bonneville Dam. During supercritical flow, the velocities are near or exceed the critical swim velocity of ($U=0.8 m\cdot s^{-1}$). Pacific lamprey would likely switch to saltatory swimming modes (burst swimming and oral attachment). If the flow depth is thin enough and slope steep enough they would begin climbing (Quintella et al. 2004, Reinhardt et al. 2008, and Keefer et al. 2013b). The difficulty of ascending supercritical flow increases as the flow depth increases because of the relationship to the drag force on the fish where:

$$F_{drag} = C_D \cdot \frac{1}{2} \rho \cdot U_{mean}^2 \cdot A_s \quad (\text{Eqn. 9})$$

A_s is the submerged cross section and a function of flow depth, V is the mean velocity, and C_D is the coefficient of drag.

The function above relates drag force to mean velocity and submerged area. The submerged area will vary with the size of the Pacific lamprey and water depth in the duct, but should be proportional based on the girth, or circumference of the fish for a given depth. We created a simple model of the drag force on a *fully submerged* lamprey by assuming that the shape of a lamprey is cylindrical. Assuming this simple shape is overly conservative as the true shape of lamprey is more hydrodynamic, but it allows us to relate lamprey size to drag force. We first solved for the cross sectional area as a function of girth by assuming the girth is equal to the circumference of a circle:

$$C = \pi D \quad ; \quad G = \pi D \quad ; \quad D = \frac{G}{\pi} \quad (\text{Eqn. 10})$$

Where D is the diameter, C is the circumference, and G is the girth of the fish.

The cross sectional, submerged area is therefore determined using the formula for the area of a circle and substituting (Eqn. 10) for the diameter:

$$A_s = \pi \cdot \left(\frac{D}{2}\right)^2 \quad ; \quad A_s = \frac{G^2}{4\pi} \quad (\text{Eqn. 11})$$

Finally, by substituting the resulting submerged area as a function of girth into (Eqn. 9), we create a model to relate lamprey size to drag force:

$$F_{\text{drag}} := C_D \cdot \frac{1}{2} \cdot \rho \cdot U_{\text{mean}}^2 \cdot \frac{G^2}{4\pi} \quad (\text{Eqn. 12})$$

Our simple model correlates drag force with the girth of the fish by assuming a similar shape between all sizes of adult Pacific lamprey. We then determined the resulting drag force acting on three girths: $G=8$ cm, $G=10$ cm, and $G=12$ cm (Figure 3.3). We can see that at a given velocity the drag force increases with increasing girth. The critical swim threshold is represented by the dashed lines and is assumed constant for all girths ($U_{crit}=0.8$ m·sec⁻¹). The velocity barrier is represented by dotted lines, and is also assumed constant for all girths ($U_{vb}=2.5$ m·sec⁻¹).

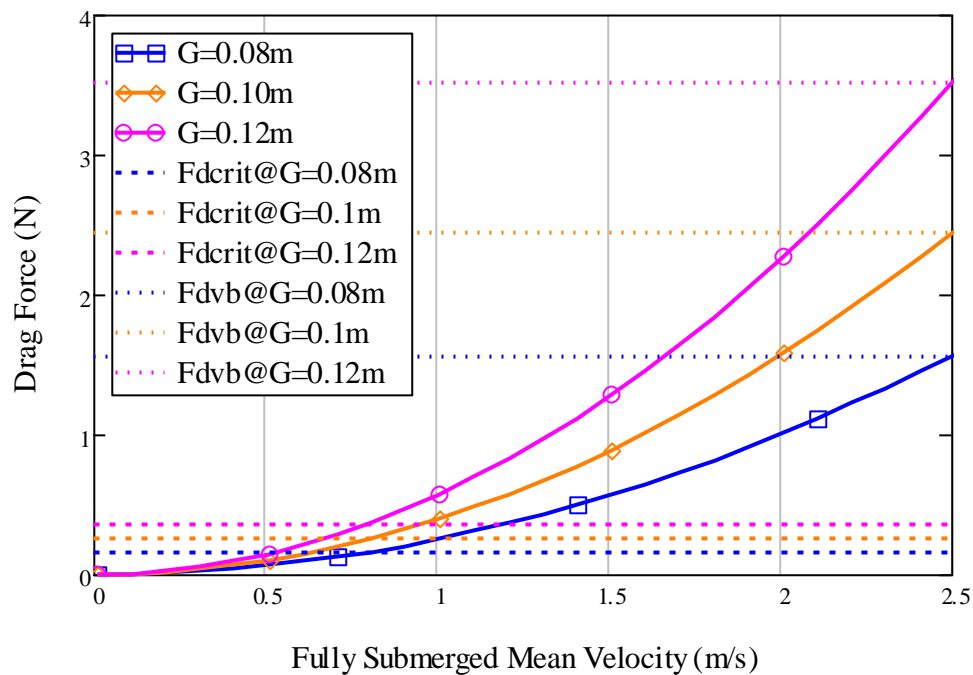


Figure 3.3: Drag force as a function of velocity. The fish is fully submerged in the flow. Blue lines represent a fish with girth, $G=0.08$ m; Orange lines represent a fish with $G=0.10$ m, and pink lines represent a fish with $G=0.12$ m. F_{dcrit} is the drag force at the critical swim velocity of 0.8 m·sec⁻¹ and the respective girth. F_{dvb} is the drag force at the upper swimming limit of 2.5 m·sec⁻¹ and the respective girth.

The smallest fish has less drag at a given velocity, but still can only swim up to the critical velocity. Our model assumes that the reported critical velocity for lamprey within this range of girths is constant, and approximately equal to ($U_{crit}=0.8$ m·sec⁻¹) (Mesa et al. 2003). Therefore, the advantage of a smaller cross section is lost presumably due to decreased body size and potential swimming thrust. The largest fish girth has higher drag

force, but also a larger body that can swim up to the same critical swim velocity. Above the critical swim velocities and the resulting drag represented by the dashed lines, the fish will begin saltatory swimming. Once the velocity increases to the velocity barrier value of ($U_{vb}=2.5 \text{ m}\cdot\text{s}^{-1}$) the fish cannot progress, and that threshold is represented by the dotted lines. With the constant velocity barrier model we eliminate the advantage of lower drag due to smaller girth because the critical velocity and velocity barrier are assumed constant for the range of girths. Using the correlation for length to girth from Keefer et al. (2012 unpub. Data) we found the predicted girth size of Mesa et al. (2003) was between 10-11 cm, and within the range we set. Assuming that the critical velocity is constant may only be valid for a certain range of girths, and will need further research to determine if it is valid.

We also investigated the fish drag force within the duct work to try to understand potential limits on swimming. We created our model based off of (Eqn. 12) as we did before, but this time we modeled flow depth with varying slopes and maintained a constant discharge of $Q=7.8 \text{ L}\cdot\text{s}^{-1}$ for a channel width of 19cm. The relationship between slope, flow depth, and velocity is given (Figure 3.4).

The critical slope condition occurs when the Froude number is equal to 1.0, ($S_c=0.0047$ for $b=19\text{cm}$ and $Q=7.8 \text{ L}\cdot\text{s}^{-1}$) (Table 3.3). The traversing duct is very sensitive to slope changes at low slopes, and small changes in slope will have large effects on flow depth and velocity (Figure 3.4a). Within the supercritical flow, the depth changes are more gradual (Figure 3.4b). With increasing slope, velocity increases, and the depth decreases.

We combined (Eqn. 12) with (Eqn. 7) to relate the drag force to the changing flow depth and developed the following relationship:

$$F_{\text{drag}} := C_D \cdot \frac{1}{2} \cdot \rho \cdot \left(\frac{Q}{b \cdot y} \right)^2 \cdot \frac{G^2}{4\pi} \quad (\text{Eqn. 13})$$

The flow is subcritical for all cases when the fish is fully submerged. We only evaluated (Eqn. 13) when the flow depth was greater than, or equal to the girth of the fish. The flow depth increases with decreasing slope in (Figure 3.5). There are no results until the fish is fully submerged. The smallest fish becomes submerged first, but we can see from (Figure 3.5), that the drag forces are above the critical swim threshold and the fish will exhibit saltatory swim behavior. Girth determines the protrusion of the fish into the flow. Smaller fish will protrude less, but are more submerged for any given slope. With increasing flow depth (decreasing slope), the drag force decreases until the fish passes the critical drag force threshold ($F_{d,\text{crit}, @G=0.8\text{m}}$) and begins to swim. The larger fish will not be submerged until lower slope values for a given discharge.

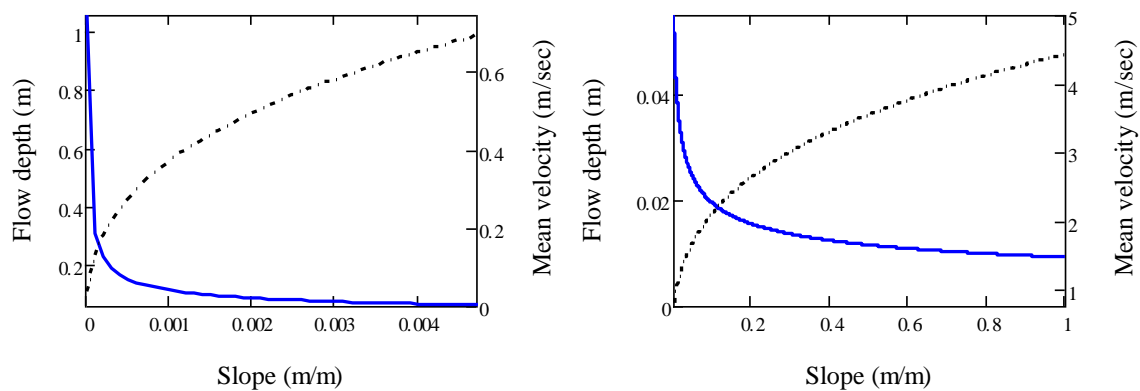


Figure 3.4: Flow Depth with Increasing Slope. The duct shown is the traversing width ($b=19\text{cm}$) and ($Q=7.8\text{L}\cdot\text{s}^{-1}$). Flow depth is represented by the solid, blue line, and velocity is represented by the dashed, black line. a) Represents subcritical slopes $< S_c=0.0047$ b) represents supercritical slopes where $\text{Slope} > S_c=0.0047$

The critical slopes vary with width and discharge for the ductwork, and are relatively low values compared with the climbing slopes (Table 3.3). Reducing the slope may not result in increased climbing efficiency for Pacific lamprey because the fish will be in deeper flow as the slope decreases. The depth changes will be most significant at slopes near the critical slope. Fully submerged supercritical flows will result in drag forces higher than $F_{d_{crit}}$ for all girths (Table 3.5) causing fish to switch to saltatory swimming according to our constant velocity model where ($U_{crit}=0.8 \text{ m}\cdot\text{s}^{-1}$). The fish will be partially submerged within the LPS systems at functional discharges for all supercritical flows. Partially submerged fish will have less drag, but how it relates to the girth of the fish is still unknown. Further research is necessary to better understand the effects of fully submerged and partially submerged drag force over the full range of sizes of migrating Pacific lamprey.

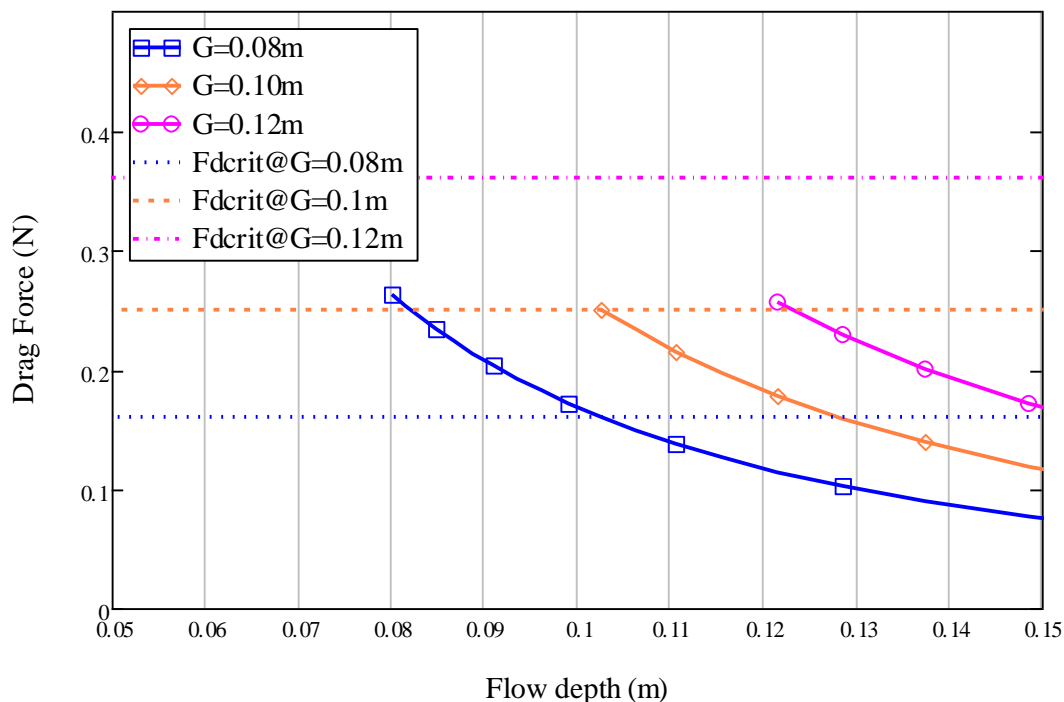


Figure 3.5: Drag force with decreasing slope ($S < S_c$) and constant discharge ($Q=7.8L\cdot\text{s}^{-1}$) for a given duct width, ($b=19\text{cm}$). Blue represents $G=0.08\text{m}$, Orange represents $G=0.1\text{m}$, and Pink represents $G=0.12\text{m}$. Dashed lines represent the $F_{d_{crit}}$ calculated from the girth and ($U_{crit}=0.8 \text{ m}\cdot\text{s}^{-1}$)

Table 3.5: Flow parameters of supercritical flow where Pacific lamprey are fully submerged. Girth=Flow depth, flow is supercritical for all cases shown with a constant Froude number. Results of the critical drag force ($F_{d,crit}$) and the velocity barrier drag force ($F_{d,vb}$), and corresponding Froude numbers for the two conditions are in bold

	Fr	Velocity ($m \cdot s^{-1}$)	So	Fd (N)	$F_{r,crit}$	$F_{d,crit}$ (N) @ $U_{crit}=0.8$ $m \cdot s^{-1}$	$F_{r,vb}$	$F_{d,vb}$ (N) @ $U_{vb}=2.5$ $m \cdot s^{-1}$
G1=y1=0.08m	1.01	0.9	0.0061	0.2	0.9	0.16	2.82	1.56
G2=y2=0.10m	1.01	1	0.0064	0.39	0.81	0.25	2.53	2.44
G3=y3=0.12m	1.01	1.1	0.0068	0.68	0.74	0.36	2.30	3.52

The climbing duct velocities increase with discharge. Implications of this are that although the flow depth will remain thin, the drag force will quadratically increase. The drag force opposing climbing lamprey may overcome the fish and result in fallback, greater exertion, exhaustion leading to fatigue, and possibly death. Therefore, any scaling of these systems should be done carefully to ensure the mean velocities are as low as possible while still providing an attractant flow. Within the climbing duct we were not able to model the flows below ($Q=7.8 L \cdot s^{-1}$) due to the ambiguity of the flow condition. Careful calibration of the effective roughness and perhaps a more comprehensive hydraulic model over all flow regimes may be necessary to effectively scale the LPS systems.

Our simple constant critical velocity model relies on the fish being fully submerged due to the complexities of calculating the submerged cross-sectional area, the coefficient of drag, and the additional component of wave drag that results when bodies are partially submerged. However, the drag force *thresholds* calculated above will apply to partially submerged Pacific lamprey. Higher flow depth resulting from increased discharge could explain why some Pacific lamprey lost ground at the highest discharge during experiments (Reinhardt et al. 2008). Smaller fish may also have an advantage climbing as their drag is lower due to smaller body diameter (Moser et al. 2006). Although this may only be true for low discharges and steep slopes. Future research is needed to explore how the area, drag

coefficient, and wave drag varies with submergence in order to fully understand Pacific lamprey climbing behavior and how it relates to discharge and flow depth.

Lamprey may have greater difficulty ascending the low slope supercritical flow due to the increased flow depth and increased drag. This is supported in experimental results where greater efficiency for the climbing behavior was observed when ($S=1.0$) compared to ($S=0.325$) at low discharge ($Q=3.9 \text{ L}\cdot\text{s}^{-1}$) (Reinhardt et al. 2008). We recommend that traversing ducts be set at a slope ($S\approx 0.003$) and the climbing ducts have slopes of ($S=1.0$), with a possible advantage for decreasing the discharge in climbing ducts to the low flow condition ($Q=3.9 \text{ L}\cdot\text{s}^{-1}$).

However, reduced discharge in experimental trials has not provided clear improvements in passage. Full scale fishway experiments indicate there is little advantage with lower flows (Moser et al. 2006, Moser et al. 2008, and Moser et al. 2011). While laboratory experiments indicate lower flows improve climbing performance, with slope compounding the results (Reinhardt et al. 2008, Keefer et al. 2012). Research on Pacific lamprey climbing behavior indicates that some lamprey can ascend vertical ducting with velocities around $3.7 \text{ m}\cdot\text{s}^{-1}$ (Kemp et al. 2009). Therefore, Pacific lamprey may be able to ascend climbing duct with velocities exceeding their maximum burst swim speed at very steep slopes. The full range of slopes has not been studied and more research will be necessary to implement slopes ($S>1.0$ or $S<1.0$). The effect of discharge may be confounded due to research that indicates it affects lamprey attraction to the systems (Moser et al. 2008, Johnson et al. 2012, and Keefer et al. 2012). Reducing the discharge may improve climbing, but it would likely adversely affect the attraction and guidance of Pacific lamprey to the entrances of LPS structures. A potential hybrid approach would be to supplement

flow at or near the LPS entrance to provide guidance and attraction flow while holding discharge within the LPS to low values, particularly in structures with long vertical runs.

The material roughness of aluminum is comparable to that of steel or copper and has a roughness value estimated to be ($\epsilon = 0.002\text{mm}$) (White 2003). Chow acknowledges that shape has an effect on the roughness value, and rectangular ductwork is the most extreme case (1959). This is attributed to friction effects of the side walls, which diminish as the aspect ratio increases (Nezu & Nakagawa 1993). The aspect ratio is the relationship of channel width to flow depth: $\alpha = b/y$. In wide channels, where $\alpha > 10$, the effects of the walls are considered negligible (Chow 1959). Increasing the aspect ratio also tends to increase the penetration of the roughness into the flow. The effective roughness of the ductwork will therefore vary some with aspect ratio in addition to material, and discharge. From observations of open channel flow we understand that lower aspect ratios will have higher effective roughness because of these and other effects.

The predicted roughness for the climbing duct is appropriate based on the smooth aluminum surfaces. The large aspect ratios indicate that the effect of the sidewalls is negligible (Table 3.2). Our effective roughness value used in our hydraulic modeling was based on discharge and velocity measurements within the climbing duct. The value of $\epsilon=0.18\text{mm}$ is valid for the climbing duct above discharges of $Q=7.8 \text{ L}\cdot\text{s}^{-1}$. There may be some additional roughness effects within the traversing ducts due to the low aspect ratios: $\alpha<10$ (Table 3.2). Smaller widths will have a greater effect, but the values should still be comparable to the climbing effective roughness. Therefore, we applied the climbing duct effective roughness for all traversing ducts. The traversing duct flow is turbulent for all discharges within the range we investigated. The climbing duct flow regime is more

sensitive to varying discharges because of the thin flow. One of the conclusions of studying the hydraulic conditions within the climbing duct flow is the need to assess different flow regimes. Our model is valid only within the turbulent flow regime. There is currently no research relating Pacific lamprey climbing behavior to flow regime.

Our estimates of effective roughness are based on reported values from literature. We matched reported values for depth and discharge for the traversing duct. The roughness value for the traversing duct is unreasonably high given the smooth surface of aluminum. We attribute the high value to nominal measurements of the depth and discharge. Careful measurements of depth, discharge and slope are necessary to predict the roughness accurately. Another potential problem with using the reported measurements for the traversing duct is that the measurement location may have been in areas of gradually varying or unsteady flows. The equations used in the analysis are valid only for fully developed uniform flows. We recommend independent validation of roughness prior to implementing the operating curves.

6. Acknowledgements

Work supported by the United States Army Corp of Engineers, Portland office

The author acknowledges the guidance and support of Ralph Budwig in the development of this model.

7. References

Barret, J. and M. Mallen-Cooper. 2006. The Murray River's 'Sea to Hume Dam' fish passage program: Progress to date and lessons learned, *Ecological Management & Restoration*, 7:3 173-183

- Beck, L.M. 1995. Fish Behavior at Submerged Orifices, Overflow Weirs, and Vertical Slots in the Fish Ladder at Bonneville Second Powerhouse 1993-1994, Report of Research for U.S. Army Corp of Engineers
- Beamish, R.J. 1980. Adult biology of the river lamprey (*Lampetra ayresi*) and the Pacific lamprey (*Lampetra tridentata*) from the Pacific coast of Canada. *Can. J. Fish Aquat. Sci.* 37:1906-1923
- Caudill, C.C., W.R. Daigle, M.L. Keefer, C.T. Boggs, M.A. Jepson, B.J. Burke, R.W. Zabel, T.C. Bjornn, and C.A. Peery. 2007. Slow dam passage in adult Columbia River salmonids associated with unsuccessful migration: delayed negative effects of passage obstacles or condition-dependent mortality? *Can. J. Fish Aquat. Sci.* 64:979-995
- Chow, V. T., 1959. *Open Channel Hydraulics*, 3-16, 201-203
- Clabough, T., M.L. Keefer, C.C. Caudill, E.L. Johnson, & C.A. Peery. 2012. Use of Night Video to Enumerate Adult Pacific Lamprey Passage at Hydroelectric Dams: Challenges and Opportunities to Improve Escapement Estimates, *North American Journal of Fisheries Management*, 32:4, 687-695, DOI:10.1080/02755947.2012.690820
- Clemens, B.J., M.G. Mesa, R.J. Magie, D.A. Young, C.B. Schreck. 2012. Pre-spawning migration of adult Pacific lamprey, *Entosphenus tridentatus*, in the Willamette River, Oregon, U.S.A. *Environ Biol Fish*, 93:245-254, doi10.1007/s10641-011-9910-3
- Close, D.A., M. S. Fitzpatrick, & H. W. Li. 2002. The Ecological and Cultural Importance of a Species at Risk of extinction, *Pacific Lamprey, Fisheries*, 27:7, 19-25, DOI:10.1577/1548-8446(2002)027<0019:TEACIO>2.0.CO;2
- Hard, A., B. Kynard. 1997. Video evaluation of passage efficiency of American Shad and Sea Lamprey in a modified Ice Harbor fishway, *North American Journal of Fisheries Management*, 17:4, 981-987, DOI:10.1577/1548-8675(1997)017<0981:VEOPEO>2.3.CO;2
- Hunn, J.B., & W.D. Youngs. 1980. Role of Physical Barriers in the Control of Sea Lamprey (*Petromyzon marinus*), *Can. J. Fish. Aquat. Sci.* 37:2118-2122
- Johnson, R.L. & L.Z. Perkins. 1968. Fish ladders for John Day Dam, Columbia River, Oregon and Washington; hydraulic model investigations. U.S. Army Corps of Engineers, North Pacific Division, Technical Report 103-1, Bonneville Oregon.
- Johnson, E.L., C.C. Caudill, M.L. Keefer, T.S. Clabough, C.A. Peery, M.A. Jepson, & M.L. Moser. 2012. Movement of Radio-Tagged Adult Pacific Lamprey during a Large-Scale Fishway Velocity Experiment, *Transactions of the American Fisheries Society*, 141:3, 571-579, DOI: 10.1080/0028487.2012.683468

- Johnson, E.L., T.S. Clabough, M.L. Keefer, C.C. Caudill, and C.A. Peery, and M.L. Moser. 2009. Effects of Lowered Nighttime Velocities on Fishway Entrance Success by Pacific Lamprey at Bonneville Dam and Fishway Use Summaries for Lamprey at Bonneville and The Dalles Dams, 2008, Report of research to U.S. Army Corps of Engineers Portland Oregon.
- Kakac, S., R.K. Shah, W. Aung. 1987. Haaland Correlation, Handbook of single phase convective heat transfer, Table 4.3
- Kemp, P.S., T. Tsuzaki, & M.L. Moser. 2009. Linking behavior and performance: intermittent locomotion in a climbing fish, *Journal of Zoology*, 277: 171-178
- Keefer, M.L., M.L. Moser, C.T. Boggs, W.R. Daigle, & C.A. Peery. 2009. Variability in migration timing of adult Pacific lamprey (*Lampetra tridentata*) in the Columbia River, U.S.A. *Environmental Biology of Fishes*, 85:253-264. DOI 10.1007/s10641-009-9490-7
- Keefer, M. L., M.L. Moser, C.T. Boggs, W.R. Daigle, & C.A. Peery. 2009. Effects of Body Size and River Environment on the Upstream Migration of Adult Pacific Lampreys. *North American Journal of Fisheries Management*, 29:5, 1214-1224, DOI: 10.1577/M08-239
- Keefer, M. L., W. R. Daigle, C. A. Peery, H. T. Pennington, S. R. Lee, & M. L. Moser. 2010. Testing adult Pacific lamprey performance at structural challenges in fishways. *North American Journal of Fisheries Management*, 30:2, 376-385.
- Keefer, M.L., C.A. Peery, S.R. Lee, W.R. Daigle, and E.L. Johnson. 2011a. Behaviour of adult Pacific lamprey in near-field flow and fishway design experiments. *Fisheries Management and Ecology* 18:177-189
- Keefer, Matthew L., William R. Daigle, Christopher A Peery, Howard T. Pennington, Steven R. Lee, and Mary L. Moser. 2011b. Testing Adult Pacific Lamprey Performance at Structural Challenges in Fishways. *North American Journal of Fisheries Management* 30:2, 376-385
- Keefer, M.L., C.C. Caudill, E.L. Johnson, T.S. Clabough, M.A. Jepson, C.T. Boggs, S.C. Corbett, and M.L. Moser. 2012. Adult Pacific Lamprey Migration in the Lower Columbia River: 2011 Half-Duplex PIT Tag Studies, A Report for Study Code ADS-P-00-8 for the U.S. Army Corp of Engineers, Portland Office.
- Keefer, M.L., T.C. Clabough, M.A. Jepson, E.L. Johnson, C.T. Boggs, and C.C. Caudill. 2012. Adult pacific lamprey passage: data synthesis and fishway improvement prioritization tools, Technical Report 2012-8 for US Army Corp of Engineers Walla Walla District

- Keefe, M.L., C.C. Caudill, T.S. Clabough, M.A. Jepson, E.L. Johnson, C.A. Peery, M.D. Higgs, & M.L. Moser. 2013a. Fishway passage bottleneck identification and prioritization: a case study of Pacific lamprey at Bonneville Dam. *Canadian Journal of Fisheries and Aquatic Science*, 70: 1551-1565. [Dx.doi.org/10.1139/cjfas-2013-0164](https://doi.org/10.1139/cjfas-2013-0164)
- Keefe, M. L., C. C. Caudill, C. A. Peery, and M. L. Moser. 2013b. Context-dependent diel behavior of upstream-migrating anadromous fishes. *Environmental Biology of Fishes* 96:691-700
- Moser, M.L., & D. Close. 2003. Assessing Pacific Lamprey Status in the Columbia River Basin. *Northwest Science* 77: 116-125
- Mallen-Cooper, M., D.A. Brand. 2007. Non-salmonids in a salmonid fishway: what do 50 years of data tell us about past and future fish passage? *Fisheries Management and Ecology*, 14:319-332
- Mesa, M.G., J.M. Bayer, and J.G. Seelye. 2003 Swimming Performance and Physiological Responses to Exhaustive Exercise in Radio-Tagged and Untagged Pacific Lamprey, *Transactions of the American Fisheries Society*, 132:3, 483-492
- Moser, M.L., A.L. Matter, L.C. Stuehrenberg, and T.C. Bjornn. 2002a. Use of an extensive radio receiver network to document Pacific lamprey (*Lampetra tridentata*) entrance efficiency at fishways in the lower Columbia River. *Hydrobiologia* 483: 45-53
- Moser, M.L., P.A. Ocker, L.C. Stuehrenberg, and T.C. Bjornn. 2002b. Passage efficiency of adult Pacific lampreys at hydropower dams on the lower Columbia River, U.S.A. *Transactions of the American Fisheries Society* 131:956-965
- Moser, M.L., D.A. Close. 2003. Assessing Pacific Lamprey Status in the Columbia River Basin, *Northwest Science*, 77:2, 116-125
- Moser, M.L., D.A. Ogden, B.J. Burke, & C.A. Peery. 2005. Evaluation of a Lamprey Collector in the Bradford Island Makeup Water Channel, Bonneville Dam, 2003. Report of research to U.S. Army Corps of Engineers Portland Oregon.
- Moser, M.L. & D.A. Ogden, D.L. Cummings, C.A. Peery. 2006. Development and Evaluation of a Lamprey Passage Structure in the Bradford Island Auxiliary Water Supply Channel, Bonneville Dam, 2004. Report of Research to U.S. Army Corp of Engineers Portland Oregon.
- Moser, M.L., & D.A. Ogden, H. T. Pennington, W.R. Daigle & C.A. Peery. 2008. Development of Passage Structures for Adult Pacific Lamprey at Bonneville Dam, 2005. Report of Research to U.S. Army Corp of Engineers Portland Oregon
- Moser, M.L., M.L. Keefer, H.T. Pennington, D.A. Ogden, and J.E. Simonsen. 2011. Development of Pacific lamprey fishways at a hydropower dam. *Fisheries Management and Ecology* 18: 190-200

- Monk, B., D. Weaver, C. Thompson, F. Ossiander. 1989. Effects of Flow and Weir Design on the Passage Behavior of American Shad and Salmonids in an Experimental Fish Ladder, *North American Journal of Fisheries Management* 9:60-67
- Nezu, I., H. Nakagawa. 1993. Turbulence in open-channel flows. 88-96
- Perkins, L.Z. & P.M. Smith. 1973. Modification of fish ladders Bonneville Dam, Columbia River Oregon and Washington Hydraulic Model Investigation, Technical Report No 141-1 for U.S. Army Corp of Engineers Portland Oregon
- Quintella, B.R., N.O. Andrade, A. Koed, & P.R. Ameida. 2004. Behavioural patterns of sea lampreys' spawning migration through difficult passage areas studied by electromyogram telemetry, *Journal of Fish Biology*, 65: 961-972
- Russon, I.J. and P.S. Kemp. 2011. Experimental quantification of the swimming performance and behavior of spawning run river lamprey *Lampetra fluviatilis* and European eel *Anguilla*, *Journal of Fish Biology* 78: 1965-1975, DOI:10.1111/j.1095-8649.2011.02965.x
- Reinhardt, U.G., L. Eidietis, S.E. Friedl, and M.L. Moser. 2008. Pacific lamprey climbing behavior. *Canadian Journal of Zoology* 86: 1264-1272
- White, F.M. 2003. *Fluid Mechanics* fifth edition. pg. 366-367.

CHAPTER FOUR: INTEGRATING DIVERSE INFORMATION SOURCES WITH 3D VISUAL MODELS TO CREATE A FISH PASSAGE WIKI

Hattie Zobott¹, Ralph Budwig¹, Chris Caudill², and Matthew Keefer²

¹Center for Ecohydraulics Research

University of Idaho, Boise, ID

²Department of Fish and Wildlife Sciences

University of Idaho, Moscow, ID, 83844-1136

1. Abstract

Improving fish passage at dams can be data-intensive and typically requires close collaboration between researchers, dam managers, and other stakeholders during prioritization and implementation of improvements. Planning for and implementing structural or operational changes at fishways often occurs in an adaptive management context, where data are gathered incrementally and decision makers must integrate information on fish biology and behavior with engineering and cost constraints. We developed a ‘fish passage wiki’ to communicate information to a diverse group of stakeholders tasked with improving upstream migration success in Pacific lamprey (*Entosphenus tridentatus*) as part of a large the recovery and management effort. The study site was Bonneville Dam on the Columbia River, which is a large complex multi-fishway hydroelectric facility where substantial efforts have been made to improve passage for lamprey. The stakeholders included regional dam managers, Federal and state government agencies, researchers and Tribal authorities. We developed a collaborative model where qualitative and quantitative information could be visually presented within the spatial context of the Bonneville Dam infrastructure. We did this by using a three dimensional

visual “wiki” model (3D wiki) as the basis upon which spatially explicit information is mapped on layers or by using interactive links. The 3D wiki developed for lamprey passage at Bonneville Dam could be implemented for other species, other facilities, or in any situation where visualization of multiple data types in a spatially complex environment is needed.

2. Introduction

Wiki technology is a collaborative communication tool where a group maintains webpages based on their knowledge (Hester 2011). The most familiar reference to wiki use is Wikipedia/ With over 12 million users, the platform is a proven communication tool (Shu and Chuang 2011). Learning through use of wiki tools has also been documented in various contexts (Moskaliuk, et al. 2009, Kimmerle et al. 2011) and have found that groups with intermediate understanding of the subject have the greatest opportunity to learn (Kimmerle et al. 2011). Ultimately, many organizations and groups are using wikis as their knowledge management system (KMS) with the tool evolving through use (Hester 2011).

Collaborative modeling is a growing field of research (Budhathoki & Haythornthwaite 2013, Langsdale et al. 2013, Michaud 2013, Palmer et al. 2013, Sandoval-Solis et al. 2013, Török et al. 2013) wherein diverse groups of stakeholders can increase their knowledge and improve their decision making (Michaud 2013). Collaborative modeling is relatively untested in fish management, but potentially very useful because it is flexible and accommodates diverse groups of stakeholders. Collaborative modeling interfaces are designed to be easily accessible to non-technical, decision makers, managers and researchers alike. Lagsdale et al. (2013) outline eight principles for the successful development of a collaborative model:

1. Collaborative modeling is appropriate for complex, conflict laden, and decision making processes where stakeholders are willing to work together.
2. All stakeholder representatives participate early and often to ensure that all relevant interests are included.
3. Both the model and the process remain accessible and transparent to all participants
4. Collaborative modeling builds trust and respect among parties
5. The model supports the decision process by easily accommodating new information and quickly simulating alternatives.
6. The model addresses questions that are important to decision makers and stakeholders.
7. Parties share interests and clarify the facts before negotiating alternatives
8. Collaborative modeling requires both modeling and facilitation skills

We used the framework to develop our current model. The iterative nature of collaborative modeling ensures that the process refines and fulfills the original goal, helps stakeholders align their interests, and implicitly recognizes that the model is a “work-in-progress on a living document”.

Our group of stakeholders was assembled in response to the Columbia Basin Fish Accords in 2008 (“Columbia River Fish Accords Salmon Restoration, Salmon Protection” 2013). In which Pacific Lamprey (*Entosphenus tridentatus*) was established as a priority species. The ten-year plan set out in the Accords included mandated effort to improve

Pacific Lamprey passage efficiency at hydroelectric dams in the Columbia River basin. The existing management structure included communicating progress through regular reporting, but it became difficult for the stakeholder group to effectively integrate the diverse information into a coherent understanding. The difficulty increased through time as research effort and results increased and more structural and operational features were implemented. In addition, Pacific lamprey passage issues were identified and the first five years of the Columbia Basin Fish Accords yielded numerous technical reports, peer-reviewed papers, planning documents, and on-the-ground changes at the dams. Consequently, after the first five years, the stakeholder desired a way to succinctly tracking of fishway retrofits and other improvements in parallel with prioritizing future projects and research.

Our goal was to develop a novel approach to the integration of various information types onto a three dimensional model in support of stakeholder needs that could release, maintained and used as a Wiki. Here, we illustrate the potential of such models in adaptive management situations by documenting our Bonneville Dam experience as a case study. In order to develop this integrative tool we needed to: 1) Choose the software platform 2) Build the visual 3D model 3) populate the visual 3D model with different information types 4) Distribute and allow for feedback. A refined model will then be provided to the stakeholder group and converted to a Wiki. An additional major advantage of the model is that users can rapidly view the model from multiple perspectives and spatial scales by “flying” through the fishway and turning data layers on and off.

3. Methods

The study site was Bonneville Dam, located on the Columbia River (Figure 4.1). We selected the location because all lamprey migrating to the interior Columbia Basin must pass

the dam, it is spatially complex, and because a large amount of data on passage and lamprey improvements were available for the site. Bonneville Dam is made up of several fishways, two powerhouses, a spillway, locks for ship navigation, and fish passage research facilities. We implemented the 3D wiki as a collaborative communication tool. The research we integrated focused on lamprey passage difficulties including monitoring (e.g., Clabough et al. 2012), pacific lamprey movements in the fishway (e.g., Johnson et al. 2012), passage bottlenecks (e.g., Keefer et al. 2013a), and behavior (e.g., Keefer et al. 2013b). We developed a comprehensive model of the site, but focus on the Washington Shore Fishway for this case study.

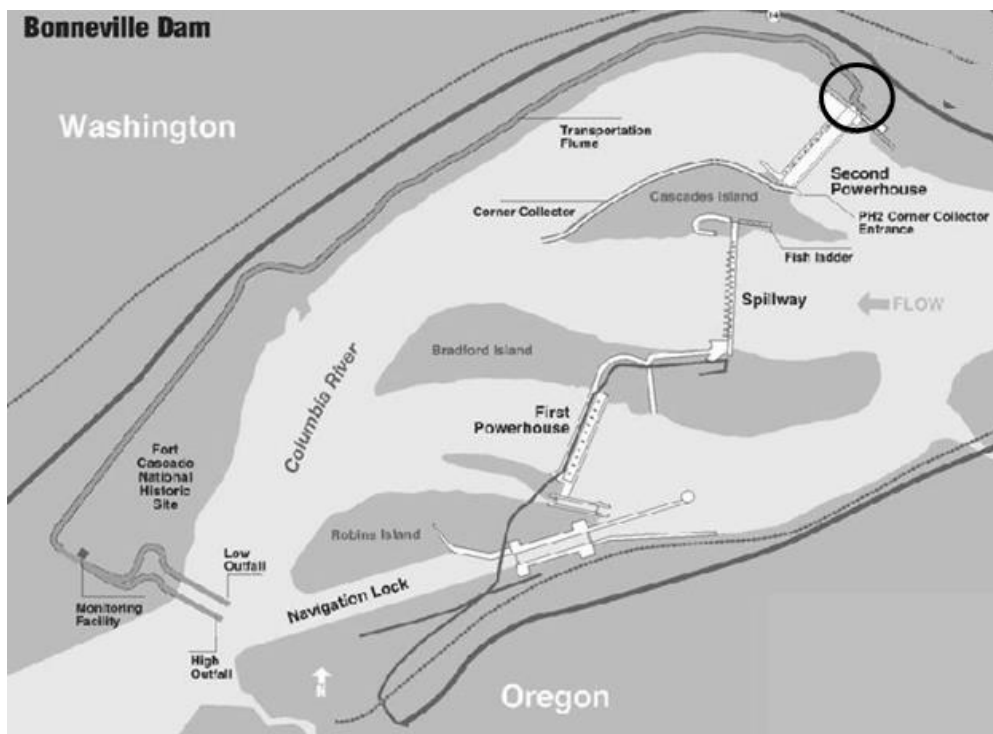


Figure 4.1: Site Overview of Bonneville Dam Complex, The Washington North Shore Fishway is circled

Different 3D modeling platforms were researched during development including: SolidWorks, AutoCAD, HyperCosm, ArcGIS, and SketchUp. Some of the more traditional engineering modeling platforms were accessible to individuals of the group, but they would

have been cost prohibitive to supply to all stakeholders. We needed a low cost and user friendly platform of our visual 3D model. Our selection criteria were equally weighted and were cost, adaptability, and sharing. Cost was based on basic modeling functionality. We determined a model was adaptable if it could incorporate diverse information types and handle the cataloging of research within the model. Part of that adaptability included the function of hyperlinks within the model to external data. The sharing criterion was measured by how easily users could access the model and develop their skills from novice to competent user level (defined as a user who could both navigate and contribute data sources). We compared the tools using qualitative assessments derived from trial use and data sheets. We compared several open source visual modeling tools. We also researched visual modeling tools that are commonly used in industry 3D visual modeling including SolidWorks, AutoCAD, and ProEngineer. Each platform had benefits, but most were geared towards an industry application, not an adaptive 3D wiki model of a fishway. Platforms with specific application spaces were less likely to pass our adaptability requirement. We compared the different options using a simple qualitative assessment criteria (high vs. low; Table 4.1).

Table 4.1: Software platform selection table. Google Sketchup was the best suited based on our criteria

Software Platform	Cost	Adaptability	Sharing
AutoCAD	High	Low	High
Solidworks	High	Low	High
ProE	High	Low	High
ArcGIS	Low	Low	Low
Hypercosm	Low	Low	Low
SketchUp	Low	High	High

An important consideration in the development of a Wiki is the trade-off between spatial accuracy and cost. For our application, we chose to build a structurally representative model, but did not strive for architectural or engineering precision. We developed the 3D visual model by incorporating import and drafting methods. The accuracy of the rendering depended on the information source and importing technique. The most basic level was done by drawing over the top of imported images from Google Earth, photos, technical drawings, and selected research results. Detail and accuracy increased when we worked off of technical drawings to develop realistic rendering of more complex fishway features. We also directly imported 2D files that were then extended to 3D, which added flexibility to our development process. The 3D model has a series of layers that enable the user to easily compare different perspectives and data types. We used this feature to create visual representations of some research results that could be shown on specific layers depending on relevance.

The 3D model was populated with different pieces of information to create the wiki functionality. Some information, like graphs, charts, reports, and photo albums, were saved as (.pdf) file types and then linked to from the model. Other information was synthesized into layers and overlaid on the visual 3D model. We then created different “scenes” that the basic user could use to navigate to key perspectives with little or no technical training. Each scene highlighted a broader perspective of the involved research.

We needed the model to hyperlink to external data to create the “wiki” functionality. After extensive research on various Sketchup blogs and forums, we found a solution call “Links Manager” plugin (“[Plugin] Update Links Manager, SketchUcation Community Forums” 2013). A key advantage of Wiki models is they can be fully web based, but

internet access and security issues required that we develop our model to be independent of the internet. We distributed the resulting model as a DVD rather than using the Internet due to security issues. Each copy had everything the user needed to access the model including software, plugins, data, and manual. Because of the hyperlinks function, we implemented self-executing files to install data onto the user's computer.

Development of the model was an iterative process. We would create a visual model and then distribute for feedback. Users would ask for more detail, or an expanded view of the model. We started with one piece of the fishway and expanded it to the entire complex. The level of detail decreased as the scale increased to save time. Our modeling was implemented by one technical user that managed the 3D visual modeling and data integration. The core group of users that provided most of the feedback would also provide information sources and sort through data to determine relevance.

Periodically during development, we hosted workshops to garner feedback from stakeholders. These sessions helped the stakeholders explore the functionality of the tool and break down insecurities in using the tool. More technical users were able to explore the model independently; while novice users relied on the manual we developed to gain necessary skills to install and access the model. We continually iterated the 3D wiki based on feedback from the users and stakeholder throughout the development process.

4. Results

The 3D visual model encompasses the entire complex (Figure 4.2). Most of it was drawn from the Google Earth images, and the resolution is low. The goal was to provide a broad spatial context for the dam complex at coarse detail and much finer detail at the Washington Shore Fishway (WSF) where most modifications have occurred (Figure 4.3).

We were interested in fine scale features of the WSF that negatively impact Pacific lamprey passage including orifices of overflow weirs, grating, fishway opening, and picket leads.

We also needed higher accuracy to model the tailrace elevation changes and their interactions with the overflow weirs. We can see that higher tailrace elevation results in flooding of more overflow weirs (Figure 4.3).

We created unique model shapes representative of research results to better communicate passage problems within the fishway (Figure 4.4). The layers were organized into an index so that users could filter the information based on their interests or questions (Figure 4.5). We added additional functionality by creating scenes that were snapshots of important data. For instance, we separated modifications and data-monitoring into two different scenes (Figure 4.4). Hyperlinks were an important tool that we implemented to simplify the model and minimize visual interference. We also cataloged the hyperlinks based on content and add them to specific layers as shown in (Figure 4.4). The structure of the model was a result of feedback and multiple iterations. Each milestone and review session lead to development, which kept the model relevant and interesting to the users. A copy of the model is available from the authors, including video clips illustrating major features that do not require installation of any software.

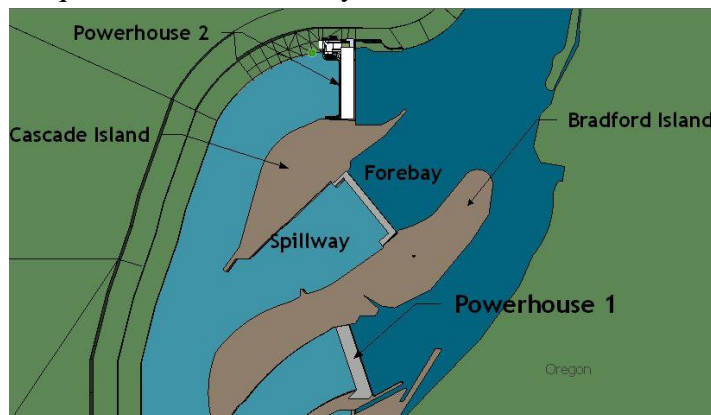


Figure 4.2: Plan view of Bonneville Dam Complex 3D wiki model

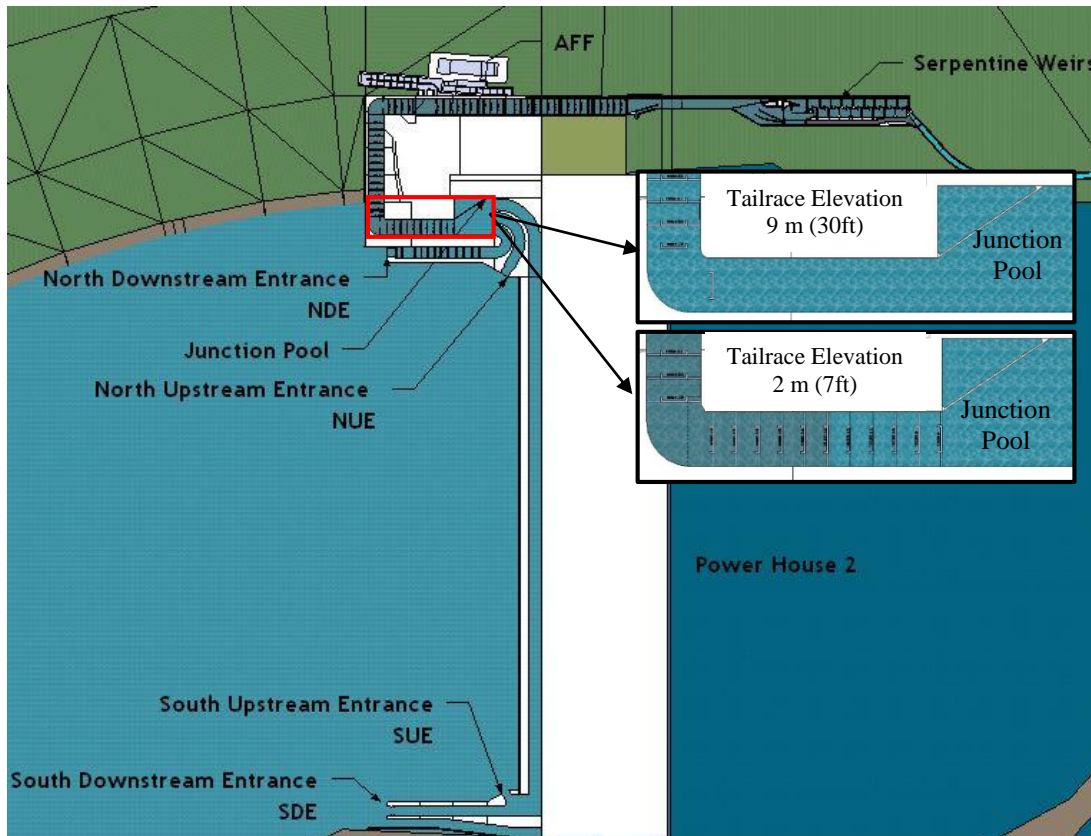


Figure 4.3: Plan view of Powerhouse 2. Insets show tailrace elevation change and resulting overflow weir flooding

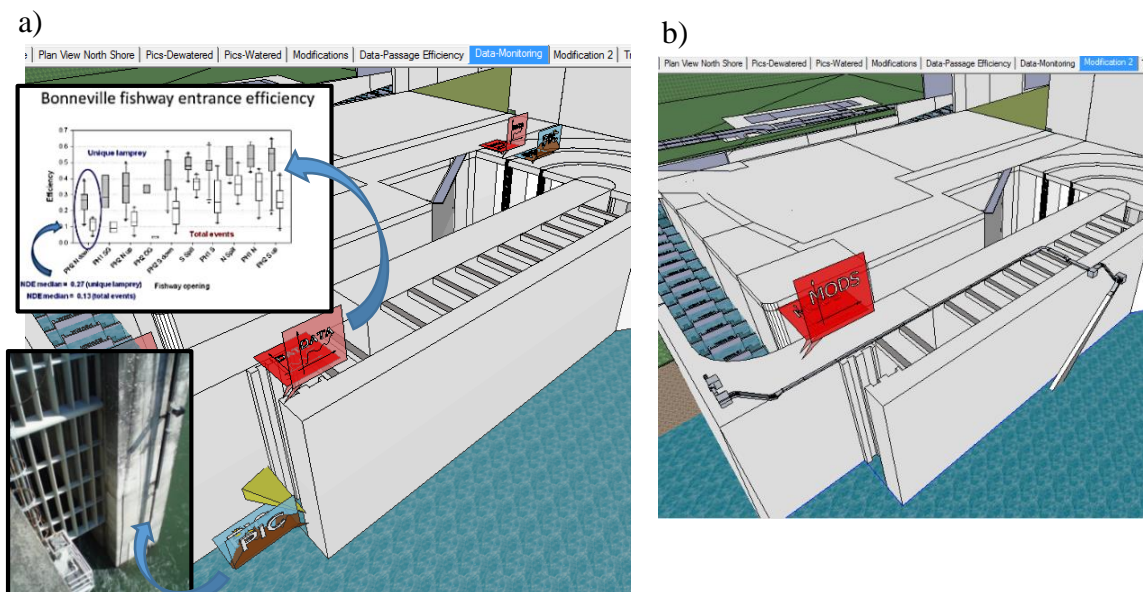


Figure 4.4: Snapshots of the 3D wiki functionality. The brightly colored objects are references to external data pertaining to their location (e.g. reports, charts, or pictures). a) Arrows show the hyperlinked external data of a graph and a picture of the North Downstream Entrance of the fishway (Inset pictures). b) Scene where the recent Lamprey Passage Flume modifications of the Washington North Shore Fishway are shown.

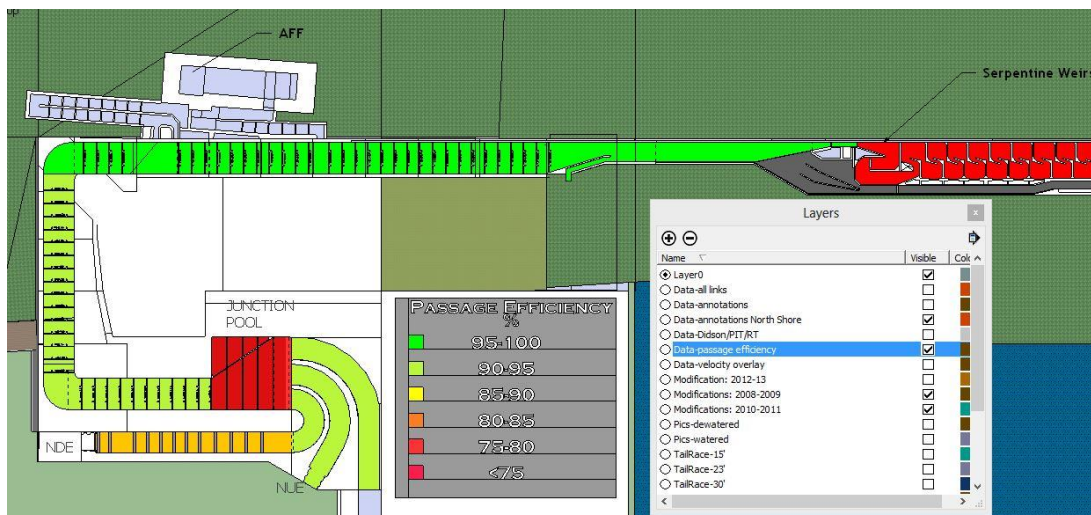


Figure 4.5: Data passage overlay on the visual 3D base model. The inset “Layers” box shows which layers are active in this view.

5. Discussion

The resulting 3D wiki model is a collaborative tool with a broad array of potential applications. With one user taking the initiative to be the technical master of the 3D model, other users can benefit by sharing a common perspective. The model can be detailed or abstract, depending on time and resources. Layers of information make the model interactive like a “wiki” page. Each user has the ability to edit the information based on their perspective, or for content. Users develop confidence in the model through iterative workshops where they can learn basic modeling skills or applications of the 3D wiki model. The content of our model was Pacific lamprey passage at Bonneville North Shore Fishway, but the base model could include other species and perhaps overlays of their migration difficulties. This type of information synthesis leads to clearer understanding of migration problems and potential solutions within the spatial context of the obstruction.

Our specific application at Bonneville Dam enabled the group of stakeholders to develop a more comprehensive view of Pacific lamprey passage. Previously difficult to access structural information became the basis of the model. Now all stakeholders could use

the information at will. The large and scattered information within a literature synthesis was transformed into a visual synthesis that is easy to understand (Figure 4.4). Users could compare the research (Figure 4.4) with resulting modifications (Figure 4.5b). The additional functionality of hyperlinks allowed us to catalog photos, and other information about the fishway in one place (Figure 4.5a). Now the stakeholders had the information that they needed to understand the difficulties Pacific lamprey face during passage at Bonneville Dam.

Development of the tool roughly followed the guidelines outlined by Lagsdale (2013). Except we had difficulty making the model accessible to users at all times due to the research involved in creating it. We had to find a way for multiple users to access the same file, and manage versions because Sketchup as a platform does not have data management services. We recognized that if the model had glitches or inaccuracies the stakeholders would likely lose interest and discontinue using the model. Therefore, periodic rebuilds of the visual model occurred as the technical master of the visual model became more adept. This resulted in a prolonged timeline between workshops, which could be problematic as it reduced transparency in the process along with feedback opportunities. The usefulness of wiki pages as a collaboration tool has also been investigated, and coordinating timelines for edits has been shown to be a limiting factor (Bonk et al. 2009). Future applications of this model will have a shorter turnaround. Storing the model on the web would reduce or eliminate the time between edits because the users could access it independently at will.

The risks of prolonged time periods between iterations is that the results diverge from expectations. One part of the group may also have greater opportunity to work on the

model resulting in bias towards that group. There are many limiting factors to the success of a collaborative model such as the 3D wiki, and many practitioners find the results don't meet up to their expectations (Bonk et al. 2009). Therefore it is important that the model be constantly adaptable in order for it to succeed.

We found that working with a smaller group on technical issues helped the 3D wiki model develop to a higher quality. By limiting the input of users during the beginning stages we were able to simplify the initial scope. Then, as the technical master of the visual model gained experience, the model grew in complexity. It is important to note that the technical master had no prior experience with the Sketchup platform. This is encouraging for the application of this platform for 3D wiki models because any group could implement it with relative ease. Ultimately, we found the Sketchup platform to be adaptable to our needs for a visual 3D wiki model. Our results were collaborative, and involved numerous iterations to align the product with group's needs. We started with a simple concept and expanded it in detail and complexity as the technical skills of the group increased. The result was a fish passage wiki that a group of diverse stakeholders implemented to develop solutions for Pacific lamprey passage difficulties. Although, this tool would be suitable for many complex problems facing fish recovery efforts.

6. Acknowledgements

Work supported by the United States Army Corp of Engineers, Portland office

The author acknowledges the guidance and support of Christopher Caudill, Matthew Keefer, and Ralph Budwig

7. References

- “ArcGIS - Mapping and Spatial Analysis for Understanding Our World.” 2013. Accessed July 31. <http://www.esri.com/software/arcgis>.
- “AutoCAD Design Suite, CAD Design Software, Autodesk.” 2013. Accessed July 31. <http://www.autodesk.com/suites/autocad-design-suite/overview>.
- “Columbia River Fish Accords | Salmon Restoration, Salmon Protection.” 2013. *Columbia River Inter-Tribal Fish Commission*. Accessed July 31. <http://www.critfc.org/fish-and-watersheds/fish-and-habitat-restoration/columbia-basin-fish-accords/>.
- Bonk, C.J., M.M. Lee, N. Kim, and M. G. Lin. 2009. “The Tensions of Transformation in Three Cross-institutional Wikibook Projects.” *Internet & Higher Education* 12: 126–135
- Budhathoki, N.R., and C. Haythornthwaite. 2013. “Motivation for Open Collaboration: Crowd and Community Models and the Case of OpenStreetMap.” *American Behavioral Scientist*, 57:5, 548–575.
- Clabough, T. S., M. L. Keefer, C. C. Caudill, E. L. Johnson, and C. A. Peery. 2012. Use of night video to enumerate adult Pacific lamprey passage at hydroelectric dams: challenges and opportunities for improved escapement estimates. *North American Journal of Fisheries Management* 32:687-695.
- “Google Earth.” 2013. Accessed July 31. <http://www.google.com/earth/index.html>.
- “Hypercosm - Interactive, Web-Based, 3D Simulations.” 2013. Accessed July 31. <http://www.hypercosm.com/>.
- Hester, A. 2011. “A Comparative Analysis of the Usage and Infusion of Wiki and Non-wiki-based Knowledge Management Systems.” *Information Technology & Management* 12:4 335–355
- Johnson, E. L., C. C. Caudill, M. L. Keefer, T. S. Clabough, C. A. Peery, M. A. Jepson, and M. L. Moser. 2012. Movement of radio-tagged adult Pacific lampreys during a large-scale fishway velocity experiment. *Transactions of the American Fisheries Society* 141:571-579.
- Keefer, M. L., C. C. Caudill, T. S. Clabough, M. A. Jepson, E. L. Johnson, C. A. Peery, M. D. Higgs, and M. L. Moser. *In press*. Fishway passage bottleneck identification and prioritization: a case study of Pacific lamprey at Bonneville Dam. *Canadian Journal of Fisheries and Aquatic Sciences*.

- Kefer, M. L., C. C. Caudill, C. A. Peery, and M. L. Moser. 2013. Context-dependent diel behavior of upstream-migrating anadromous fishes. *Environmental Biology of Fishes* 96:691-700.
- Kimmerle, J., J. Moskaliuk, and U. Cress. 2011. "Using Wikis for Learning and Knowledge Building: Results of an Experimental Study." *Journal of Educational Technology & Society*, 14:4, 138–148
- Langsdale, S., A. Beall, E. Bourget, E. Hagen, S. Kudlas, R. Palmer, D. Tate, and W. Werick. 2013. "Collaborative Modeling for Decision Support in Water Resources: Principles and Best Practices Collaborative Modeling for Decision Support in Water Resources: Principles and Best Practices." *Journal of the American Water Resources Association*, 49:3, 629–638
- Michaud, W.R. 2013. "Evaluating the Outcomes of Collaborative Modeling for Decision Support Evaluating the Outcomes of Collaborative Modeling for Decision Support." *Journal of the American Water Resources Association*, 49:3 693–699
- Moskaliuk, J., J. Kimmerle, and U. Cress. 2009. "Wiki-supported Learning and Knowledge Building: Effects of Incongruity between Knowledge and Information." *Journal of Computer Assisted Learning*, 25:6, 549–561
- "[Plugin] Update Links Manager SketchUcation Community Forums." 2013. Accessed July 31. <http://sketchucation.com/forums/viewtopic.php?t=33534>.
- Sandoval-Solis, S., R.L. Teasley, D.C. McKinney, G.A. Thomas, and C. Patiño-Gomez. 2013. "Collaborative Modeling to Evaluate Water Management Scenarios in the Rio Grande Basin Collaborative Modeling to Evaluate Water Management Scenarios in the Rio Grande Basin." *Journal of the American Water Resources Association*, 49:3,639–653.
- "SketchUp 3D for Everyone." 2013. Accessed July 31. <http://www.sketchup.com/>.
- "SolidWorks 2013 Data Sheets." 2013. Accessed July 31. http://www.solidworks.com/sw/products/9694_ENU_HTML.htm.
- Török, J., G. Iñiguez, T. Yasseri, M. San Miguel, K. Kaski, and J. Kertész. 2013. "Opinions, Conflicts, and Consensus: Modeling Social Dynamics in a Collaborative Environment." *Physical Review Letters*, 110:8 088701–1
- Shu, W., Y. Chuang. 2011. "THE BEHAVIOR OF WIKI USERS." *Social Behavior & Personality: An International Journal*, 39:6, 851–864

APPENDIX A-REPORTED PARAMETERS INVESTIGATED DURING
ROUGHNESS CALCULATIONS*

b (m)	y (m)	α	S	U_{mean} (m/s)	f	Re #	Fr #	Source
0.50	0.0039	130	1	4.05	0.018	1.17E+04	20.8	Reinhardt et al. 2008
0.50	0.0044	114	1	3.56	0.027	1.16E+04	17.2	Reinhardt et al. 2008
0.50	0.00222	226	1	3.52	0.014	5.87E+03	23.9	Reinhardt et al. 2008
0.50	0.0021	238	1	3.67	0.012	5.90E+03	25.6	Reinhardt et al. 2008
0.50	0.0020	245	1	3.82	0.011	5.87E+03	27.0	Reinhardt et al. 2008
0.50	0.0031	163	0.325	2.55	0.012	5.85E+03	14.7	Reinhardt et al. 2008
0.50	0.0029	172	0.325	2.69	0.02	5.90E+03	15.9	Reinhardt et al. 2008
0.50	0.0028	181	0.325	2.83	0.0087	5.86E+03	17.2	Reinhardt et al. 2008
0.50	0.0043	117	0.325	1.82	0.032	5.82E+03	8.9	Reinhardt et al. 2008
0.50	0.004	125	0.325	1.97	0.026	1.20E+04	9.9	Reinhardt et al. 2008
0.50	0.00368	136	0.325	2.12	0.021	5.83E+03	11.2	Reinhardt et al. 2008

*All parameter combinations above did not converge to a roughness value for ϵ in the Haaland correlation, the values that converged are shown in the results.

APPENDIX B-ROUGHNESS CALCULATION METHOD

Hattie Zobott Darcy friction factor analysis,
LPS systems, using reported values in literature for to determine friction factors and roughness

$$\mu := 2.730 \cdot 10^{-5} \frac{\text{lb} \cdot \text{s}}{\text{ft}^2} \quad \rho := 992 \frac{\text{kg}}{\text{m}^3} \quad \nu := \frac{\mu}{\rho} = 1.318 \times 10^{-6} \frac{\text{m}^2}{\text{s}} \quad 50 \text{ deg F}$$

Sensitivity analysis at bottom of worksheet, summary:

Traversing duct: for $0.003 < S < 0.004$
 $0.68 < f < 0.91$, $6\text{mm} < \epsilon < 16\text{mm}$

Climbing duct: $1.0 < S < 1.1$
for $0.4 < f < 0.46$, $0\text{mm} < \epsilon < 3\text{mm}$

traversing more sensitive to slope error. also,
ranges do not overlap

Summary of Reinhardt et al 2008 for $S=1$, $V=3.56 \text{ m/s} \pm 0.49\text{m/s}$, $Q=7.8\text{L/s}$

at $v=4\text{m/s}$	$y := 3.9 \times 10^{-3}$	$f := .018$	imaginary result
at $v=3.56$	$y := 4.382 \times 10^{-3}$	$f := 0.027$	imaginary result
at $v=3.07\text{m/s}$	$y := 3.852$	$f := .041$	$\epsilon := 1.828 \times 10^{-4} \text{ m}$

Summary of Reinhardt et al 2008 for $S=1$, $V=3.67 \text{ m/s} \pm 0.15\text{m/s}$, $Q=3.9\text{L/s}$

imaginary

Summary of Reinhardt et al 2008 for $S=0.314$, $V=2.69 \text{ m/s} \pm 0.14\text{m/s}$, $Q=7.8\text{L/s}$

imaginary

Summary of Reinhardt et al 2008 for $S=0.314$, $V=1.97 \text{ m/s} \pm 0.15\text{m/s}$, $Q=3.9\text{L/s}$

imaginary

Preliminary Calculations based on Reported hydraulic conditions and Duct Geometry

$b := 7.5\text{in}$	$y := 10\text{cm}$	$Q := 7.8 \frac{\text{L}}{\text{sec}}$
---------------------	--------------------	--

Determine the darcy friction factor from the energy equation using the reported discharge and depth of flow:

$$A := b \cdot y \quad S_o := \frac{.25\text{in}}{6\text{ft}} = 3.472 \times 10^{-3} \quad \text{Horizontal section, slope } 1/4" \text{ per } 6'$$

$$V := \frac{Q}{A} = 0.409 \frac{\text{m}}{\text{s}}$$

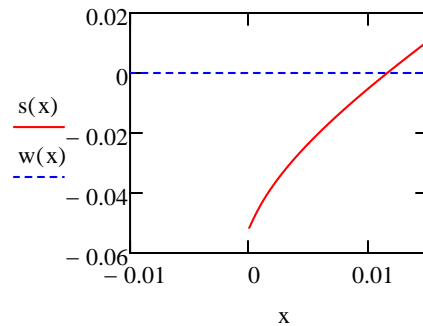
$$f := \frac{S_o \cdot 4 \cdot \left(\frac{y \cdot b}{2 \cdot y + b} \right) \cdot 2 \cdot g}{(V)^2} = 0.079 \quad \text{Re} := \frac{V \cdot \left(\frac{y \cdot b}{2 \cdot y + b} \right)}{\nu} = 1.516 \times 10^4$$

$$s(\epsilon) := 4 \left[3.4735 - 1.5635 \cdot \ln \left[2 \cdot \frac{\epsilon}{4 \left(\frac{y \cdot b}{2 \cdot y + b} \right)} \right] \right]^{1.11} + 63.635 \cdot \frac{\nu}{\left(\frac{y \cdot b}{2 \cdot y + b} \right) \cdot V} \right]^{-2} - f \quad \text{Haaland Correlation}$$

$$w(x) := 0$$

$$y1 := 0 \text{ mm}$$

$$\epsilon := \text{root}(s(y1), y1) = 11.581 \cdot \text{mm}$$



Now determine the friction factor for the climbing $S=1$ duct reported velocities at 7.8L/sec
Reignhardt et al 2009

$$So := 1$$

$$V := 3.07 \frac{\text{m}}{\text{sec}} = 3.07 \frac{\text{m}}{\text{s}}$$

$$b := 50 \text{ cm}$$

$$\text{Velocity was measured to } \pm .49 \text{ m/s}$$

$$A := \frac{Q}{V} = 2.541 \times 10^{-3} \text{ m}^2$$

$$y := \frac{A}{b} = 5.081 \times 10^{-3} \text{ m}$$

$$f := \frac{So \cdot 4 \cdot \left(\frac{y \cdot b}{2 \cdot y + b} \right) \cdot 2 \cdot g}{V^2} = 0.041$$

$$Re := \frac{V \cdot \left(\frac{y \cdot b}{2 \cdot y + b} \right)}{\nu} = 1.16 \times 10^4$$

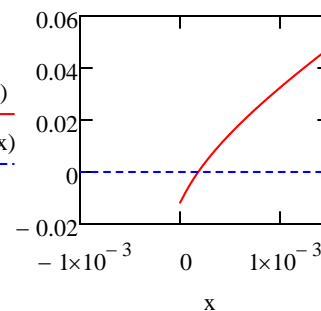
$$Rh := \frac{y \cdot b}{2 \cdot y + b} = 4.98 \times 10^{-3} \text{ m}$$

Use the Haaland Correlation to determine f

$$s(\epsilon) := 4 \left[3.4735 - 1.5635 \cdot \ln \left[2 \cdot \frac{\epsilon}{4 \left(\frac{y \cdot b}{2 \cdot y + b} \right)} \right] \right]^{1.11} + 63.635 \cdot \frac{\nu}{\left(\frac{y \cdot b}{2 \cdot y + b} \right) \cdot V} \right]^{-2} - f$$

$$y1 := .0002 \text{ m}$$

$$\epsilon := \text{root}(s(y1), y1) = 0.182 \cdot \text{mm}$$



Now determine the friction factor for the climbing S=1 duct reported velocities at 7.8L/sec
Reignhardt et al 2009

$$So := 1$$

$$V := 3.56 \frac{\text{m}}{\text{sec}} = 3.56 \frac{\text{m}}{\text{s}} \quad b := 50\text{cm}$$

Velocity was measured to +/- .49m/s

$$A := \frac{Q}{V} = 2.191 \times 10^{-3} \text{ m}^2$$

$$y := \frac{A}{b} = 4.382 \times 10^{-3} \text{ m}$$

$$Rh := \frac{y \cdot b}{2 \cdot y + b} = 4.307 \times 10^{-3} \text{ m}$$

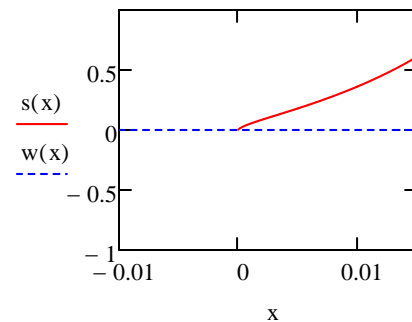
$$f := \frac{So \cdot 4 \cdot \left(\frac{y \cdot b}{2 \cdot y + b} \right) \cdot 2 \cdot g}{V^2} = 0.027$$

$$Re := \frac{V \cdot \left(\frac{y \cdot b}{2 \cdot y + b} \right)}{\nu} = 1.164 \times 10^4$$

$$s(\epsilon) := 4 \cdot \left[3.4735 - 1.5635 \cdot \ln \left[2 \cdot \frac{\epsilon}{4 \left(\frac{y \cdot b}{2 \cdot y + b} \right)} \right] \right]^{1.11} + 63.635 \cdot \frac{\nu}{\left(\frac{y \cdot b}{2 \cdot y + b} \right) \cdot V} \Bigg]^{-2} - f \quad \text{Haaland Correlation}$$

$$y1 := .001\text{m}$$

$$\epsilon := \text{root}(s(y1), y1) = (-2.787 \times 10^{-5} - 8.968i \times 10^{-6}) \cdot \text{m}$$



Now determine the friction factor for the climbing S=1 duct reported velocities at 7.8L/sec
Reignhardt et al 2009

$$So := 1$$

$$V := 4.05 \frac{\text{m}}{\text{sec}} = 4.05 \frac{\text{m}}{\text{s}}$$

b := 50cm Velocity was measured to +/- .49m/s

$$A := \frac{Q}{V} = 1.926 \times 10^{-3} \text{ m}^2$$

$$y := \frac{A}{b} = 3.852 \times 10^{-3} \text{ m}$$

$$Rh := \frac{y \cdot b}{2 \cdot y + b} = 3.793 \times 10^{-3} \text{ m}$$

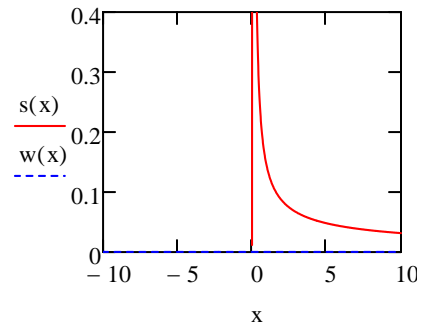
$$f := \frac{So \cdot 4 \cdot \left(\frac{y \cdot b}{2 \cdot y + b} \right) \cdot 2 \cdot g}{V^2} = 0.018$$

$$Re := \frac{V \cdot \left(\frac{y \cdot b}{2 \cdot y + b} \right)}{\nu} = 1.166 \times 10^4$$

$$s(\epsilon) := 4 \cdot \left[3.4735 - 1.5635 \cdot \ln \left[2 \cdot \frac{\epsilon}{4 \left(\frac{y \cdot b}{2 \cdot y + b} \right)} \right]^{1.11} + 63.635 \cdot \frac{\nu}{\left(\frac{y \cdot b}{2 \cdot y + b} \right) \cdot V} \right]^{-2} - f \quad \text{Haaland Correlation}$$

$$y1 := .00002\text{m}$$

$$\epsilon := \text{root}(s(y1), y1) = (-5.846 \times 10^{-5} + 1.881i \times 10^{-5}) \cdot \text{m}$$



Decrease discharge: 3.9L/sec Reinhart et al 2008, +/- .15m/sec

$$So := 1$$

$$V := 3.67 \frac{\text{m}}{\text{sec}} = 3.67 \frac{\text{m}}{\text{s}}$$

$$b := 50\text{cm}$$

$$Q := 3.9 \frac{\text{L}}{\text{sec}}$$

$$A := \frac{Q}{V} = 1.063 \times 10^{-3} \text{m}^2$$

$$y := \frac{A}{b} = 2.125 \times 10^{-3} \text{m}$$

$$f := \frac{So \cdot 4 \cdot \left(\frac{y \cdot b}{2 \cdot y + b} \right) \cdot 2 \cdot g}{V^2} = 0.012$$

$$Re := \frac{V \cdot \left(\frac{y \cdot b}{2 \cdot y + b} \right)}{\nu} = 5.87 \times 10^3$$

$$Rh := \frac{y \cdot b}{2 \cdot y + b} = 2.107 \times 10^{-3} \text{m}$$

$$s(\epsilon) := 4 \cdot \left[3.4735 - 1.5635 \cdot \ln \left[2 \cdot \frac{\epsilon}{4 \left(\frac{y \cdot b}{2 \cdot y + b} \right)} \right]^{1.11} + 63.635 \cdot \frac{\nu}{\left(\frac{y \cdot b}{2 \cdot y + b} \right) \cdot V} \right]^{-2} - f$$

$$y1 := .2\text{m}$$

$$\epsilon := \text{root}(s(y1), y1) = 1.026 \times 10^3 \cdot \text{m}$$

$$So := 1$$

$$V := (3.67 + x \cdot 15) \frac{\text{m}}{\text{sec}} = 3.82 \frac{\text{m}}{\text{s}} \quad b := 50\text{cm}$$

$$Q := 3.9 \frac{\text{L}}{\text{sec}}$$

$$x := 1$$

Reinhart et al 2008, +/- 15m/sec

$$A := \frac{Q}{V} = 1.021 \times 10^{-3} \text{ m}^2$$

$$y := \frac{A}{b} = 2.042 \times 10^{-3} \text{ m}$$

$$f := \frac{So \cdot 4 \cdot \left(\frac{y \cdot b}{2 \cdot y + b} \right) \cdot 2 \cdot g}{V^2} = 0.011$$

$$Re := \frac{V \cdot \left(\frac{y \cdot b}{2 \cdot y + b} \right)}{\nu} = 5.872 \times 10^3 \quad Rh := \frac{y \cdot b}{2 \cdot y + b} = 2.025 \times 10^{-3} \text{ m}$$

$$s(\epsilon) := 4 \cdot \left[3.4735 - 1.5635 \cdot \ln \left[2 \cdot \frac{\epsilon}{4 \left(\frac{y \cdot b}{2 \cdot y + b} \right)} \right]^{1.11} + 63.635 \cdot \frac{\nu}{\left(\frac{y \cdot b}{2 \cdot y + b} \right) \cdot V} \right]^{-2} - f$$

$$y1 := .1\text{m}$$

$$\epsilon := \text{root}(s(y1), y1) = 1.875 \times 10^3 \cdot \text{m}$$

For 18 deg slope and Q 7.8L/s

$$So := .325 \quad V := (2.69 + x \cdot 14) \frac{\text{m}}{\text{sec}} = 2.55 \frac{\text{m}}{\text{s}} \quad b := 50\text{cm}$$

$$x := -1$$

Reinhardt et al 2008 +/- 0.15m/s
change x to change +, -, or 0

$$A := \frac{Q}{V} = 1.529 \times 10^{-3} \text{ m}^2$$

$$y := \frac{A}{b} = 3.059 \times 10^{-3} \text{ m}$$

$$f := \frac{So \cdot 4 \cdot \left(\frac{y \cdot b}{2 \cdot y + b} \right) \cdot 2 \cdot g}{V^2} = 0.012$$

$$Re := \frac{V \cdot \left(\frac{y \cdot b}{2 \cdot y + b} \right)}{\nu} = 5.848 \times 10^3 \quad Rh := \frac{y \cdot b}{2 \cdot y + b} = 3.022 \times 10^{-3} \text{ m}$$

$$s(\epsilon) := 4 \cdot \left[3.4735 - 1.5635 \cdot \ln \left[2 \cdot \frac{\epsilon}{4 \left(\frac{y \cdot b}{2 \cdot y + b} \right)} \right]^{1.11} + 63.635 \cdot \frac{\nu}{\left(\frac{y \cdot b}{2 \cdot y + b} \right) \cdot V} \right]^{-2} - f$$

$$y1 := .2\text{m}$$

$$\epsilon := \text{root}(s(y1), y1) = 1.771 \times 10^3 \cdot \text{m}$$

$$x := -1$$

Reinhardt et al 2008 +- 0.14m/s

change x to change +, -, or 0

For 18 deg slope and Q 3.9L/s

$$So := .325 \quad V := (1.97 + x \cdot 0.15) \frac{\text{m}}{\text{sec}} = 1.82 \frac{\text{m}}{\text{s}} \quad b := 50\text{cm} \quad Q := 3.9 \frac{\text{L}}{\text{sec}}$$

$$A := \frac{Q}{V} = 2.143 \times 10^{-3} \text{m}^2$$

$$y := \frac{A}{b} = 4.286 \times 10^{-3} \text{m}$$

$$f := \frac{So \cdot 4 \cdot \left(\frac{y \cdot b}{2 \cdot y + b} \right) \cdot 2 \cdot g}{V^2} = 0.032$$

$$Re := \frac{V \cdot \left(\frac{y \cdot b}{2 \cdot y + b} \right)}{\nu} = 5.82 \times 10^3 \quad Rh := \frac{y \cdot b}{2 \cdot y + b} = 4.213 \times 10^{-3} \text{m}$$

$$s(\epsilon) := 4 \cdot \left[3.4735 - 1.5635 \cdot \ln \left[2 \cdot \frac{\epsilon}{4 \left(\frac{y \cdot b}{2 \cdot y + b} \right)} \right]^{1.11} + 63.635 \cdot \frac{\nu}{\left(\frac{y \cdot b}{2 \cdot y + b} \right) \cdot V} \right]^{-2} - f$$

$$y1 := .0001\text{m}$$

$$\epsilon := \text{root}(s(y1), y1) = (-4.723 \times 10^{-5} + 1.52i \times 10^{-5}) \cdot \text{m}$$

Slope sensitivity analysis, traversing duct

$$\frac{.25\text{in}}{6\text{ft}} = 3.472 \times 10^{-3} \quad Q := 7.8 \frac{\text{L}}{\text{sec}}$$

$$y := 10\text{cm} \quad b := 7.5\text{in}$$

$$V := \frac{Q}{y \cdot b} = 0.409 \frac{\text{m}}{\text{s}}$$

$$i := 0..10$$

$$f(S_0) := \frac{S_0 \cdot 4 \cdot \left(\frac{y \cdot b}{2 \cdot y + b} \right) \cdot 2 \cdot g}{V^2}$$

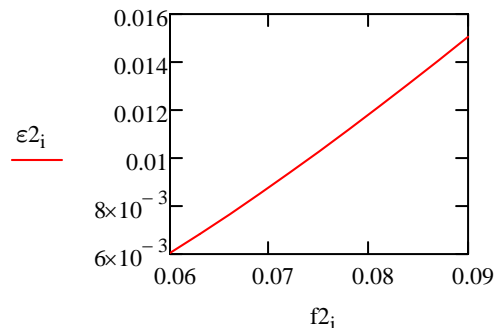
$$S_i := 0.003 + \frac{i}{10000}$$

$$s(\epsilon, f) := 4 \cdot \left[3.4735 - 1.5635 \cdot \ln \left[2 \cdot \frac{\epsilon}{4 \left(\frac{y \cdot b}{2 \cdot y + b} \right)} \right]^{1.11} + 63.635 \cdot \frac{\nu}{\left(\frac{y \cdot b}{2 \cdot y + b} \right) \cdot V} \right]^{-2} - f$$

$$y1(x, f) := \text{root}(s(x, f), x)$$

y1 is a function where x is the guess and f is the friction factor

$$y2 := \begin{cases} \text{for } k \in 0..10 & i := 0..10 \\ \left| \begin{array}{l} f2 \leftarrow .06 + \frac{3k}{1000} \\ y2_k \leftarrow y1(.05\text{mm}, f2) \end{array} \right. & f2_i := .06 + \frac{3i}{1000} \\ y2 \\ \epsilon2 := y2 \end{cases}$$



range from 6mm to 16mm,
possible that the slope is off...

Slope sensitivity analysis, climbing duct

$$Q := 7.8 \frac{\text{L}}{\text{sec}} \quad V := 3.07 \frac{\text{m}}{\text{sec}} \quad b := 50\text{cm}$$

$$y := \frac{Q}{V \cdot b} = 5.081 \times 10^{-3} \text{ m}$$

$$i := 0..10$$

$$S_0 := 1 + \frac{i}{100}$$

$$f(S_0) := \frac{S_0 \cdot 4 \cdot \left(\frac{y \cdot b}{2 \cdot y + b} \right) \cdot 2 \cdot g}{V^2}$$

$$s(\epsilon, f) := 4 \cdot \left[3.4735 - 1.5635 \cdot \ln \left[2 \cdot \frac{\epsilon}{4 \left(\frac{y \cdot b}{2 \cdot y + b} \right)} \right]^{1.11} + 63.635 \cdot \frac{\nu}{\left(\frac{y \cdot b}{2 \cdot y + b} \right) \cdot V} \right]^{-2} - f$$

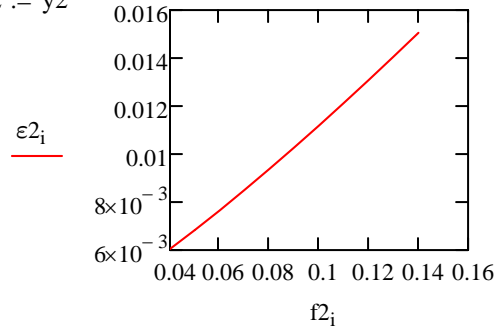
$y1(x,f) := \text{root}(s(x,f), x)$

$y1$ is a function where x is the guess and f is the friction factor

$y2 :=$

for $k \in 0..10$	$i := 0..10$				
<table style="border-collapse: collapse;"> <tr> <td style="border-right: 1px solid black; padding-right: 10px;">$f2 \leftarrow .04 + \frac{k}{100}$</td> <td style="padding-left: 10px;">$f2_i := .04 + \frac{i}{100}$</td> </tr> <tr> <td style="border-right: 1px solid black; padding-right: 10px;">$y2_k \leftarrow y1(.05\text{mm}, f2)$</td> <td></td> </tr> </table>	$f2 \leftarrow .04 + \frac{k}{100}$	$f2_i := .04 + \frac{i}{100}$	$y2_k \leftarrow y1(.05\text{mm}, f2)$		
$f2 \leftarrow .04 + \frac{k}{100}$	$f2_i := .04 + \frac{i}{100}$				
$y2_k \leftarrow y1(.05\text{mm}, f2)$					
$y2$					

$\epsilon2 := y2$



range from 0 ish to 3mm, much different from traversing climbing duct

APPENDIX C-CLIMBING DUCT HYDRAULIC MODEL CALCULATIONS

Climbing Duct for LPS system, b=50cm

$$\mu := 2.730 \cdot 10^{-5} \frac{\text{lb} \cdot \text{s}}{\text{ft}^2}$$

$$\mu = 1.307 \times 10^{-3} \frac{\text{kg}}{\text{sec} \cdot \text{m}}$$

$$\nu := \frac{\mu}{\rho} = 1.318 \times 10^{-6} \frac{\text{m}^2}{\text{s}}$$

$$\rho := 992 \frac{\text{kg}}{\text{m}^3}$$

$$g = 32.174 \frac{\text{ft}}{\text{sec}^2}$$

Properties of water 50 deg F

$$S_o := \frac{.25 \text{in}}{6 \text{ft}} = 3.472 \times 10^{-3}$$

Horizontal section, slope 1/4" per 6'

$$b := 7.5 \text{in} = 0.191 \text{m}$$

Nominal width of traversing ductwork

$$A(y) := b \cdot y$$

Area of flow

$$Rh(y) := \frac{y \cdot b}{2 \cdot y + b}$$

Hydraulic Radius

$$D_h := 4 \cdot Rh(y)$$

Hydraulic Diameter

$$Re := \frac{V \cdot Rh(y)}{\nu}$$

Reynolds Number

$$Fr := \frac{V}{\sqrt{g \cdot y}}$$

Froude Number

Comparison of roughness values

$$Q := 7.8 \frac{\text{L}}{\text{sec}}$$

$$b := 50 \text{cm}$$

$$S_o := 1$$

$$\varepsilon := 11 \text{mm}$$

use the traversing duct roughness

$$s(y) := 8 \cdot S_o \cdot \left(\frac{y \cdot b}{2 \cdot y + b} \right) \cdot g - 4 \cdot \left[3.4735 - 1.5635 \cdot \ln \left[2 \cdot \frac{\varepsilon}{4 \left(\frac{y \cdot b}{2 \cdot y + b} \right)} \right]^{1.11} + 63.635 \cdot \frac{\nu}{4 \left(\frac{y \cdot b}{2 \cdot y + b} \right) \cdot \frac{Q}{b \cdot y}} \right]^{-2} \frac{Q^2}{(b \cdot y)^2}$$

$$y := 1 \text{mm}$$

$$y1 := \text{root}(s(y), y)$$

$$y := y1 = 8.928 \times 10^{-3} \text{m}$$

Resulting depth for the roughness

$$Q := 7.8 \frac{\text{L}}{\text{sec}} \quad b := 50\text{cm} \quad S_o := 0.325 \quad \varepsilon := .18\text{mm}$$

use the climbing duct roughness

$$s(y) := 8 \cdot S_o \cdot \left(\frac{y \cdot b}{2 \cdot y + b} \right) \cdot g - 4 \cdot \left[3.4735 - 1.5635 \cdot \ln \left[2 \cdot \frac{\varepsilon}{4 \left(\frac{y \cdot b}{2 \cdot y + b} \right)} \right]^{1.11} + 63.635 \cdot \frac{\nu}{4 \left(\frac{y \cdot b}{2 \cdot y + b} \right) \cdot \frac{Q}{b \cdot y}} \right]^{-2} \frac{Q^2}{(b \cdot y)^2}$$

$$y := 1\text{mm}$$

$$y1 := \text{root}(s(y), y)$$

$$y := y1 = 6.983 \times 10^{-3} \text{ m}$$

Resulting depth for the roughness

$$A(y) := b \cdot y$$

$$V := \frac{Q}{A(y)} = 2.234 \frac{\text{m}}{\text{s}}$$

$$\text{Fr} := \frac{V}{\sqrt{g \cdot y}} = 8.537$$

For the Climbing Duct, 20", S=1

From Reinhardt et al 2008 Q:7.8L/s, V:3.05m/sec

$$Q := 7.8 \frac{\text{L}}{\text{sec}} \quad b := 50\text{cm} \quad \varepsilon := 1.8 \cdot 10^{-4} \text{ m} \quad S_o := 1$$

$$s(y, Q) := 8 \cdot S_o \cdot \left(\frac{y \cdot b}{2 \cdot y + b} \right) \cdot g - 4 \cdot \left[3.4735 - 1.5635 \cdot \ln \left[2 \cdot \frac{\varepsilon}{4 \left(\frac{y \cdot b}{2 \cdot y + b} \right)} \right]^{1.11} + 63.635 \cdot \frac{\nu}{\left(\frac{y \cdot b}{2 \cdot y + b} \right) \cdot \frac{Q}{b \cdot y}} \right]^{-2} \frac{Q^2}{(b \cdot y)^2}$$

$$y1(x, Q) := \text{root}(s(x, Q), x) \quad y1 \text{ is a function where } x \text{ is the guess and epsilon is the channel roughness}$$

$$y2 := \left| \begin{array}{l} \text{for } k \in 0..1000 \\ \left| \begin{array}{l} Q2 \leftarrow .001 \frac{\text{m}^3}{\text{sec}} + \frac{k \cdot \frac{\text{m}^3}{\text{sec}}}{1000} \\ y2_k \leftarrow y1(.2\text{mm}, Q2) \end{array} \right. \\ y2 \end{array} \right.$$

$$i := 0..1000$$

$$Q2_i := .001 \frac{\text{m}^3}{\text{sec}} + \left(\frac{i}{1000} \right) \frac{\text{m}^3}{\text{sec}}$$

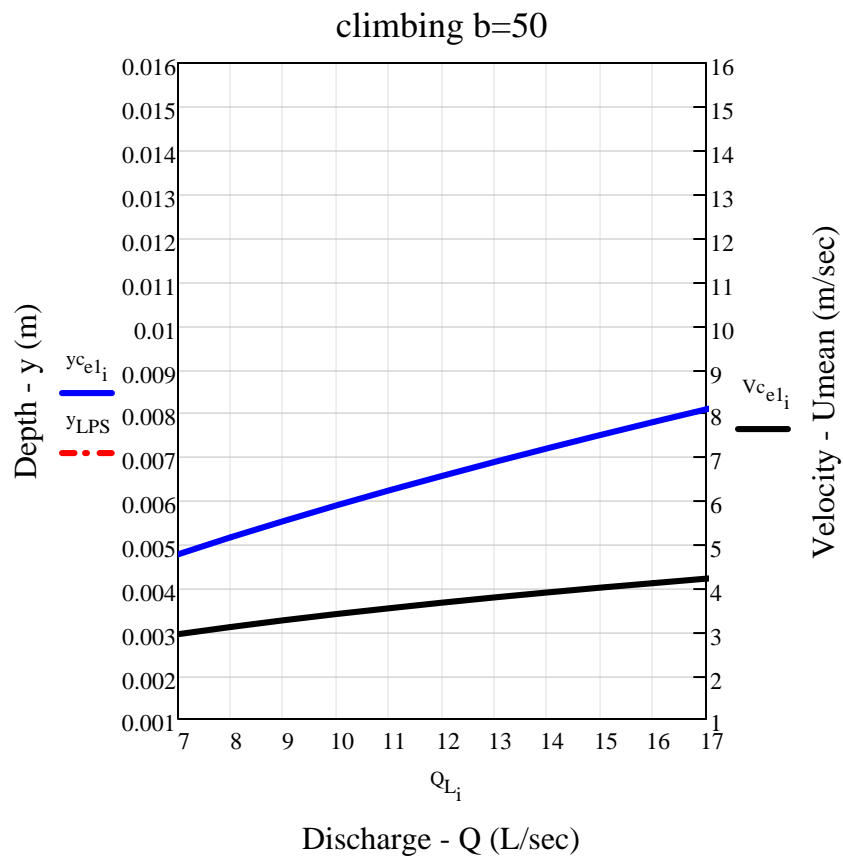
$$Q_L := Q2 \cdot 1000$$

$$y_{c_{e1}} := y2$$

$$A(y) := b \cdot y$$

$$A_{c_{e1}} := A(y2)$$

$$V_{c_{e1}} := \frac{Q2}{A_{c_{e1}}}$$



Assume roughness from the S=1.0 solution is valid for all climbing slope

$$b := 50\text{cm}$$

$$\varepsilon = 1.8 \times 10^{-4}\text{ m}$$

Change slope to 18 degrees,

$$So := \tan\left(\frac{18 \cdot \pi}{180}\right) = 0.325$$

$$s(y, Q) := 8 \cdot So \cdot \left(\frac{y \cdot b}{2 \cdot y + b}\right) \cdot g - 4 \cdot \left[3.4735 - 1.5635 \cdot \ln\left[2 \cdot \left(\frac{\varepsilon}{4 \cdot \left(\frac{y \cdot b}{2 \cdot y + b}\right)}\right)^{1.11} + 63.635 \cdot \frac{\nu}{4 \cdot \left(\frac{y \cdot b}{2 \cdot y + b}\right) \cdot \frac{Q}{b \cdot y}} \right] \right]^2 \cdot \frac{Q^2}{(b \cdot y)^2}$$

$$y1(x, Q) := \text{root}(s(x, Q), x)$$

y1 is a function where x is the guess and Q is the discharge

$$y2 := \begin{cases} \text{for } k \in 0..1000 \\ \left| \begin{array}{l} Q2 \leftarrow .001 \frac{\text{m}^3}{\text{sec}} + \frac{k \cdot \frac{\text{m}^3}{\text{sec}}}{1000} \\ y2_k \leftarrow y1(.9\text{mm}, Q2) \end{array} \right. \\ y2 \end{cases}$$

$$i := 0..1000$$

$$Q2_i := .001 \frac{\text{m}^3}{\text{sec}} + \left(\frac{i}{1000}\right) \frac{\text{m}^3}{\text{sec}}$$

$$Q_L := \frac{Q2 \cdot 1000}{\frac{\text{m}^3}{\text{sec}}}$$

$$ycS18_{e5} := y2$$

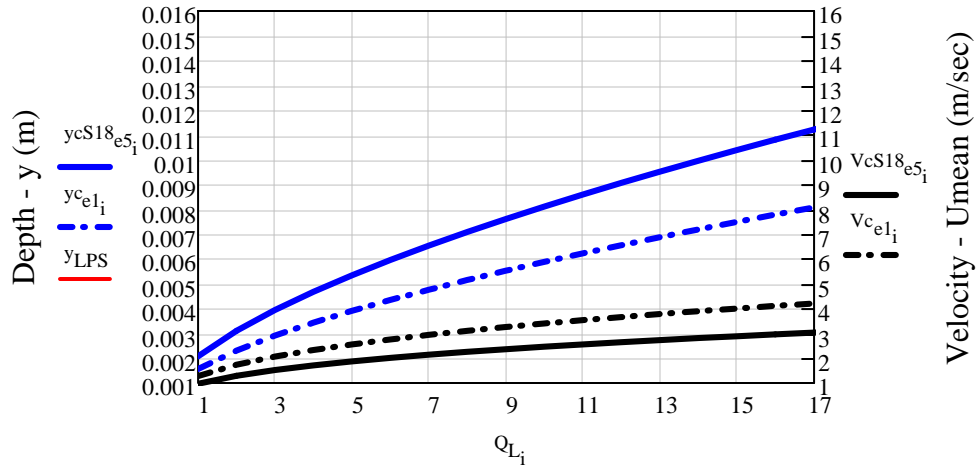
$$AcS18_{e5} := A(y2)$$

$$VcS18_{e5} := \frac{Q2}{AcS18_{e5}}$$

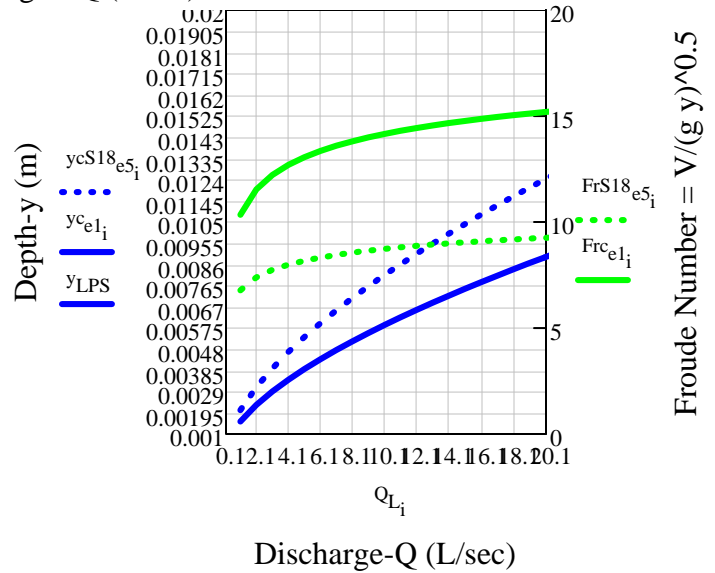
$$FrS18_{e5} := \frac{VcS18_{e5}}{\sqrt{g \cdot ycS18_{e5}}}$$

$$Frc_{e1} := \frac{Vc_{e1}}{\sqrt{g \cdot yc_{e1}}}$$

Climbing Duct, Varying Slope, b=50cm



Discharge - Q (L/sec)



Change width in climbing duct, increase by 20%

$$S_o := 1$$

$$b := 60\text{cm}$$

$$\epsilon = 1.8 \times 10^{-4} \text{ m}$$

$$s(y, Q) := 8 \cdot S_o \cdot \left(\frac{y \cdot b}{2 \cdot y + b} \right) \cdot g - 4 \cdot \left[3.4735 - 1.5635 \cdot \ln \left[2 \cdot \frac{\epsilon}{4 \left(\frac{y \cdot b}{2 \cdot y + b} \right)} \right]^{1.11} + 63.635 \cdot \frac{\nu}{4 \left(\frac{y \cdot b}{2 \cdot y + b} \right) \cdot \frac{Q}{b \cdot y}} \right]^{-2} \frac{Q^2}{(b \cdot y)^2}$$

$y1(x, Q) := \text{root}(s(x, Q), x)$ $y1$ is a function where x is the guess and ϵ is the channel roughness

$y2 :=$ for $k \in 0..1000$

$$Q2 \leftarrow .001 \frac{\text{m}^3}{\text{sec}} + \frac{k \cdot \frac{\text{m}^3}{\text{sec}}}{1000}$$

$$y2_k \leftarrow y1(.9\text{mm}, Q2)$$

$y2$

$i := 0..1000$

$$Q2_i := .001 \frac{\text{m}^3}{\text{sec}} + \left(\frac{i}{1000} \right) \frac{\text{m}^3}{\text{sec}}$$

$$Q_L := \frac{Q2 \cdot 1000}{\frac{\text{m}^3}{\text{sec}}}$$

$$y_{c_{e5b60}} := y2$$

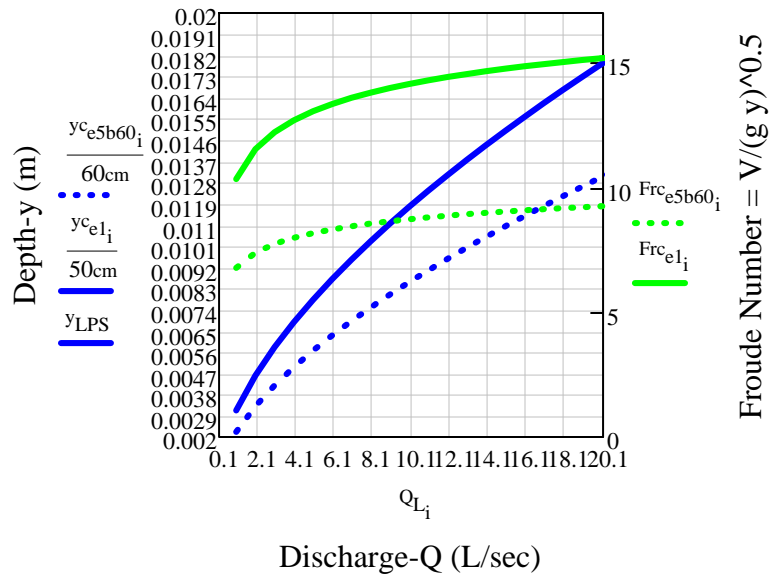
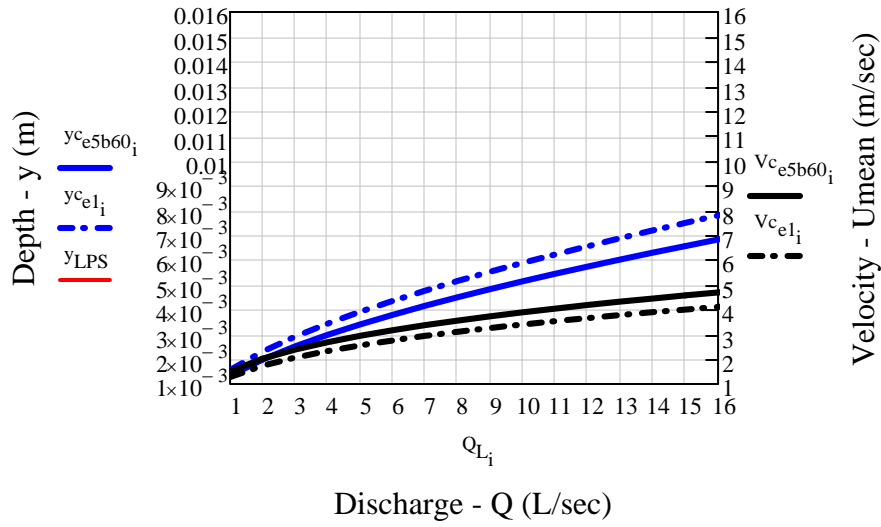
$$y_{\max} := 1.3\text{cm}$$

$$A_{c_{e5b60}} := A(y2)$$

$$V_{c_{e5b60}} := \frac{Q2}{A_{c_{e5b60}}}$$

$$Frc_{e5b60} := \frac{V_{c_{e5b60}} S_{18_{e5}}}{\sqrt{g \cdot y_{c_{e5b60}} S_{18_{e5}}}}$$

Climbing Duct, Varying Width



APPENDIX D-TRAVERSING DUCT HYDRAULIC MODEL CALCULATIONS

Traversing Duct Hydraulic Model

Modification of duct calculations, change roughness to 0.18 for all traversing

Variables that are changed are highlighted and outlined on right hand side of worksheet

$$\mu := 2.730 \cdot 10^{-5} \frac{\text{lbf} \cdot \text{s}}{\text{ft}^2} \quad \rho := 992 \frac{\text{kg}}{\text{m}^3} \quad \nu := \frac{\mu}{\rho} = 1.318 \times 10^{-6} \frac{\text{m}^2}{\text{s}} \quad \text{constants at 50 deg F}$$

$$S_o := \frac{.25 \text{in}}{6 \text{ft}} = 3.472 \times 10^{-3} \quad \text{Horizontal section, slope } 1/4" \text{ per } 6'$$

Equation and solution for flow depth at a given slope, width, and discharge

$$\epsilon := .18 \text{mm}$$

$$b := 7.5 \text{in} \quad y := 4.445 \text{cm}$$

$$S_o = 3.472 \times 10^{-3}$$

$$s(Q) := 8 \cdot S_o \cdot \left(\frac{y \cdot b}{2 \cdot y + b} \right) \cdot g - 4 \cdot \left[3.4735 - 1.5635 \cdot \ln \left[2 \cdot \frac{\epsilon}{4 \left(\frac{y \cdot b}{2 \cdot y + b} \right)} \right]^{1.11} + 63.635 \cdot \frac{\nu}{\left(\frac{y \cdot b}{2 \cdot y + b} \right) \cdot \frac{Q}{b \cdot y}} \right]^{-2} \frac{Q^2}{(b \cdot y)^2}$$

$$y1 := .1 \frac{\text{m}^3}{\text{sec}}$$

$$Q := \text{root}(s(y1), y1)$$

$$Q = 4.322 \cdot \frac{\text{L}}{\text{sec}} \quad V := \frac{Q}{b \cdot y} = 0.51 \frac{\text{m}}{\text{s}} \quad \frac{b}{y} = 4.286$$

$$\text{Re} := \frac{\rho \cdot V \cdot \left(\frac{b \cdot y}{2 \cdot y + b} \right)}{\mu} = 1.174 \times 10^4 \quad \text{Fr} := \frac{V}{\sqrt{g \cdot y}} = 0.773$$

Equation and solution for flow depth at a given slope, width, and discharge

$$\epsilon := .18 \text{mm}$$

$$b := 50 \text{cm}$$

$$Q := 7.8 \frac{\text{L}}{\text{sec}}$$

$$S_o = 3.472 \times 10^{-3}$$

$$s(y) := 8 \cdot S_o \cdot \left(\frac{y \cdot b}{2 \cdot y + b} \right) \cdot g - 4 \cdot \left[3.4735 - 1.5635 \cdot \ln \left[2 \cdot \frac{\epsilon}{4 \left(\frac{y \cdot b}{2 \cdot y + b} \right)} \right]^{1.11} + 63.635 \cdot \frac{\nu}{\left(\frac{y \cdot b}{2 \cdot y + b} \right) \cdot \frac{Q}{b \cdot y}} \right]^{-2} \frac{Q^2}{(b \cdot y)^2}$$

$$y1 := 1 \text{mm}$$

$$y := \text{root}(s(y1), y1) \quad y = 3.204 \cdot \text{cm} \quad V := \frac{Q}{b \cdot y} = 0.487 \frac{\text{m}}{\text{s}}$$

$$\text{Re} := \frac{\rho \cdot V \cdot \left(\frac{b \cdot y}{2 \cdot y + b} \right)}{\mu} = 1.049 \times 10^4 \quad \text{Fr} := \frac{V}{\sqrt{g \cdot y}} = 0.869$$

Traversing, wide ductwork b=50cm

b := 50cm

$$s(y, Q) := 8 \cdot \text{So} \cdot \left(\frac{y \cdot b}{2 \cdot y + b} \right) \cdot g - 4 \cdot \left[3.4735 - 1.5635 \cdot \ln \left[2 \cdot \frac{\epsilon}{4 \left(\frac{y \cdot b}{2 \cdot y + b} \right)} \right]^{1.11} + 63.635 \cdot \frac{\nu}{\left(\frac{y \cdot b}{2 \cdot y + b} \right) \cdot \frac{Q}{b \cdot y}} \right]^{-2} \frac{Q^2}{(b \cdot y)^2}$$

$y1(x, Q) := \text{root}(s(x, Q), x)$ $y1$ is a function where x is the guess and epsilon is the channel roughness

Write a loop to solve flow depth for varying discharges

$$y2 := \begin{array}{l} \text{for } k \in 0..1000 \\ \left| \begin{array}{l} Q2 \leftarrow .001 \frac{\text{m}^3}{\text{sec}} + \frac{k \cdot \frac{\text{m}^3}{\text{sec}}}{1000} \\ y2_k \leftarrow y1(.09\text{mm}, Q2) \end{array} \right. \\ y2 \end{array}$$

$$i := 0..1000$$

$$Q2_i := .001 \frac{\text{m}^3}{\text{sec}} + \left(\frac{i}{1000} \right) \frac{\text{m}^3}{\text{sec}}$$

$$yc_{e3} := y2$$

$$A(y) := b \cdot y$$

$$Ac_{e3} := \overrightarrow{A(yc_{e3})}$$

$$Vc_{e3} := \frac{Q2}{Ac_{e3}}$$

Solve for the area, velocity, and reynolds number for the entire matrix $y2$

Traversing, ductwork b=23cm

b := 23cm

$$s(y, Q) := 8 \cdot \text{So} \cdot \left(\frac{y \cdot b}{2 \cdot y + b} \right) \cdot g - 4 \cdot \left[3.4735 - 1.5635 \cdot \ln \left[2 \cdot \frac{\epsilon}{4 \left(\frac{y \cdot b}{2 \cdot y + b} \right)} \right]^{1.11} + 63.635 \cdot \frac{\nu}{\left(\frac{y \cdot b}{2 \cdot y + b} \right) \cdot \frac{Q}{b \cdot y}} \right]^{-2} \frac{Q^2}{(b \cdot y)^2}$$

$y1(x, Q) := \text{root}(s(x, Q), x)$ $y1$ is a function where x is the guess and epsilon is the channel roughness

$$y3 := \begin{array}{l} \text{for } k \in 0..1000 \\ \left| \begin{array}{l} Q2 \leftarrow .001 \frac{\text{m}^3}{\text{sec}} + \frac{k \cdot \frac{\text{m}^3}{\text{sec}}}{1000} \\ y3_k \leftarrow y1(9\text{mm}, Q2) \end{array} \right. \\ y3 \end{array}$$

$$yc_{e5} := y3$$

$$A(y) := b \cdot y$$

$$Ac_{e5} := \overrightarrow{A(yc_{e5})}$$

$$Vc_{e5} := \frac{Q2}{Ac_{e5}}$$

Solve for the area, velocity, and reynolds number for the entire matrix $y2$

Traversing, narrow width b=19cm

b := 19cm

$$s(y, Q) := 8 \cdot S_o \cdot \left(\frac{y \cdot b}{2 \cdot y + b} \right) \cdot g - 4 \cdot \left[3.4735 - 1.5635 \cdot \ln \left[2 \cdot \frac{\epsilon}{4 \cdot \left(\frac{y \cdot b}{2 \cdot y + b} \right)} \right]^{1.11} + 63.635 \cdot \frac{\nu}{\left(\frac{y \cdot b}{2 \cdot y + b} \right) \cdot \frac{Q}{b \cdot y}} \right]^{-2} \cdot \frac{Q^2}{(b \cdot y)^2}$$

y1(x, Q) := root(s(x, Q), x) y1 is a function where x is the guess and epsilon is the channel roughness

```

y4 := for k ∈ 0..1000
    |
    |   Q2 ← .001  $\frac{m^3}{sec} + \frac{k \cdot \frac{m^3}{sec}}{1000}$ 
    |   y4k ← y1(9mm, Q2)
    |
    | y4
    
```

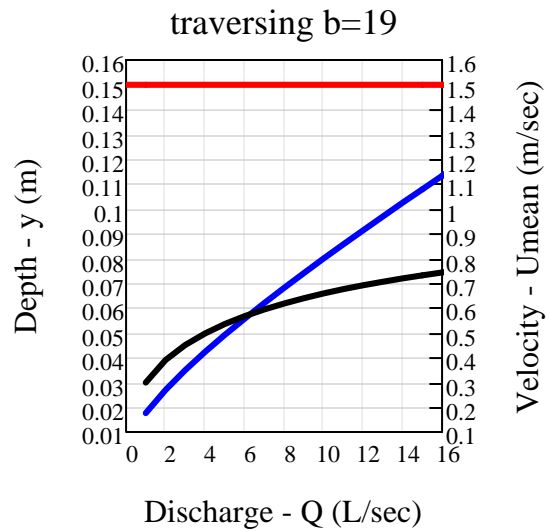
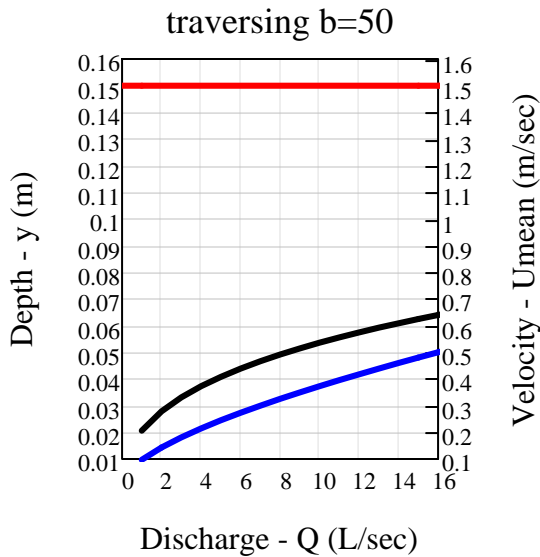
Q_L := Q2 · 1000 change Q to L/sec
 y_{LPS} := .15m depth of channel

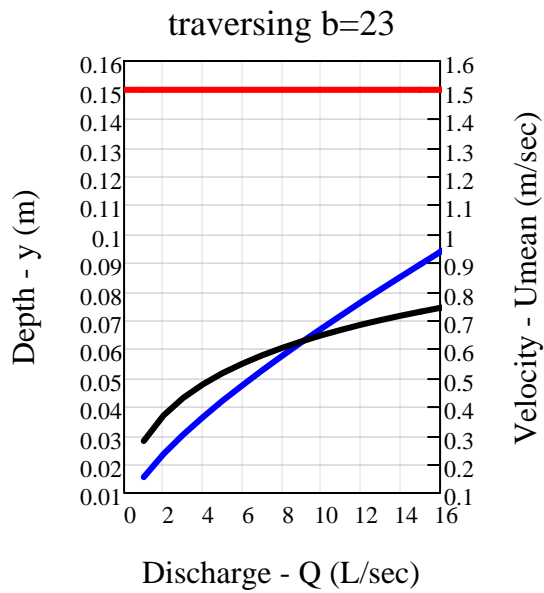
yc_{e7} := y4

A(y) := b · y

A_{c_{e7}} := A(yc_{e7})

V_{c_{e7}} := $\frac{Q2}{A_{c_{e7}}}$





Critical Slope Calculations

$$Q := 7.8 \frac{\text{L}}{\text{sec}} \quad b := 19 \text{cm}$$

$$s(y, S_0) := 8 \cdot S_0 \cdot \left(\frac{y \cdot b}{2 \cdot y + b} \right) \cdot g - 4 \cdot \left[3.4735 - 1.5635 \cdot \ln \left[2 \cdot \frac{\epsilon}{4 \left(\frac{y \cdot b}{2 \cdot y + b} \right)} \right]^{1.11} + 63.635 \cdot \frac{\nu}{4 \left(\frac{y \cdot b}{2 \cdot y + b} \right) \cdot \frac{Q}{b \cdot y}} \right]^2 \cdot \frac{Q^2}{(b \cdot y)^2}$$

$y_1(x, S_0) := \text{root}(s(x, S_0), x)$ y_1 is a function where x is the guess and epsilon is the channel roughness

$$y_2 := \begin{cases} \text{for } k \in 0..10000 \\ \quad \left| \begin{array}{l} S_{02} \leftarrow .00001 + \frac{k}{10000} \\ y_{2k} \leftarrow y_1(.9 \text{mm}, S_{02}) \end{array} \right. \\ y_2 \end{cases}$$

$$i := 0..10000$$

$$S_{02_i} := .00001 + \frac{i}{10000}$$

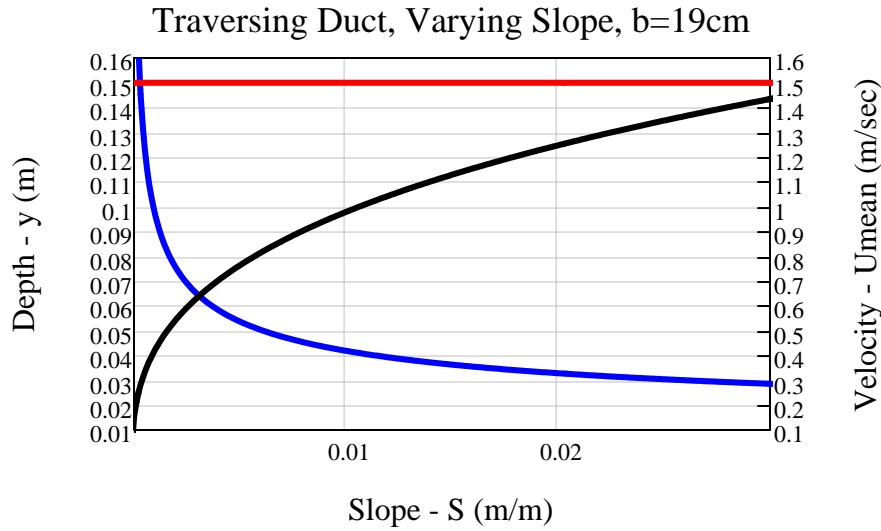
$$y_c := y_2$$

$$A(y) := b \cdot y$$

$$A_c := A(y_c)$$

$$V_c := \frac{Q}{A_c}$$

$$Fr_c := \frac{V_c}{\sqrt{g \cdot y_c}}$$



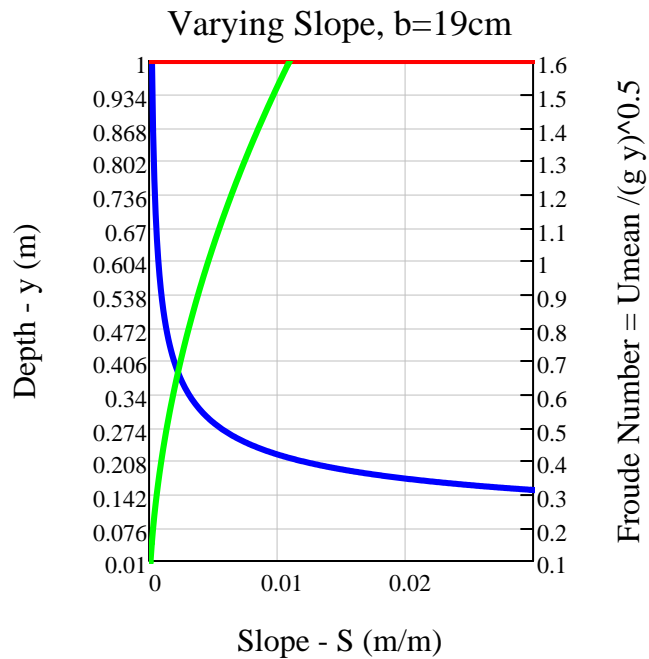
$Fr_c =$

	0
0	0.016
1	0.098
2	0.153
3	0.198
4	0.237
5	0.272
6	...

$y_{c47} = 0.055 \text{ m}$

$V_{c47} = 0.743 \frac{\text{m}}{\text{s}}$

$So_{247} = 4.71 \times 10^{-3}$



Critical Slope Calculations

b := 23cm

$$s(y, So) := 8 \cdot So \cdot \left(\frac{y \cdot b}{2 \cdot y + b} \right) \cdot g - 4 \cdot \left[3.4735 - 1.5635 \cdot \ln \left[2 \cdot \frac{\epsilon}{4 \cdot \left(\frac{y \cdot b}{2 \cdot y + b} \right)} \right]^{1.11} + 63.635 \cdot \frac{\nu}{4 \cdot \left(\frac{y \cdot b}{2 \cdot y + b} \right) \cdot \frac{Q}{b \cdot y}} \right]^{-2} \cdot \frac{Q^2}{(b \cdot y)^2}$$

$y1(x, So) := \text{root}(s(x, So), x)$ $y1$ is a function where x is the guess and epsilon is the channel roughness

```

y2 := | for k ∈ 0.. 10000
      |   So2 ← .00001 +  $\frac{k}{10000}$ 
      |   y2k ← y1(.9mm, So2)
      | y2
  
```

```

i := 0.. 10000
So2i := .00001 +  $\frac{i}{10000}$ 
  
```

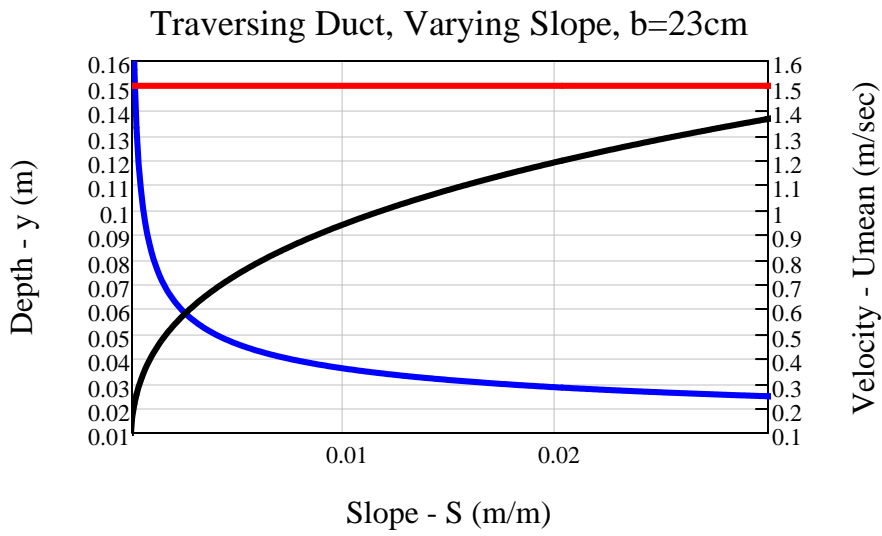
$$y_c := y2$$

$$A(y) := b \cdot y$$

$$A_c := A(y_c)$$

$$V_c := \frac{Q}{A_c}$$

$$Fr_c := \frac{V_c}{\sqrt{g \cdot y_c}}$$



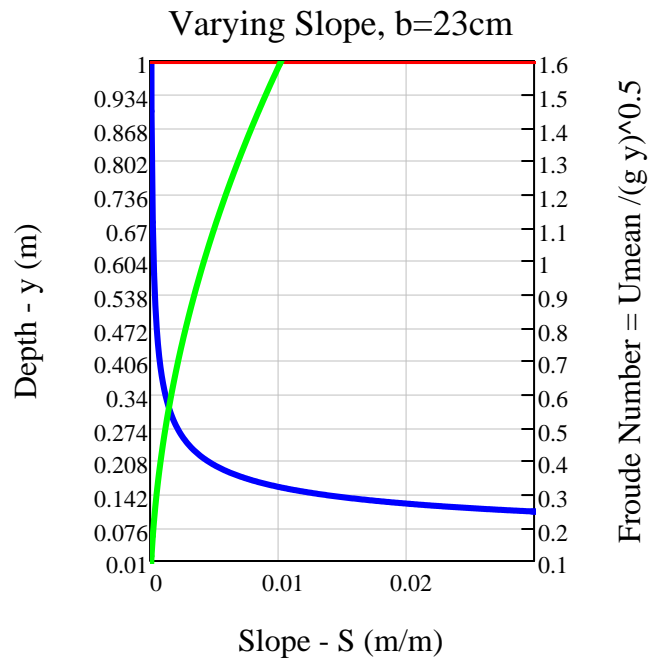
	0
0	0.021
1	0.115
2	0.175
3	0.223
4	0.265
5	0.302
6	0.336
7	...

Fr_c =

$$y_{c42} = 0.049 \text{ m}$$

$$V_{c42} = 0.693 \frac{\text{m}}{\text{s}}$$

$$So_{242} = 4.21 \times 10^{-3}$$



Critical Slope Calculations

b := 50cm

$$s(y, So) := 8 \cdot So \cdot \left(\frac{y \cdot b}{2 \cdot y + b} \right) \cdot g - 4 \cdot \left[3.4735 - 1.5635 \cdot \ln \left[2 \cdot \frac{\epsilon}{4 \cdot \left(\frac{y \cdot b}{2 \cdot y + b} \right)} \right]^{1.11} + 63.635 \cdot \frac{\nu}{4 \cdot \left(\frac{y \cdot b}{2 \cdot y + b} \right) \cdot \frac{Q}{b \cdot y}} \right]^2 \cdot \frac{Q^2}{(b \cdot y)^2}$$

y1(x, So) := root(s(x, So), x) y1 is a function where x is the guess and epsilon is the channel roughness

```

y2 := for k ∈ 0..10000
    | So2 ← .00001 + k / 10000
    | y2k ← y1(.9mm, So2)
    | y2
i := 0..10000
So2i := .00001 + i / 10000

```

y_c := y2

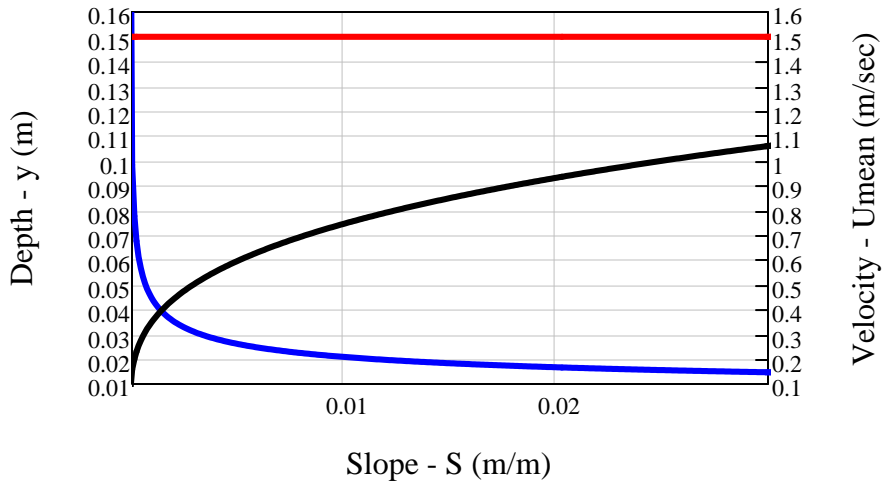
$$A(y) := b \cdot y$$

$$A_c := A(y_c)$$

$$V_c := \frac{Q}{A_c}$$

$$Fr_c := \frac{V_c}{\sqrt{g \cdot y_c}}$$

Traversing Duct, Varying Slope, b=50cm



	0
0	0.04
1	0.161
2	0.23
3	0.283
4	0.328
5	0.368
6	0.404
7	0.437
8	...

$$y_{c_{37}} = 0.029 \text{ m}$$

$$V_{c_{37}} = 0.538 \frac{\text{m}}{\text{s}}$$

$$So_{2_{37}} = 3.71 \times 10^{-3}$$

Varying Slope, b=50cm

